Cretaceous Research 170 (2025) 106095

Contents lists available at ScienceDirect

Cretaceous Research

journal homepage: www.elsevier.com/locate/CretRes

Age and palaeoenvironmental constraints on the earliest dinosaur-bearing strata of the Densuș-Ciula Formation (Hațeg Basin, Romania): Evidence of their late Campanian-early Maastrichtian syntectonic deposition

Gáspár Albert [a], Soma Budai [b], Zoltán Csiki-Sava [c], László Makádi [d], Daniel Țabără [e], Valentin Árvai [f], Ramona Bălc [g, h], Raluca Bindiu-Haitonic [i], Mihai N. Ducea [c, j], Gábor Botfalvai [k, l, *]

[a] Eötvös Loránd University, Institute of Cartography and Geoinformatics, Budapest, Hungary
[b] Università degli Studi di Pavia, Dipartimento di Scienze della Terra e dell'Ambiente, Pavia, Italy
[c] University of Bucharest, Department of Geology, Mineralogy and Palaeontology, Bucharest, Romania
[d] Supervisory Authority for Regulatory Affairs, Geological Directorate, Department of Collections, Budapest, Hungary
[e] Al. I. Cuza University of Iași, Department of Geology, Iași, Romania
[f] Eötvös Loránd University, Doctorate School of Earth Sciences, Budapest, Hungary
[g] Babeș-Bolyai University, Faculty of Environmental Science and Engineering, Cluj-Napoca, Romania
[h] Babeș-Bolyai University, Interdisciplinary Research Institute on Bio-Nano Sciences, Cluj-Napoca, Romania
[i] Babeș-Bolyai University, Department of Geology and Research Centre for Integrated Geological Studies, Cluj-Napoca, Romania
[j] Department of Geosciences, University of Arizona, Tucson, USA
[k] ELTE Eötvös Loránd University, Institute of Geography and Earth Sciences, Department of Palaeontology, Budapest, Hungary
[l] HUN-REN–MTM–ELTE Research Group for Paleontology, Budapest, Hungary

ARTICLE INFO

Article history:
Received 2 September 2024
Received in revised form
20 January 2025
Accepted in revised form 21 January 2025
Available online 30 January 2025

Keywords:
Syntectonic sedimentation
Late Cretaceous
Geological mapping
Dinosaur beds
Strike-slip basin
Campanian/Maastrichtian boundary

ABSTRACT

The Hațeg Basin is famous for its rich uppermost Cretaceous continental vertebrate assemblages, with some of the most important ones originating from the Densuș-Ciula Formation. The present study aims to provide a more accurate picture of the geological and palaeoenvironmental context of this important dinosaur-bearing succession through complex spatial analysis based on detailed geological mapping combined with results of zircon U–Pb geochronology, sedimentology, vertebrate palaeontology and micropalaeontology investigations. This integrated stratigraphical survey revealed that the important environmental shift from marine to continental deposition in western Hațeg Basin occurred significantly earlier (by middle late Campanian) than hitherto considered, and that the lower Densuș-Ciula Formation – previously thought to be restricted to the Maastrichtian – covers a good part of the upper Campanian as well. Sedimentological investigations, aimed to characterize palaeoenvironmental changes during basin evolution, identify two, vertically superimposed fining-upward successions within the lower Densuș-Ciula Formation, reconstructed as alluvial fan environments linked to distinct stages of basin tectonic evolution. Contrary to previous interpretations as a post-orogenic molasse, the lower Densuș-Ciula Formation is here re-interpreted as a largely syntectonic unit deposited in a transtensional, dextral strike-slip basin initiated during the late Campanian. The stratigraphic positions and palaeoenvironmental settings of all major vertebrate sites from this area are re-assessed using our new age constraints and improved tectonic-stratigraphic-sedimentologic framework, documenting a significantly earlier start of the accumulation of vertebrate-bearing deposits than thought before, and challenging previous ideas about the timing of assembly, isolation and evolution of the Hațeg Island faunas.

* Corresponding author. Pázmány Péter sétány 1/C, Budapest 1117, Hungary.
E-mail address: botfalvai@staff.elte.hu (G. Botfalvai).

https://doi.org/10.1016/j.cretres.2025.106095

1. Introduction

The Upper Cretaceous Densuș-Ciula Formation (Hațeg Basin) has long been known for its rich dinosaur sites, from which hundreds of well-preserved vertebrate fossils have been collected over one hundred years (Nopcsa, 1915; Kadić, 1916; Therrien, 2005; Csiki et al., 2010; Csiki-Sava et al., 2016; Venczel et al., 2016; Botfalvai et al., 2017, 2021 and references therein). However, excepting the Tuștea nesting locality (Botfalvai et al., 2017) and a few microvertebrate sites (e.g. Vasile and Csiki, 2010; Vasile et al., 2011), geological, stratigraphical and sedimentological context is poorly documented for a large part of the fossils collected from this formation, and often the exact locations of the individual sites remain unknown (e.g. Buffetaut et al., 2002; Weishampel et al., 2003). Detailed geological mapping of the investigated area was first conducted in the early 20th century (Schafarzik, 1910). This early mapping study has already shown that the older deposits of the uppermost Cretaceous continental successions are located in the western part of Hațeg Basin, where at the same time the first significant dinosaur finds were also reported (Nopcsa, 1915; Kadić, 1916). Following a long break, mapping in this area resumed in the 1970s and 1980s (Maier and Lupu, 1979; Lupu et al., 1993) but the relationships between the different sedimentary sequences and the bone-bearing beds has not been fully resolved. Despite the presence of vertebrate fossils, the age of the entire uppermost Cretaceous sedimentary succession was uncertain at that time: since fossils were only collected from the lower-intermediate part of the unit, its upper part was considered as Paleocene. The structural line bounding the basin to the north was interpreted on these maps as a normal fault, and although the steep nature and alternating azimuth of the dip of the deposits was recognised, no ductile deformation is marked in any of the Upper Cretaceous formations.

However, several major discoveries starting with the 1980s rendered the published maps obsolete. First of all, detailed palaeontological studies supported a Late Cretaceous age for the quasi-entirety of the Densuș-Ciula Formation, the unit that was defined to include all continental beds from northwestern Hațeg Basin, starting with the uppermost Cretaceous (Grigorescu, 1983, 1992; Csiki et al., 2010; Vasile et al., 2011; Csiki-Sava et al., 2016). New data have narrowed down the depositional period of this thousands-metres thick terrestrial sedimentary succession to the Maastrichtian. Further new results included the recognition of the folded nature of the Upper Cretaceous marine deposits underlying the Densuș-Ciula Formation, in the western part of the basin (Grigorescu and Melinte, 2001), and the identification of the dextral strike-slip nature of the fault in the northwestern part of the basin (Bărzoi and Şeclăman, 2010).

Although the main nappe structures in the wider region of the western Southern Carpathians were recognised early (Murgoci, 1912; Codarcea, 1940) and presented on several maps (see Stelea and Ghenciu, 2020), there was no consensus on the nature and position of the Upper Cretaceous continental deposits overlying these nappes, including those from Hațeg Basin. These were regarded to be not, or only slightly, deformed by tectonic activity, despite the fact that Schafarzik (1910) already reported that the Upper Cretaceous conglomerates (now belonging to the basal Densuș-Ciula Formation) are affected by tectonic forces. Laufer (1925) has similarly pointed out the tilted position of the uppermost Cretaceous continental beds, and Grigorescu (1983) also noted the synorogenic character of the Upper Cretaceous (Maastrichtian) sedimentary rocks. Nonetheless, the uppermost Cretaceous continental sedimentary record of Hațeg Basin was widely considered as not involved in nappe thrusts, resulting instead from post-orogenic deposition (e.g., Mațenco and Schmid, 1999; Iancu et al., 2005). These conflicting interpretations have prompted renewed geological mapping of the northwestern Hațeg Basin area in order to clarify the discrepancies between previous observations.

Since 2019 a large-scale systematic prospecting and geological mapping were conducted around Vălioara Valley (in westernmost part of Hațeg Basin: Fig. 1). During these activities, several areas with palaeontological potential were investigated, resulting in hundreds of vertebrate remains recovered over the past 5 years (Kadić, 1916; see detailes in Botfalvai et al., 2021). Overall, the five-year study resulted in the detailed mapping of an area of about 10 km^2, aiming to address the following main scientific objectives: (i) to resolve and synthesize the often conflicting previously published tectonic and stratigraphic interpretations as well as, specifically, to assess the syn- or post-tectonic nature of the Densuș-Ciula Formation; (ii) to assess the depositional environments and potential ages/stratigraphic relationships of the numerous macro- and microvertebrate sites known in the Vălioara area; (iii) to investigate in greater detail the general depositional setting of the uppermost Cretaceous around Vălioara, first addressed by Botfalvai et al. (2021); and (iv) to produce an updated geological map for the Vălioara area based on the integrated interpretation of the various geological and stratigraphic features observed in the field.

Our results provide important new data prompting the reassessment of the stratigraphical, tectonic and sedimentological conditions that controlled the evolution of the world-renowned dwarf dinosaur assemblages from Hațeg Basin, and allow large-scale reconstructions of the tectonic processes operating, as well as of the palaeoenvironmental evolution, during the emergence of these assemblages. Furthermore, the results discussed in this report are also useful for understanding the circumstances of tectonic evolution that affected areas wider than the basin itself (i.e. the South Carpathians).

2. Geological background

The Hațeg Basin is located in the northwestern part of the Southern Carpathians in Romania (Fig. 1). The geological build-up of the region is the result of large-scale nappe overthrusts associated with the Late Cretaceous Alpine orogeny, and reflect the evolution of extensional basins adjacent to the main collision front (Mațenco and Schmid, 1999; Willingshofer et al., 2001; Iancu et al., 2005). The largely metamorphic basement of the wider study area consists of the lower Danubian Unit and the overlying Getic-Supragetic units. Tectonically (and once palaeogeographically) wedged between the two main units, and currently cropping out further southwest of Hațeg Basin, lies a third unit of oceanic and thinned continental lithosphere known as the Severin Unit (Săndulescu, 1994; van Hinsbergen et al., 2020). During the late Early to early Late Cretaceous a minor continent-continent-type collision between the Getic-Supragetic and the Danubian units closed the intervening Severin Basin, and while the Danubian units were underthrust, a marine piggy-back basin formed on top of the overriding Getic-Supragetic units as the prelude of Hațeg Basin (Willingshofer et al., 2001). The sedimentary rocks of this basin are mainly Upper Cretaceous (including Campanian) deep-marine siliciclastic turbidites, often referred to as 'flysch' in the literature (Grigorescu and Melinte, 2001; Melinte-Dobrinescu, 2010).

Overlying these marine beds, the sedimentary infill of the 80 km^2 large Hațeg Basin comprises two main uppermost Cretaceous continental sedimentary units: the Densuș-Ciula and Sînpetru formations, well-known for their vertebrate fossil occurrences (Grigorescu, 1992; Therrien, 2006; Csiki-Sava et al., 2016; Botfalvai et al., 2021). In the western part of Hațeg Basin, encompassing the study area, the lower part of the Densuș-Ciula Formation is made up of coarse conglomeratic deposits, with minor sandstones and mudstones. This lower part also contains tuff and volcanoclastic

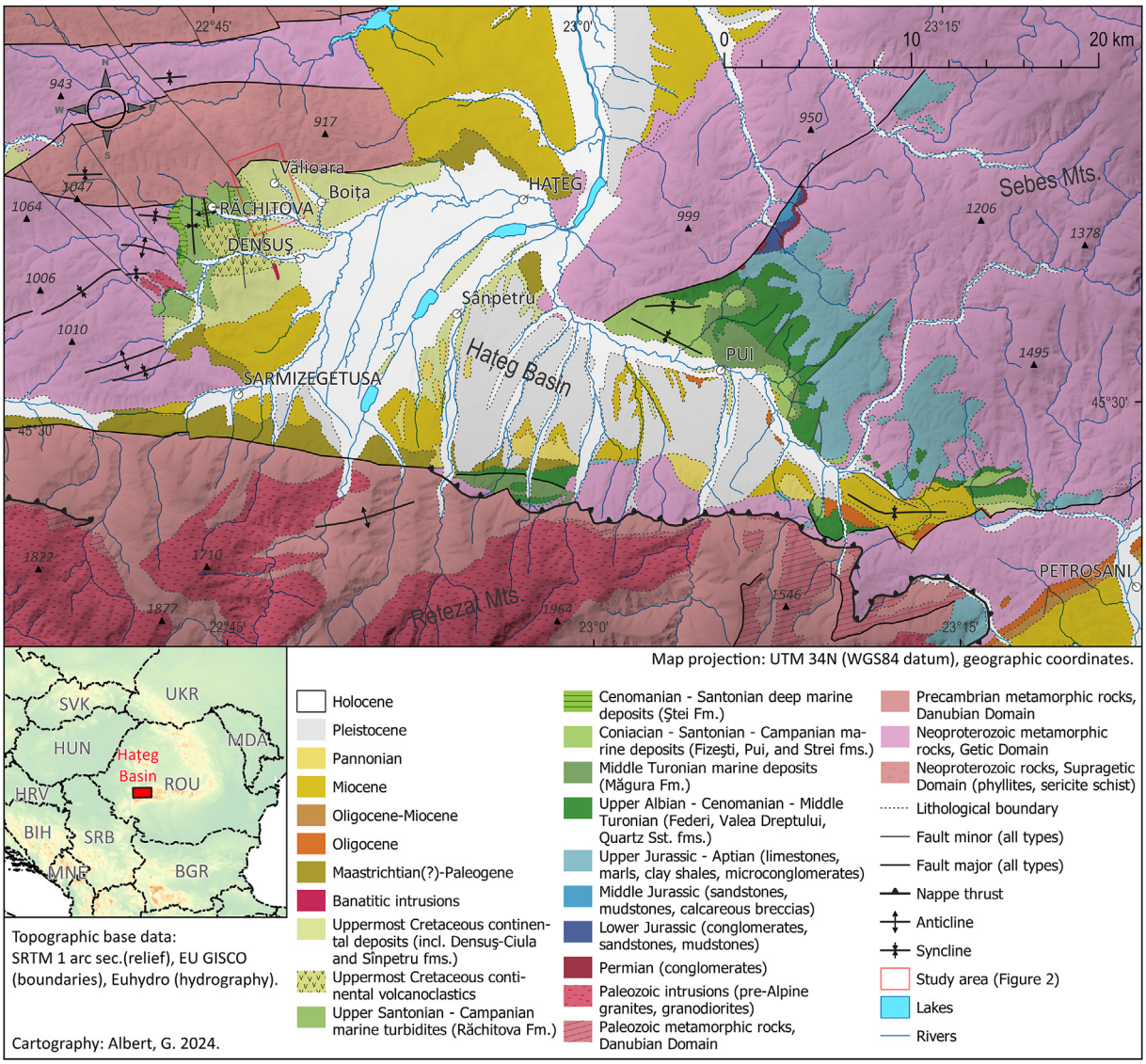

Fig. 1. Geologic map of Hațeg Basin redrawn after the 1:200,000 Geological Map of Romania and other sources (Grigorescu and Melinte, 2001; Melinte-Dobrinescu, 2010; Vasile et al., 2011; Melinte-Dobrinescu and Grigorescu, 2014; Csiki-Sava et al., 2016; Țabără and Slimani, 2019).

debris associated with pene-contemporaneous volcanic activity of the Banatitic Province, located to the west (e.g., Anastasiu and Csobuka, 1989). The middle part of the Densuș-Ciula Formation is composed of interfingering fluvial and proximal alluvial fan deposits, while its upper part also formed under dominantly alluvial conditions. The upper and, especially, middle parts of the unit yielded fossil remains previously assessed to be of early to late Maastrichtian age (e.g., Csiki-Sava et al., 2016).

The Sînpetru Formation and tentatively correlated units (see Csiki-Sava et al., 2016) crop out in the central-eastern part of the basin; these units are represented by thick and locally fossil-rich fluvial deposits (Csiki-Sava et al., 2016). The two fluvial systems that were active during the deposition of the two main units had different source areas (see details in Grigorescu, 1983; Van Itterbeeck et al., 2004; Bojar et al., 2010). The great thickness of these units suggests a rapidly deepening basin, filled up by huge amounts of deposits derived from the erosion of the uplifted Southern Carpathians nappe pile (Willingshofer et al., 2001). These Upper Cretaceous continental units are covered locally by Miocene and Quaternary sediments.

The uppermost Cretaceous continental deposits were previously thought to be largely undeformed or only slightly deformed and thus were assumed to be post-orogenic in nature (Mațenco and Schmid, 1999; Iancu et al., 2005). The main argument for their post-orogenic deposition was that the Densuș-Ciula Formation unconformably overlies some of the thrusts thought to be active during the regionally manifested Campanian to early Maastrichtian phase of the Alpine orogeny in the Southern Carpathians. Indeed, formerly two deformation phases were identified affecting the latest Cretaceous sedimentation and erosion within Hațeg Basin (Willingshofer et al., 2001): 1) a Campanian to early Maastrichtian phase, that created a piggy-back type basin which was filled up mainly by marine deposits, and 2) a late Maastrichtian phase, identified as “post-orogenic” collapse, dominated by extensional and transpressional stresses. The latter phase was considered to be responsible for the formation of the Maastrichtian continental units mentioned previously.

In the study area, the metamorphic units of Mesteacăn Range (eastern end of the Poiana-Ruscă Mountains) that bounds the basin from the northwest, and the Upper Cretaceous and younger sedimentary record of Hațeg Basin, respectively, are in tectonic contact.

The boundary fault was interpreted as either a normal fault (Lupu et al., 1993), or as a right-lateral fault (Bărzoi and Şeclăman, 2010).

3. Methods

The study area lies in the northwestern part of Haţeg Basin, near Vălioara (Fig. 1), and covers an area of about 10 km^2; its bounding coordinates in the UTM34N metric cartographic coordinate system are: easting min.: 637246, max.: 640526; northing min.: 5051150, max.: 5054426. Geological mapping and sedimentological survey of the outcrops was preceded by classification of multispectral remote sensing and topographic data, and by comparisons with the results of previous geological mappings. Field data acquisition was carried out using tablets and handheld GPS between autumn 2019 and summer 2023, and a geodatabase of 225 localities was created for the area (Albert et al., 2024). Detailed field investigations were completed by geospatial, diverse palaeontological, as well as sedimentological and geochronological analyses (see Supplementary information 1 and 2).

3.1. Geospatial data preparation

The preparation of the mapping stage included georeferencing of archive and recent maps, which was necessary to manage the data in a GIS framework. The archive material used included a manuscript map by Kadić (1916) that previously allowed the rediscovery of most of the fossil vertebrate sites he excavated over a century ago (Botfalvai et al., 2021). The maps, along with detailed satellite imagery data, were available in the field on tablets on which the freeware FieldMove program was run. The employed desktop GIS program was the freeware QGIS v3.24.1.

Preliminary geological maps were prepared from multispectral satellite images of the area using random forest classification (RFC) for sectors not or barely covered by vegetation. RFC is a machine-learning method based on decision trees and is particularly suited for classifying geological categories (Breiman, 2001; Cracknell and Reading, 2014). The satellite images were Sentinel 2A and B data from the snow-free winter of 2019, and they had already undergone atmospheric correction. These images have resolutions of 10, 20 and 60 m, and cover 13 spectral bands, those suitable for coverage and geological classification having higher resolutions (Drusch et al., 2012; van der Meer et al., 2014). Details of data preparation and methods of the RFC process are described in Supplementary information 1.

3.2. Mapping and site excavation

Since 2019, yearly excavations have been conducted in the wider Vălioara Valley area resulting in the discovery of hundreds of well-preserved vertebrate and invertebrate fossils that are housed and inventoried in the palaeontology collections of the University of Bucharest (e.g., Botfalvai et al., 2021; Magyar et al., 2024). Three of the fossiliferous sites examined (K2, Nvs and Fântânele-3) are remarkably rich in vertebrate remains, while other sites yielded only rather poorly preserved and sporadic vertebrate fossils (see Supplementary information 1). The vertebrate material is dominated by terrestrial taxa (e.g. dinosaurs), while bones from aquatic (e.g. fish) and semi-aquatic (e.g. turtles, crocodiles) organisms are subordinate.

Mapping was carried out in parallel with the palaeontological excavations. The aim was to refine and field-check the preliminary geological maps. This mapping was general in character, i.e., in addition to the documentation of the different sedimentary and volcanoclastic units, structural geological observations were also carried out. The terrain covered by the mapping has a sparse network of roads, with deep valleys and hillsides covered by dense vegetation alternating with more poorly vegetated ridges, whereas the studied units usually crop out within valleys and ravines.

3.3. Analyses of samples

In addition to the geological mapping and palaeontological prospections/excavations, samples were collected from seven sectors across the study area, in order to provide chronostratigraphic and palaeoenvironmental constraints on the investigated. These include six samples for zircon U–Pb geochronology, over 30 samples for palynological and marine micropalaeontological (calcareous nannofossils and foraminifera) investigations, as well as several microvertebrate sampling localities (see details in Supplementary information 1). Zircon U–Pb geochronology and marine micropalaeontology analyses are entirely novel for this area, whereas the palynological and microvertebrate investigations significantly expand the previous sparsely coverage (e.g. Antonescu et al., 1983; Grigorescu et al., 1999; Csiki et al., 2008; Botfalvai et al., 2021). Wherever possible, mapped successions were tightly correlated with microvertebrate, palynological, marine micropalaeontological, geochronological and/or palaeontological sampling, and often the same samples were used for multiple analyses (see Supplementary information 1). Although some of the samples were barren or quasi-barren micropalaeontologically, we nevertheless report these as well due to their palaeoenvironmental significance. Analytical methods, positions of the sampling spots, and brief interpretations of the investigations are summarised in Supplementary information 1, and their main implications are discussed below; raw measurement data from the geochronological analyses are provided in Supplementary information 2.

In interpreting and discussing the chronostratigraphic/geochronologic results of our analyses, we follow, and build upon, the (informal) subdivision scheme of the Campanian stage/age put forth by (Gradstein et al., 2020: p. 1040, Fig. 27.9) for Europe that – based on previous historical usage – recognizes two subdivisons, a relatively short (slightly less than 3 My) lower and a significantly longer (~9 Ma) upper substages, with the boundary between these being placed at roughly 81 Ma within the *G. elevata* biozone, also corresponding to the uppermost parts of the *Cataceramus balticus* biozone and the *Scaphites hippocrepis* III biozone, as well as to the base of the CC19 nannoplankton biozone, respectively. Moreover, to achieve an even better chronostratigraphic/age refinement for the studied deposits, we follow Bălc et al. (2024) in separating and using three quasi-equal subdivisions (termed its 'lower', 'middle', and 'upper' parts, respectively) of the lengthy upper Campanian, whereas employ the terms 'lower' and 'upper' to refer loosely to the first, respectively second halfs of both the shorter lower Campanian and the even shorter lower Maastrichtian (see Gradstein et al., 2020). We emphasize that all these subdivisions are not formalized; nevertheless, their usage have several practical advantages as they (1) permit a more finer-grained assessment of the chronostratigraphic position of the different geological, sedimentary and tectonic events identified in the study area, as well as (2) allow easy comparisons to the results of Bălc et al. (2024) derived from another part of the Haţeg Island using the same scheme, (3) can be tied directly to absolute ages and thus compared with our zircon U–Pb geochronometry data, and (4) can be correlated to a great extent to the different important bioevents tracked throughout the Campanian and Maastrichtian.

4. Results and sedimentological interpretation

Since the main local lithostratigraphic subdivision that is the focus of this report is represented by the uppermost Cretaceous continental sedimentary succession, i.e., the Densuş-Ciula

Formation, the different informal units observed and separated in the study area can be classified largely into those belonging to this formation, and those that are stratigraphically placed below it. Important geographical reference names, the different surveyed outcrops and local sections, and the informal lithostratigraphic units discussed in the following sections are mapped in Fig. 2. The directions referred to in the text are given within the currently existing frame of reference. Stereonet and rose diagrams of transport directions from different units, based on measurements of imbrication and forset lamination after aligning the tilted layers, are shown in Fig. 3.

4.1. Units underlying the Densuș-Ciula Formation

4.1.1. Metamorphic schists

An aggregate category of metamorphic rocks was separated as 'metamorphic schists' during the mapping. These form the 900 m high range of Mesteacăn Ridge in the northern part of the mapping area, and provide a significant proportion of the debris material found in the Vălioara Valley. These schists are metamorphosed Upper Proterozoic-Lower Paleozoic sedimentary and subordinately igneous rocks that have undergone moderate retrograde metamorphism (Maier and Lupu, 1979; Lupu et al., 1993). Although recognized in the field, detailed mapping of these rocks has not been a priority in the current palaeontology-sedimentology focused research.

Sericite schist is the main rock type present in the surveyed area. It also forms the bulk of the rock material in the debris. The most characteristic lithotype is a light greyish brown to greenish brown, fine-grained, shaly chloritic metamorphic rock, rich in muscovite mica (Fig. 4A). The schistosity data indicate that the axis of folding is roughly WSW-ENE striking, indicating a perpendicular compression direction. In some places the rocks are intensely folded. White to greyish-white quartzite vein remnants can be found in many places in the sericite schist clasts. As these features were not observed in situ, their orientation or size remains undocumented. White metacarbonates (marble, metadolomite) occurred only as debris elements, in places reaching cobble to boulder sizes of 30–40 cm. Older maps show that marble and dolomitic marble occur in thin layers in Mesteacăn Ridge adjacent to the mapped area (Maier and Lupu, 1979; Lupu et al., 1993).

The contact of the metamorphic schists with the Upper Cretaceous sedimentary rocks is tectonic, mostly observed parallel to Mesteacăn Ridge as a steep zone on its southern side. The exposure of the contact is very poor in the area, mainly marked only by the cataclastic breccia and red clayey fill of the tectonic zone; however, the fault scarp is also exposed on the hillside above the neighboring settlement of Boița, to the east of the mapped area.

4.1.2. Marine turbidites

The marine Upper Cretaceous crops out in the lower and middle reaches of Geat Valley, north of Ciula Mică settlement (Fig. 4B-D); their presence had been noticed previously by Vasile (2010), and is represented on the 1:50.000 geological map of the area, too (Lupu et al., 1993). On the later map, they are referred to the 'upper Campanian-lower Maastrichtian Pui Formation' and interpreted as dominantly distal flysch deposits. They are considered to be covered unconformably by andesitic tuff-bearing siliciclastic deposits of the 'Densuș Formation', corresponding to the Lower Member of the Densuș-Ciula Formation according to Grigorescu (1992) and Csiki-Sava et al. (2016), although Vasile (2010) remarked the tectonic nature of these formational contacts at least locally (see below).

These deposits are characterized by rhythmic alternations of 1–15 cm-thin layers of grey calcareous silt, clayey silt, and calcareous fine sandstone beds, usually tilted at a steep angle, occasionally overturned. Water escape structures are frequent, and flute marks were observed at the bases of sandstone beds (Fig. 4B) indicating an estimated NE-SW flow direction. This is consistent with previous observations that suggested an east-to-west sediment transport direction within these turbidites ('flysch') successions (Pop et al., 1972).

Fossil plant fragments were found at the base of many beds. On the western side of Geat Valley, in the Poitului Valley, conglomerate beds containing grey micritic limestone and large phyllite clasts are present. The thin-layered beds are sharply folded, sometimes with detachment planes and boudin-structures involved, and the larger clasts – probably from the conglomeratic layers – are preserved in the core of the folds (Fig. 4C-D). The folded nature of the sequence is also supported by alternating easterly and westerly dip directions with equally steep dips; however, the fold cores are rarely observed due to the dominantly strike-parallel outcrops. The strike of the axis planes of larger folds are NNW-SSE, while the smaller-magnitude folded structures have NW-SE striking axes. Some of the latter are probably slump folds.

A large number of sediment samples were collected from finer-grained, grey and dark grey turbidites; some of these samples are located close to tuffitic intercalations of the overlying continental unit (Unit 1.1.) that were sampled for zircon U–Pb geochronology (see below and Supplementary information 1), while others came from other outcropping areas of the turbidites.

We report here results for five samples studied for their palynological content and palynofacies, and for six samples investigated for calcareous nannofossils; four of these samples were also studied for foraminiferal assemblages (Supplementary information 1). All investigated samples were productive, but there were significant differences in diversity and preservation between the recovered fossil assemblages. The foraminiferal assemblages are better represented in samples LL16-1, LL16-2 and Geat AM (for detailes regarding the sampling sites and samples, see Supplementary information 1), with moderate-preserved specimens (Fig. 5) and relative abundances ranging from 12 to 16 individuals per gram. The recovered assemblages are remarkably similar in overall composition across the studied samples, and contain representatives of all three main groups: agglutinated taxa (amounting to 34 % in sample LL16-1, 29 % in sample LL16-2, respectively 37 % in sample Geat AM), as well as calcareous benthic (41 %, 43 %, respectively 32 %), and planktonic ones (25 %, 28 %, respectively 31 %). Agglutinated foraminifera are represented by tubular *Rhabdammina* sp. (Fig. 5.1), globular specimens of *Saccammina* sp. (Fig. 5.2), planoconvex trochospiral *Trochammina* sp. (Fig. 5.3), and flattened streptospiral *Paratrochamminoides* sp. (Fig. 5.4). Among the calcareous benthics, taxa such as *Cibicidoides*, *Brotzenella*, and *Laevidentalina* (Figs. 5.5-12) are the most abundant, whilst globotruncanids (Figs. 5. 13–15) dominate the planktonic foraminiferal assemblages. Nannoplankton assemblages were recovered from all analysed samples (Supplementary information 1), with 22 taxa recorded in sample Geat-2023, and 27 taxa, in sample LL17-ST2. The nannoplankton assemblages (Fig. 6) are largely homogenous across the samples. The most abundant species within the Geat Valley assemblage is by far *Watznaueria barnesiae* (53.59 % average relative abundance), followed by *Micula staurophora*, *Retecapsa crenulata*, *Prediscosphaera cretacea*, *Tranolithus orionatus*, and *Eiffellithus eximius* (average – 3.32 %). The high relative abundance of *Watznaueria barnesiae* indicates palaeoenvironmental conditions characterized by warm (Doeven, 1983; Gardin, 2002; Tantawy, 2003; Sheldon et al., 2010) and oligotrophic (Roth and Krumbach, 1986; Premoli Silvá et al., 1989; Roth, 1989; Watkins, 1989; Erba, 1992; Erba et al., 1992; Herrle et al., 2003; Thibault and Gardin, 2007; Chan et al., 2022) surface waters. These environmental indications can be supported

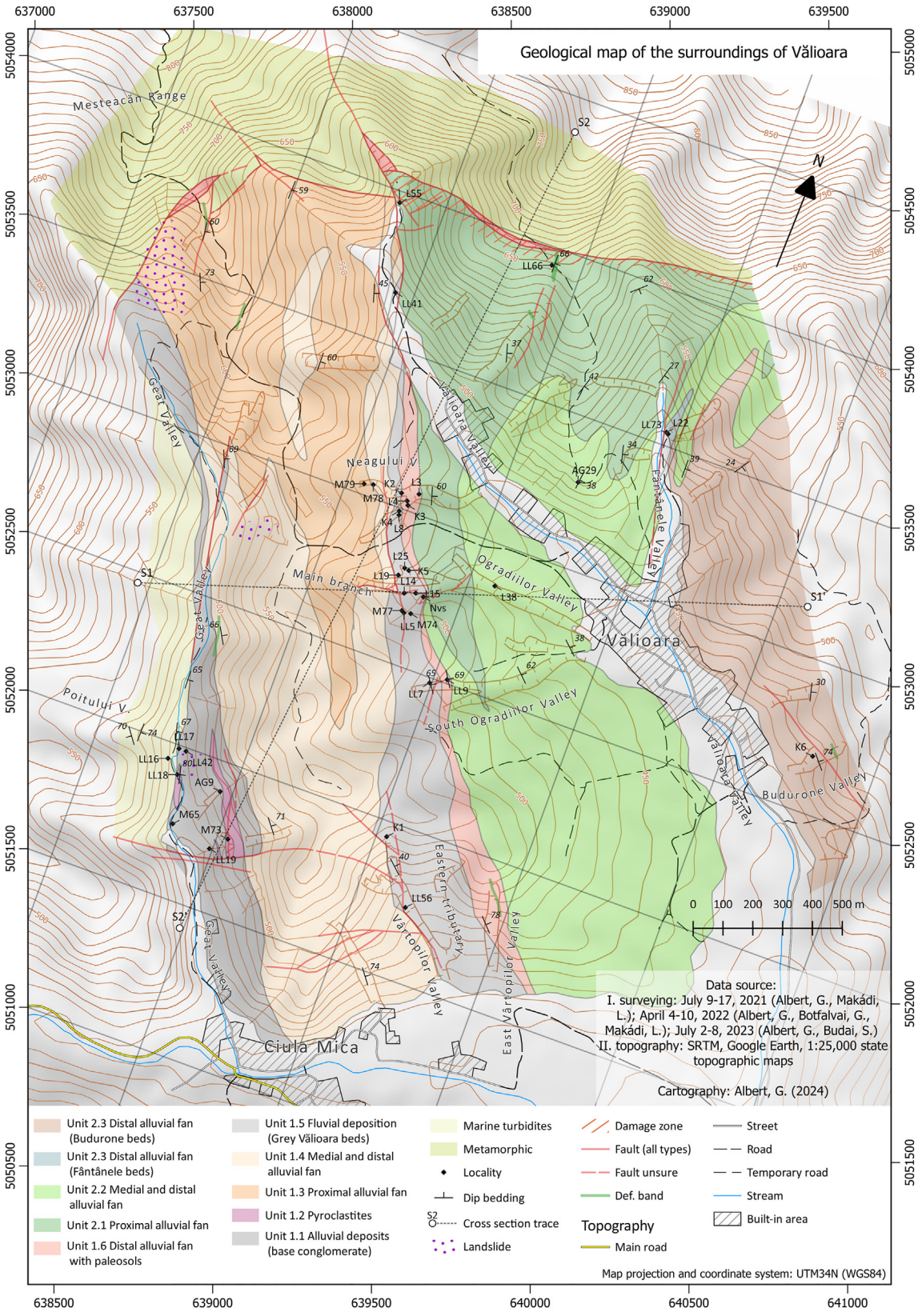

Fig. 2. Detailed geological map of the Vălioara study area, northwestern Hațeg Basin, showing the main depositional units and the locations of the surveyed/sampled sections discussed in the text.

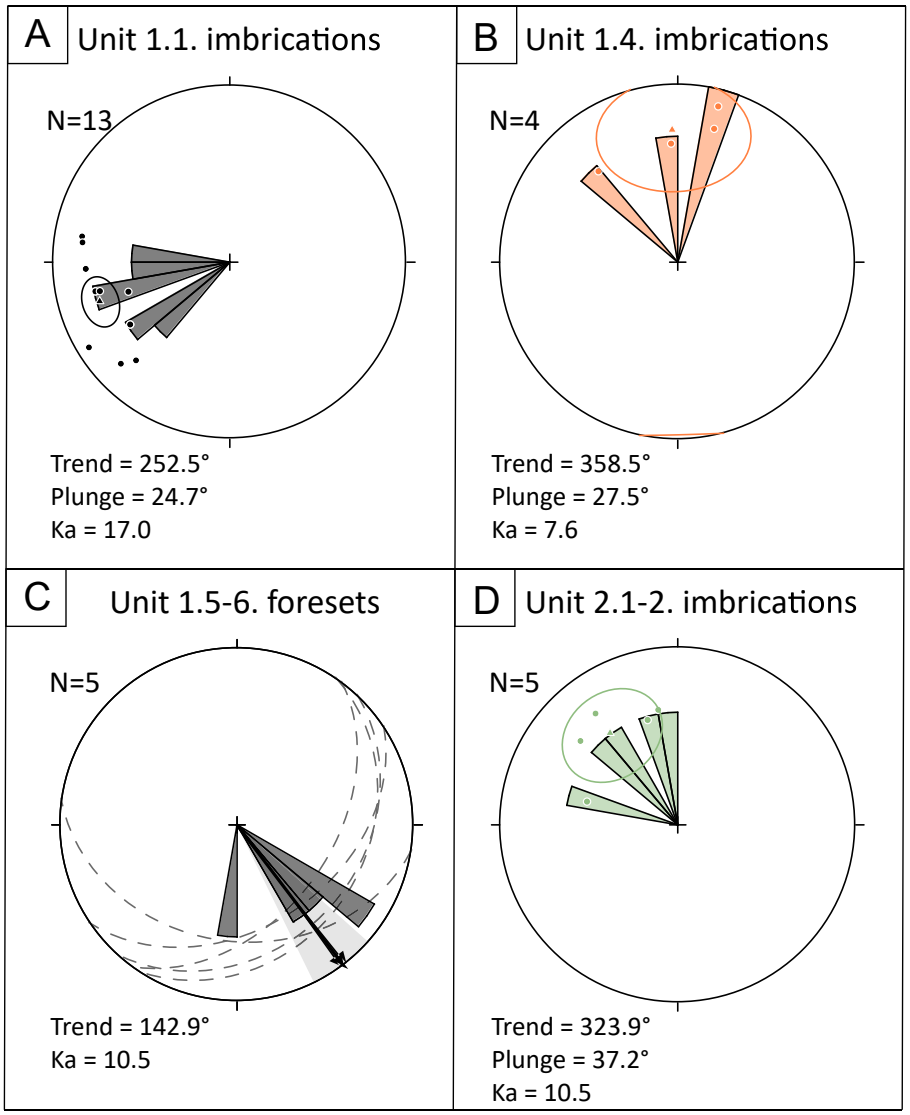

Fig. 3. Stereonet and rose diagrams of transport directions in the different depositional units, based on measurements of imbrication and foreset lamination after aligning the tilted beds. In the Equal area stereograms (southern hemispheric projection), imbrications measured as lineations are shown as dots, foresets measured as planes are shown as dashed lines. The 95 % confidence cone (α95) appears as an ellipse for points and as a range around the trend value for foresets; Ka is the Fischer concentration parameter (larger values indicate better concentrations of the measured directions). The rose diagrams show the direction of sediment supply area for the imbrications, and the sediment transport directions for the foresets. These are: A) Unit 1.1, base conglomerate = northeastward transport direction; B) Unit 1.4., conglo-breccia = southtward transport direction; C) Units 1.5 and 1.6. grey "Vălioara" & Red cyclic beds = southeastward transport direction; and D) Units 2.1 and 2.2., "upper" Vălioara breccia and green conglo-breccia = southeastward transport direction. Statistical values for mean directions are calculated from Fischer et al. (1987).

by the presence of double-keeled planktonic foraminifera which were reported from oligotrophic and warm conditions (Petrizzo, 2002; Abramovich et al., 2003, 2010). At the sea-floor, oxygenated waters are indicated by the presence of the epifaunal *Cibicidoides* and *Brotzenella*, considered as oxic indicators by Kaiho (1994), Kaiho and Hasegawa (1994), Murray (1991, 2006), Kranner et al. (2022), and Amaglio et al. (2023).

Sample LL16-1 yielded the richest and most diversified palynological assemblage, including a mix of both marine (dinoflagellates) and continental (spores, pollen) taxa (Supplementary information 1). Among the marine palynomorphs, the biostratigraphically most significant occurrences are those of *Isabelidinium microarmum bicavatum* (Fig. 7.1), *Odontochitina costata* (Fig. 7.2), and *Dinogymnium longicorne* (Fig. 7.3), while the continental palynomorph assemblage is marginally dominated by fern spores (41 % of the assemblage, with taxa such as *Vadaszisporites sacali*, Fig. 7.4; *Deltoidospora toralis*), besides those of gymnosperms (38 %; e.g. *Balmeiopsis limbatus*, Fig. 7.5) and angiosperms (e.g., *Hungaropollis* sp., Fig. 7.6; *Plicatopollis plicatus*, Fig. 7.7); remarkably, foraminiferal test linings were also recorded in the palynological slides. Both palynological assemblages and the identified palynofacies (kerogen predominantly made up of brown/opaque phytoclasts that are small-sized and rounded - Fig. 7.8; dominance of terrestrial palynomorphs over the marine ones) indicate a distal basinal depositional setting with relatively deep waters, with a prolonged transport of the continental-derived organic particles due to the activity of turbidity currents (Carvalho et al., 2013). Other samples (e.g. sample LL17-ST2; see Supplementary information 1) were less abundant in palynological remains, yielding only very rare spores (e.g., *Polypodiaceoisporites* sp.).

Although most of the microfossil taxa recovered (calcareous nannoplankton, foraminifera and palynological assemblages) are not age-diagnostic, they nevertheless constrain the age of their host deposits. The first occurrence of the calcareous nannoplankton

Fig. 4. Outcrop views of the metamorphic schists (A) and the turbidites (B–D). The latter show sole marks at the base of steeply dipping beds (B), boudin structures (C) and sharp folds (D) affecting the sandy turbidite layers. Hammer for scale.

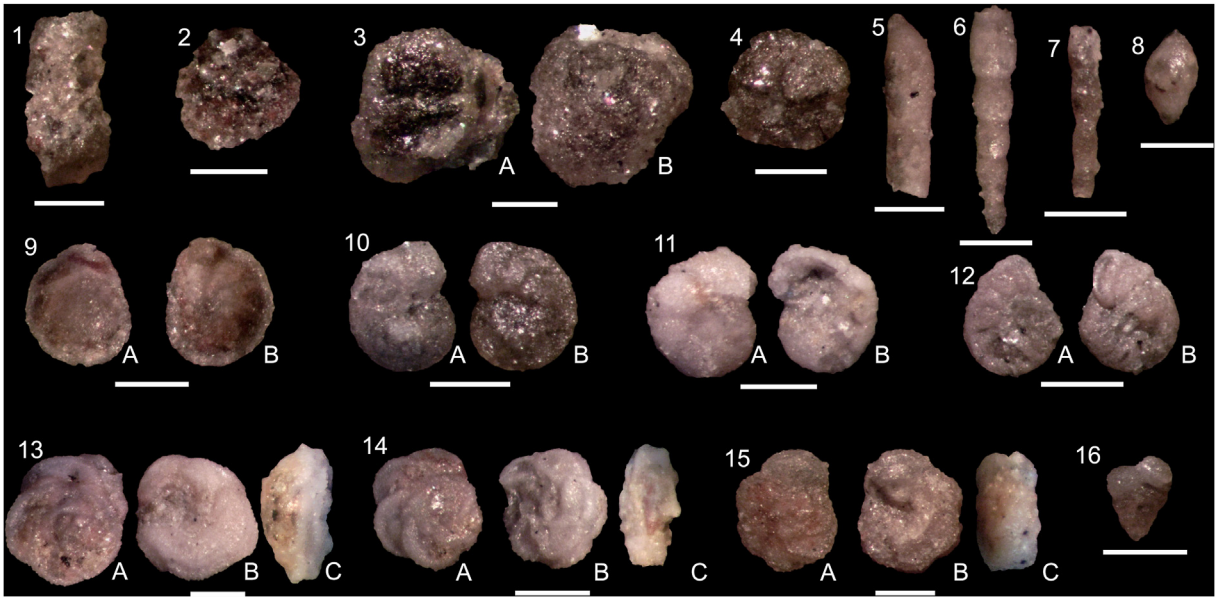

Fig. 5. Significant foraminifera taxa identified in the Geat Valley – Vălioara samples: 1. *Rhabdammina* sp. (sample LL16-1). 2. *Saccammina* sp. (sample LL16-1). 3. *Trochammina wickendeni* (sample LL16-1). 4. *Paratrochamminoides deformis* (sample LL16-1). 5. *Laevidentalina gracilis* (sample LL16-1). 6. *Siphonodosaria* sp. (sample LL16-1). 7. *Chrysalogonium polystomum* (sample LL16-1). 8. *Ellipsoglandulina velascoensis* (sample LL16-2). 9. *Globorotalites* sp. (sample LL16-1). 10. *Cibicidoides voltzianus* (sample LL16-1). 11. *Brotzenella monterelensis* (sample LL16-2). 12. *Brotzenella* sp. (sample LL16-1) 13. *Contusotruncana morozovae* (sample LL16-2). 14. *Globotruncana* sp. (sample LL16-2). 15. *Globotruncana* sp. (sample LL16-1). 16. *Planoheterohelix* sp. (sample LL16-2). Scale bars = 250 μm.

species *Broinsonia parca parca*, was originally described at the base of CC18 Biozone (Perch-Nielsen, 1985) or of the UC14a Subzone (Burnett, 1998), which was initially correlated with the lower part of the lower Campanian. However, a more recent study (Miniati et al., 2020) placed the base of CC18 Biozone in the upper Santonian, within the upper part of Chron C34n. This, combined with the presence of *Eiffellithus eximius*, with it last occurrence in the top of CC22 Biozone (middle part of upper Campanian; Perch-Nielsen, 1985; Gradstein et al., 2020), restricts the age of the marine turbidites to the latest Santonian to early part of late Campanian time interval. Even though foraminifera do not include index taxa in their composition, the correlation between the calcareous nannoplankton to the planktonic foraminifera, could likely indicate the placement in the *Globotruncanita elevata* biozone (79.33–83.65 Ma - Petrizzo et al., 2011; Gradstein et al., 2020; Miniati et al., 2020) which corresponds to the *Globotruncana arca* biozone (Peryt et al., 2022). Finally, the conclusive palynological assemblage identified in sample LL16-1 points to an early Campanian–early late Campanian age (Góczán and Siegl-Farkas, 1990; Williams et al., 2004; Ţabără and Slimani, 2019; Slimani et al., 2021). More specifically,

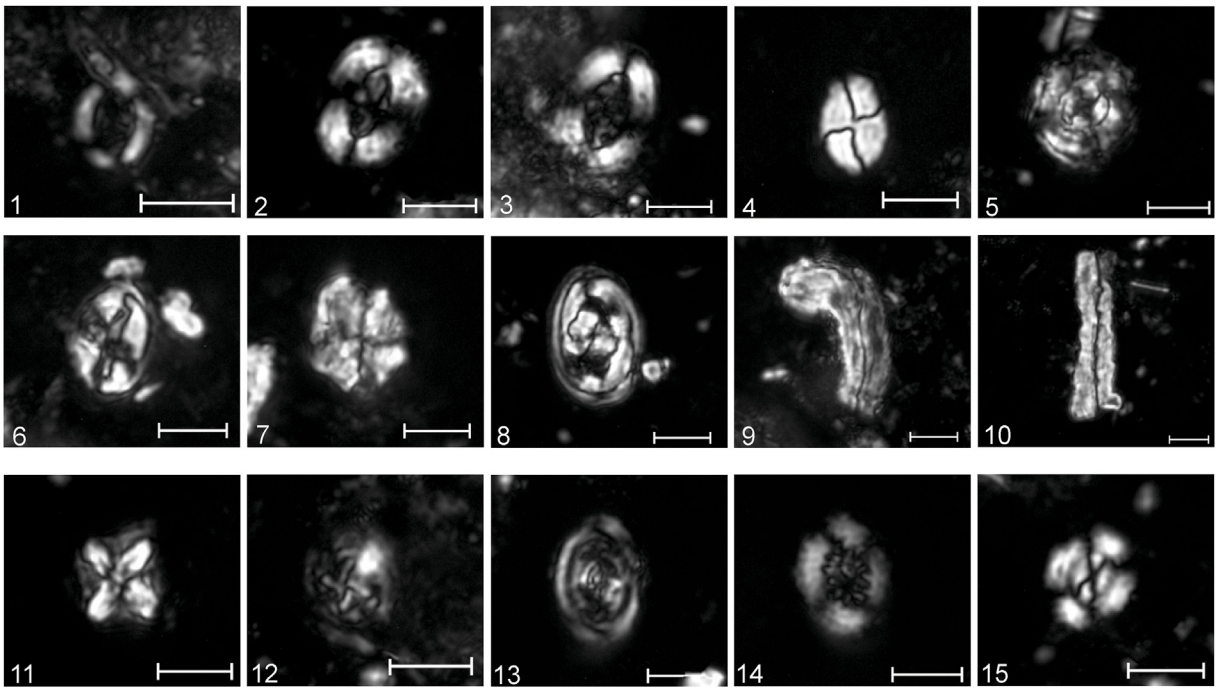

Fig. 6. Selected calcareous nannoplankton taxa identified in the Geat Valley – Vălioara samples: *Arkhangelskiella cymbiformis* (sample LL16 - 2). 2–3. *Broinsonia parca parca* (2 - sample LL16-1, 3 – LL16-2). 4. *Calculites obscurus* (sample LL16-2). 5. *Cylindralithus sculptus* (sample LL16-2). 6. *Eiffellithus eximius* (sample LL16-2). 7. *Eprolithus floralis* (sample LL16-2). 8. *Gorkaea pseudanthophorus* (sample LL16-1). 9. *Lucianorhabdus arcuatus* (sample LL16-2). 10. *Lucianorhabdus maleformis* (sample LL16-1). 11. *Micula staurophora* (sample LL16 - 1). 12. *Prediscosphaera cretacea* (sample LL16-2). 13. *Reinhardtites anthophorus* (sample LL16-2). 14. *Retecapsa crenulata* (sample LL16-2). 15. *Watznaueria barnesiae* (sample LL16-1). Scale bars = 5 μm.

the occurrence of *Isabelidinium microarmum bicavatum*, together with the overall lithology of the turbidite deposits cropping out along Geat Valley, invites correlation with the Upper Member of the Răchitova Formation from the Densuș area (Ţabără and Slimani, 2019), a 500–700 m thick marine unit with its type locality located 2 km to the west from our Geat-Vălioara mapping area (Grigorescu and Melinte, 2001; Melinte-Dobrinescu, 2010; Ţabără and Slimani, 2019).

Based on the integrated biostratigraphic evidence currently available from the turbidite deposits cropping out along Geat Valley, their age can be reliably constrained to the late early to early late Campanian, further supporting the previously suggested correlation with the Upper Member of the Răchitova Formation for which a similar age had been assessed previously by Ţ; abără and Slimani (2019).

4.2. Sequence and depositional setting of the continental beds

During the geological mapping and sedimentological investigation, the studied bone-bearing continental sedimentary deposits were categorised into fifteen facies types based on their macroscopic properties (Table 1). Furthermore, facies associations – representing distinct depositional environments – were also established (Table 2) based on recurrent joint occurrences of sets of these facies types and their relative participations, as observed in the field. The relative proportions of the identified facies associations vary both vertically and laterally in the studied area, and, considering their relative contribution ratios throughout the studied sections, informal depositional units were defined, representing distinct stages of basin evolution.

According to our investigations, the lower part of the continental Densuș-Ciula Formation (Grigorescu, 1992) cropping out in the Vălioara area is built up by a wide range of facies from muddy deposits to coarse gravels (Table 1), forming four distinct facies associations (FA 1–4; Table 2). The different facies associations are dominated by different grain sizes but all of them contain gravelly or sandy material that potentially originated from the currently still exposed metamorphic basement to the northwest (Table 1). Facies association 1 is dominated by matrix-supported gravels (facies Gms) that contain pebble to cobble sized clasts, forming beds of debrisflows (Nemec and Steel, 1984), up to several meters thick; the thickness of the beds tends to increase in the vicinity of the mapped basin bounding fault (Table 2). Finer-grained, muddy sediments with pedogenic features (Ptc) and sand and gravel clasts (Fs, Fsg), belonging to FA 3, represent the most prevalent deposits of the studied succession and they become dominant towards the basin centre (Fig. 2). Intervals dominated by this facies assocation can attain thicknesses up to 3–4 m (Fig. 9B; Table 2). These muddy and gravelly deposits are occasionally interbedded with 10 cm to 1.5 m thick channelised bodies filled up by sandy deposits (Sm, Smg) frequently showing cross-stratification (Sx, Sxg) and fining upward trends (FA 2; Fig. 9B-C, Table 2). The fourth facies association was only observed at one locality but is highly significant palaeontologically. It is composed of vertically stacked coarsening upward cycles, covering 8 m in total thickness, from dark mudstone (Fm) through sandy-siltstone (Fs), rich in plant fragments and molluscs to sandstone (Sm) (Fig. 9B).

Given the interpretations of the distinct facies and facies associations, the bone-bearing uppermost Cretaceous continental sediments from the Vălioara area are assessed to had been deposited in an alluvial fan environment (Nemec and Steel, 1984; Blair and McPherson, 1994; Blair, 1999; Fidolini et al., 2013; Gao et al., 2020), where FA 1 represents the proximal alluvial fan sector dominantly built up by debris-flow events while FA 3 is interpreted as distal, fine grained, floodplain deposits (Wright and Tucker, 1991; Wright and Marriott, 1996; Bojar et al., 2005;

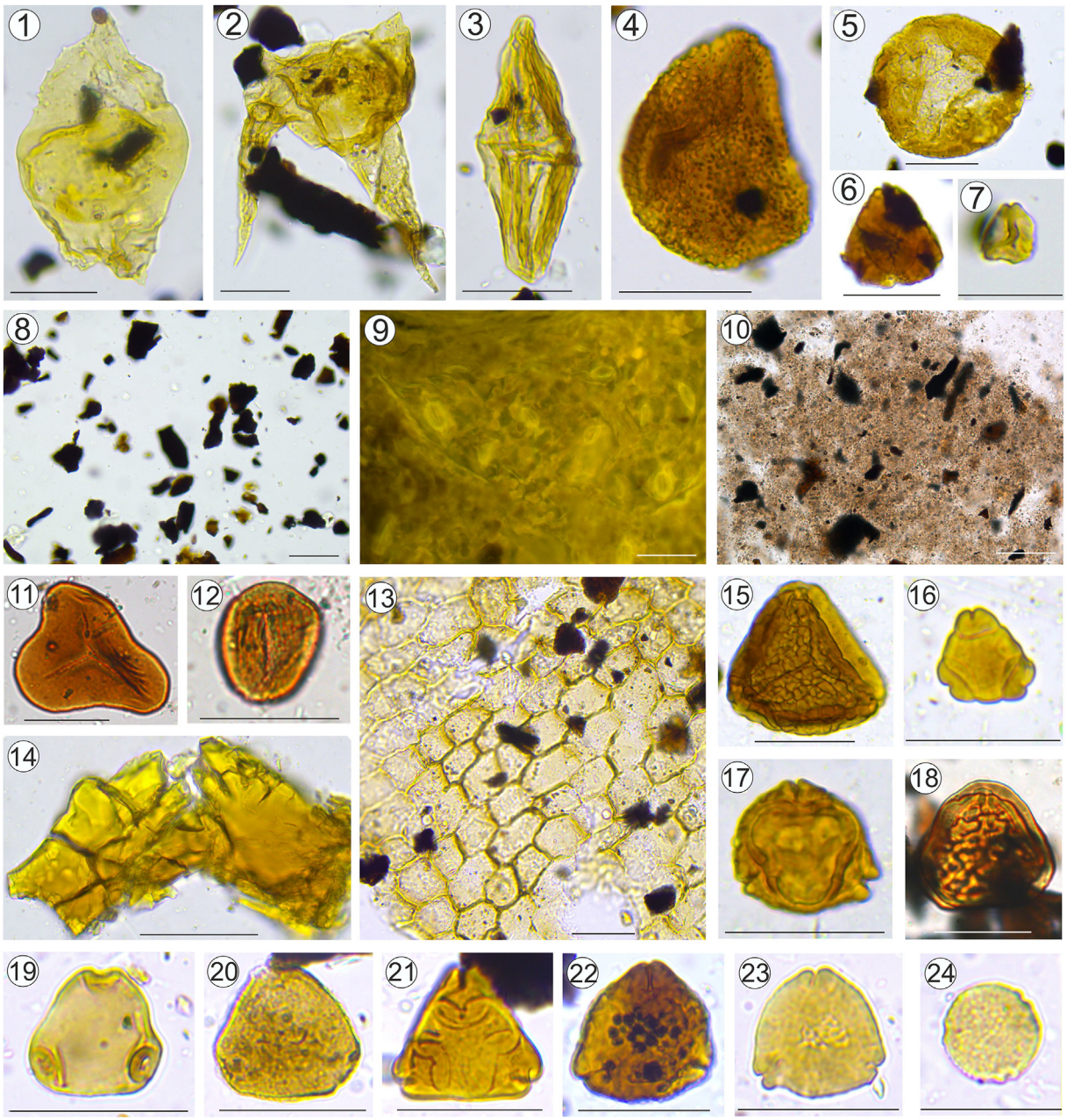

Fig. 7. Marine and terrestrial palynomorphs, as well as various palynofacies types recognized within the Upper Cretaceous deposits from the study area (all from unoxidized residues; scale bar: 30 μm). 1. *Isabelidinium microarmum bicavatum* (sample LL16-1); 2. *Odontochitina costata* (sample LL16-1); 3. *Dinogymnium longicorne* (sample LL16-1); 4. *Vadaszisporites sacali* (sample LL16-1); 5. *Balmeiopsis limbatus* (sample LL16-1); 6. *Hungaropollis* sp. (sample LL16-1); 7. *Plicatopollis plicatus* (sample LL16-1); 8. small and equi-dimensional opaque/brown phytoclasts of continental origin (sample LL16-1); 9. large cuticle fragment with stomata (incident blue light, fluorescence; sample LL17-ST3); 10. granular amorphous organic matter of marine origin mixed with opaque phytoclasts (sample 5B); 11. *Deltoidospora australis* (sample 8B); 12. *Classopollis* sp. (sample P292); 13. large fragment of cuticle (sample P425); 14. fossil resin (sample LL5-15-3); 15. *Polypodiaceoisporites hojrupensis* (sample LL5-15-3); 16. *Suemegipollis triangularis* (sample LL5-15-3); 17. *Trudopollis capsula* (sample LL5-15-3); 18. *Polypodiaceoisporites* sp. (sample 6B); 19. *Proteacidites* sp. (sample P425); 20. *Proteacidites scaboratus* (sample P425); 21. *Trudopollis conrector* (sample P425); 22. *Krutzschipollis crassis* (sample P425); 23. *Pseudopapillopollis praesubhercynicus* (sample P425); 24. *Subtriporopollenites constans* (sample P425).

Therrien, 2005). Aside these two dominant facies associations, channelised sandy-gravelly (FA 2) deposits representing fluvial channels (Therrien, 2006) and muddy-sandy heterolithics (FA 4) interpreted as floodplain lake deposits were also identified (Plint et al., 2023) (Table 2). Fluvial channel deposits are usually isolated and characterised by a simple upward fining trend from gravel-lags followed by structureless sands and occasionally capped by muddy deposits (Fig. 9B-C), a succession that points towards ephemeral braided streams, formed during flooding events, which further suggests an alluvial fan environment (Ridgway and Decelles, 1993; Blair and McPherson, 1994; Therrien, 2006; Fidolini et al., 2013; Ezquerro et al., 2019; Gao et al., 2020). These two latter facies associations are less common, but they contain the most important fossil accummulations (i.e., K2, Fântânele-3, Nvs sites; see Supplementary information 1 and Botfalvai et al., 2021). In addition, volcaniclastic-pyroclastic layers are locally interbedded within the continental sediments (Fig. 9A). Sedimentological characteristics of the individual facies and FAs display different trends in their spatial distribution that will be discussed on the following section.

Table 1
Lithofacies and their characteristics separated in the lower Densuș-Ciula Formation (uppermost Cretaceous) from the Geat Valley – Vălioara area.

Code	Lithofacies	Description	Sedimentary structures	Thickness	Fossils	Occurrence	Interpretation
Gcs	Clast-supported conglomerate	Clast-supported structureless pebble to cobble gravel. Matrix is composed of sand.	Structureless	10–50 cm	Absent	FA1, FA2	Tractional deposition on gravel bars in braided fluvial channels (e.g., Nemec and Steel, 1984; Miall, 2006; Lunt et al., 2004).
Gms	Matrix supported gravel	Matrix-supported, structureless pebble to cobble gravel. Beds are characterized by sharp non-erosional basal boundary. Beds are tabular or occasionally wedge shaped. The facies is poorly sorted, the matrix is composed of clayey, coarse to very coarse sand. Shape of the gravel clasts is angular to rounded (conglomerates), with particular sections dominated by angular clasts forming breccias. Matrix occasionally composed entirely of volcanoclastic material.	Structureless	0.15–2 m	Absent	FA1, FA2	Deposition from subaerial debris flows. (e.g., Nemec and Steel, 1984).
Gt	Gravelly channel lag deposits	Thin gravelly (granules to pebbles) deposits overlying erosional surfaces.	Structureless	1–5 cm	Absent	FA2	Channel lag deposit (Soltan and Mountney, 2016).
Gx	Cross-stratified gravel	Matrix- to clast supported granule to cobble gravel deposits showing crude trough cross-stratification. Matrix is composed of medium to very coarse-grained sand. Gravel clasts are angular to sub-rounded. Usually deposited onto erosional surfaces.	Trough-cross stratification	0.1–0.5 m	Absent	FA2	Tractional deposition on gravel bars in braided fluvial channels (Lunt et al., 2004).
Smg	Structureless gravelly sand	Structureless medium to very coarse sandstone containing granule to pebble sized gravel clasts. Frequently contains more than one sand fraction. Gravel clasts are angular to sub-rounded. The facies is frequently underlain by facies Gt or deposited directly onto erosional surfaces. Occasionally characterized by normal grading (i.e. gravel content decreasing upwards).	Structureless	0.1–1.5 m	Vertebrate fossils are very common in some cases (e.g. site NVS)	FA2	Indicate rapid deposition during flood events (Miall, 2006; Leeder, 1999).
Sxg	Cross-stratified gravelly sand	Coarse to very coarse sand containing varying amounts of angular to sub-rounded granule to pebble sized gravel clasts. The facies shows trough cross stratification. Usually characterized by an erosional lower boundary. Beds of the facies occasionally characterized by normal grading (i.e. gravel content decreasing upwards).	Trough-cross stratification	0.1–0.5 m	Absent	FA2	Tractional deposition on 3D sandy bedforms in braided fluvial channels (Miall, 2006; Soltan and Mountney, 2016).
Sm	Structureless sand	Coarse to fine grained sand, frequently deposited upon facies Smg and overlain by Fs facies.	Structureless	0.05–1.5 m	Absent	FA2, FA4	Rapid deposition during flooding events (Miall, 2006; Leeder, 1999).
Sx	Cross-stratified sand	Medium to very coarse sand showing trough cross stratification.	Trough-cross stratification	0.5–1 m	Absent	FA2	Tractional deposition on 3D sandy bedforms in braided fluvial channels (Miall, 2006; Soltan and Mountney, 2016).
Sl	Laminated sand	Fine to medium grained sand showing planar parallel lamination.	Planar-parallel lamination	0.05 –0.15 m	Rare plant fragments	FA2, FA4	Upper flow regime conditions on top of fluvial channels and shallow lacustrine deposits (crevasse delta) (Miall, 2006; Plint et al., 2023).
Fl	Finely laminated mudstone	Greyish to blackish coloured mudstone.	Lamination, sharp and non-erosive base, tabular units	0.5 m	Abundant to rare plant debris, and vertebrate fragments	FA4	Deposition from suspension settling under quiet lacustrine conditions (Fielding, 1984; Plint et al., 2023).

(*continued on next page*)

Table 1 (*continued*)

Code	Lithofacies	Description	Sedimentary structures	Thickness	Fossils	Occurrence	Interpretation
Fm	Massive mudstone and claystone	Light-grey or bluish grey mudstone and claystone.	Bioturbation, sharp and non-erosive base, common sediment deformation, tabular units	0.5–1 m	Rare plant debris and molluscs fragments	FA3, FA4	Deposition from suspension settling in standing water environment: Slackwater deposition in fluvial channel fills (FA3), under quiet lacustrine conditions (FA4) (Fielding, 1984; Plint et al., 2023).
Fs	Sandy siltstone	Massive or poorly-stratified dark grey siltstone, commonly interbedded with facies Sm.	Vertical burrows and root traces, sharp and non-erosive base, tabular units	0.5 m	Abundant molluscs, plant and vertebrate fossils	FA4	Tractional deposition of siltstone and sandstone in proximal lacustrine environment during fluvial input. Heterogeneity most likely linked to reworking through bioturbation (Jeffrey et al., 2011; Plint et al., 2023).
Fsg	Reddish sandy-gravelly mudstone	Unstratified reddish sandy-gravelly mudstone, interbedded with facies Gms.	Vertical burrows and root traces, irregular units with variable thickness	0.5–5 m	Absent	FA1, FA2, FA3	Deposited by mudflows or indicates overbank deposition of fluvial fines.
Pt	Reddish mudstone	Reddish mudstone and subordinate very fine-grained sandstone with mottles variable in colour (green, strong brown and grey).	Pedogenic features: Sporadic burial-gley, root-mottles, tiny irregular root traces, vertical burrow fills	0.5–2 m	Rare fragmentary vertebrate fossils	FA3	Moderately- or well-developed palaeosol (Bojar et al., 2005; Therrien, 2005, 2006).
Ptc	Reddish mudstone with calcareous concentrations	Red to brown mudstone with pale yellow carbonate nodules (calcrete). The calcareous concentrations show variable degrees of development, from isolated spherical concretions to thick continuous layers.	Pedogenic features: Discontinuous calcrete horizons, vertical burrows and root traces	0.5–2 m	Rare fragmentary vertebrate fossils	FA3	Well-developed palaeosol (Wright and Tucker, 1991).

Table 2
Facies associations (FA) separated in the lower Densuș-Ciula Formation (uppermost Cretaceous) from the Geat Valley – Vălioara area, and their characteristics.

Facies association	Facies (**primary**, secondary)	Description	Interpretation
FA1 – Proximal alluvial fan deposits	**Gms,** Gcs, Smg, Sxg, Fsg, Fs	Dominated by up to 2 m thick wedge- or tabular-shaped beds representing facies Gms, separated by thinner beds of facies Fsg. Grains are composed of material identical to the outcropping metamorphic bedrock. Channelized sandy-gravelly deposits (Sxg, Smg) also occur between beds of the above-mentioned facies.	The FA represents the proximal reaches of alluvial fans dominated by debrisflow events transporting material from the adjacent catchment area (Nemec and Steel, 1984; Blair and McPherson, 1994; Blair, 1999; Ezquerro et al., 2019; Gao et al., 2020). Interbedded muddy facies represents mudflows or periods of low-rate deposition.
FA2 – Fluvial channel deposits	**Smg**, **Sxg**, **Sm**, **Sx**, **Gt**, Gcs, Fm	Built up by 0.1 m–1.5 m thick, 0.3 m–10 m wide erosionally bounded channelised bodies. Infill of the sedimentary bodies is composed of thin gravelly facies (Gt) followed by structureless (Smg, Sm) or through cross-stratified (Sxg, Sx) sand or gravelly sand. Occasionally the vertical sequence is closed by grey muddy interval (Fm). Channel bodies are usually isolated within red mudstone facies (Fs) or less frequently form up to 3.5 m thick stacked sequences.	The FA is interpreted as the record of fluvial deposition within the alluvial-fan system. The usually structureless infill of the channel bodies, their isolated nature and occasional muddy capping interval point towards ephemeral braided streams (Cant and Walker, 1978; Bull, 1997; Therrien, 2006; Long, 2006, 2011).
FA3 – Floodplain deposits	**Pt**, **Ptc**,**Fm**, **Fs**, **Fsg**. Smg, Sm	Built up by pedogenetically modified, dominantly red-coloured mudstones with frequent calcareous concentrations and horizons, vertical roots and burrows. Attains up to 3–4 m in thickness. Sand and gravel grains are frequent. Infrequently the Fm and Fs facies beds are characterized by grey colours.	The FA represents floodplain deposits characterized by low water table based on the presence of pedogenic features (Wright and Tucker, 1991; Wright and Marriott, 1996; Bojar et al., 2005; Therrien, 2005, 2006). Calcrete levels indicate soil horizons. Grey mudstones indicate poorly drained areas on the floodplain.
FA4 – Floodplain lake deposits	**Fl**, **Fm**, **Fs**, **Sm**	In its sole outcrop this FA is built up by coarsening upward cycles (8 m in total) from dark mudstone (Fm) through sandy siltstone (Fs) to sandstone (Sm). Unlike FA3, the mudstones lack both sand or gravel grains and carbonate-rich horizons. Sandy siltstones are rich in plant fragments, freshwater molluscs and vertebrate fossils.	The FA represents quiet conditions located farther from the main sediment influx and a less oxidizing environment (Plint et al., 2023). Interpreted as floodplain lake environment in which coarse material accumulated during flooding events (Jeffrey et al., 2011; Montgomery and Barnes, 2012; Flaig et al., 2014).

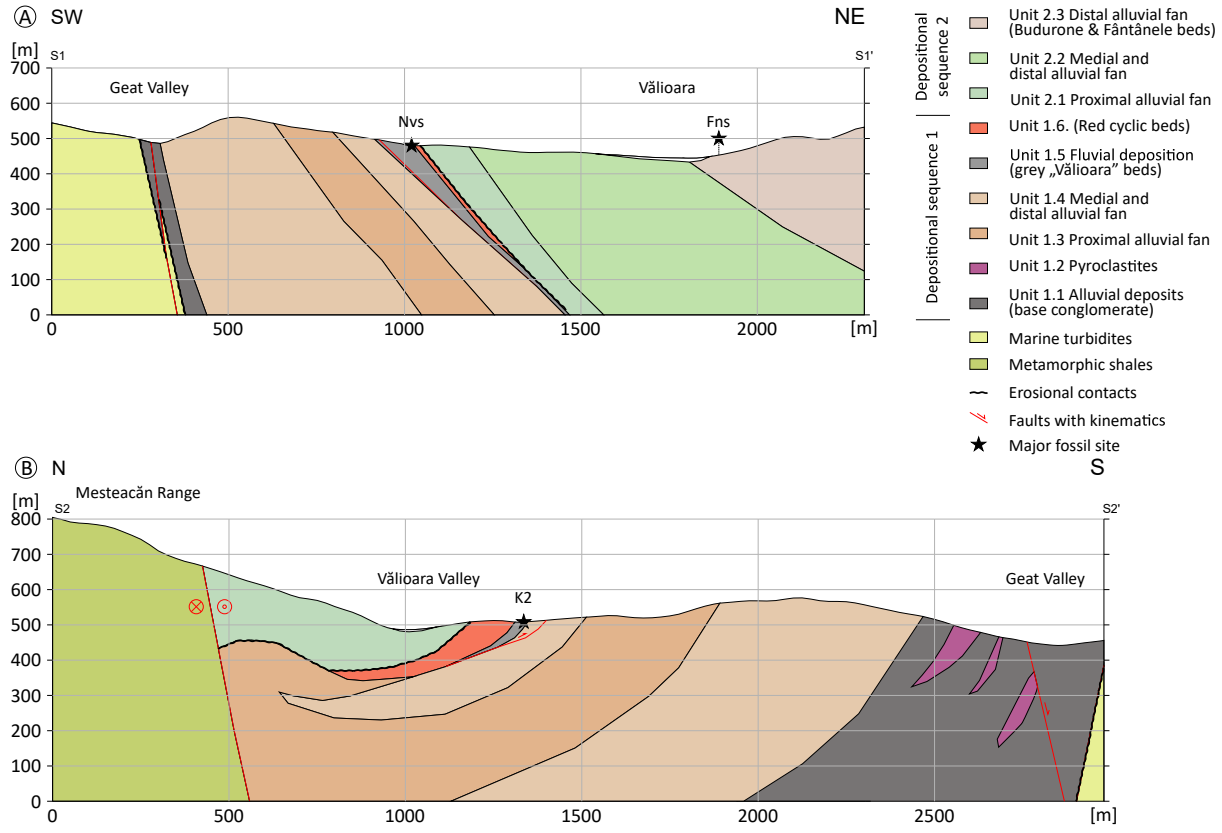

Fig. 8. General cross sections of the mapped area. Section (A) shows the decreasing eastward dip of the strata, while section (B) shows the basin-boundary fault and the relationship between the metamorphic schists and the Upper Cretaceous sedimentary strata. In (B), the apparent thickness of the strata is increased as the section is in strike direction. The tracelines of the sections are indicated on Fig. 2.

The four facies associations (Table 2) are interfingering in both vertical and lateral directions, documenting spatial and temporal changes in basin evolution. However, the exact vertical and lateral extent of the facies associations is difficult to estimate due to the relatively small size of the available outcrops and the extensive vegetation cover, coupled with the generally steep dip angles of the beds. Based on spatial patterns identified in the proportional representation of the distinct FAs, the studied continental basin fill succession of the lower Densuș-Ciula Formation from the Vălioara area can be subdivided into 9, stratigraphically successively superposed and/or laterally interfigered informal depositional/lithostratigraphic units (corresponding to distinct subenvironments; Fig. 9A), that represent the basis for our geological mapping (Fig. 2). Each of the nine units is usually dominated by one or two facies associations but tends to contain deposits from multiple FAs. The succession of the identified depositional units building up the studied uppermost Cretaceous continental basin fill can be divided into two larger scale units encompassing, vertically superimposed fining upward intervals, each of which displays an upward increase in the proportion of FA 2 and 3 deposits in tandem with the decrease in the prevalence of FA 1 deposits (Fig. 9). The lower fining-upward sequence contains the first six depositional units, including volcanoclastic-pyroclastic deposits as well, while the second sequence is built up by the remaining, upper three units.

4.2.1. Description of the continental depositional units

4.2.1.1. Depositional sequence 1. As noted, the first sequence consists of Units 1 to 6, and represents the lower ~1000m of the local continental succession. It starts with dominantly coarse-grained deposits overlying the marine turbidite beds (Fig. 9) and mostly representing FA 1; these correspond to mass flow-dominated proximal alluvial fan deposition (Units 1.1–1.4; see below) (Table 2 and Fig. 9A). These coarser deposits transition both downdip and vertically to finer grained mudstones and sandstone containing dinosaur remains, belonging to Units 1.5 and 1.6 that are built up mostly by FAs 2, 3 and 4. Meanwhile, deposits remain dominated by FA 1 throughout the whole sequence in the proximity of the basin bounding fault (Figs. 2 and 8).

4.2.2. Unit 1.1– alluvial deposits– base conglomerate

The unit is dominated by poorly sorted Gms and Gcs facies (Table 1) of the coarse FA 1 facies association, with a matrix of grey coarse-grained sand (Fig. 10). The colour of both the clasts and the matrix gives these deposits a distinctive grey colour. It crops out mainly along Geat Valley. The conglomerate clasts are rarely flattened but well-rounded grey meta-sandstones, quartzites, phyllites, as well as pyroclastites and andesitic volcanites with a porphyric texture. The conglomerate beds became gradually finer towards the top of the unit, and are further more frequently interbedded with 0.5–1.5 m thick coarse-grained sandstones in a cyclic manner (lithofacies Sxg, Sx; Table 1).

The contact with the underlying turbiditic marine deposits is unconformable and erosional (Fig. 10C-D), locally overprinted by tectonism (in the form of layer-parallel faults). The orientation of bedding is rather difficult to ascertain, but appears to steeply dip towards NE (54/73 dip.dir/dip from 6 measurements). Imbrication data – corrected with the average bedding – shows a NE transport direction in terms of current orientations (Fig. 3A).

The amount of volcanic material in the Unit 1.1. beds can represent up to a quarter of the clasts in certain locations (LL42; for

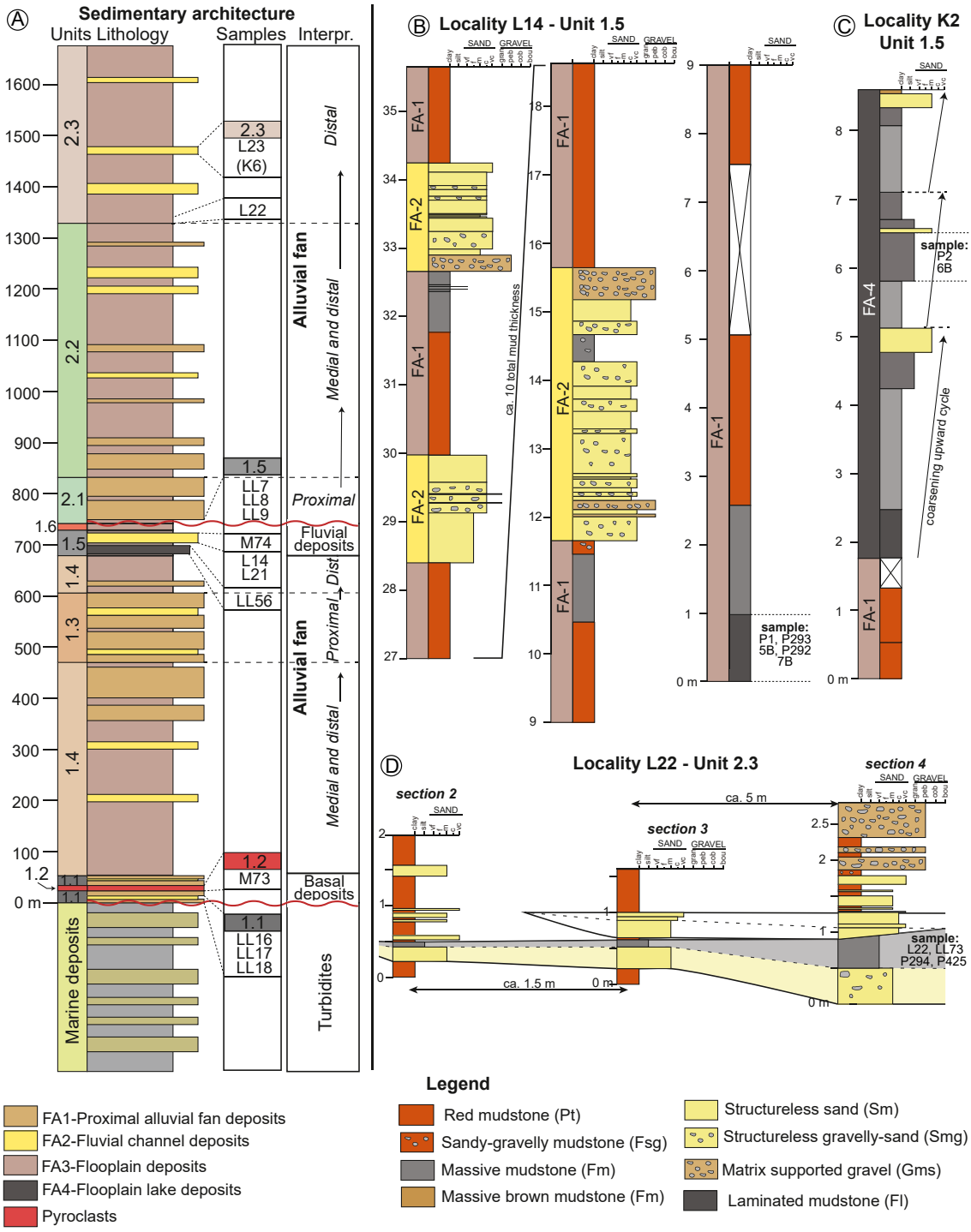

Fig. 9. Distinct depositional units (1.1–2.3) separated within the lower Densuș-Ciula Formation in the Vălioara area, based on the proportions of facies associations (see text for details). (A) Generalized lithology, environmental interpretation, and locations of samples for each unit; (B) Detailed sedimentary architecture of Unit 1.5 at locality L14: thick intervals of red floodplain mudstones (FA-3) interrupted by coarser sandy, gravelly fluvial deposits (FA-2); (C) Floodplain lake deposits (FA-4) outcropping at locality K2; (D) Braided fluvial channels of FA-2 incised into muddy beds of FA-3 at locality L22.

the location of the sampling place, see Fig. 2). In some outcrops (e.g., LL19) cobbles and smaller boulder-sized (40–50 cm) blocks, mainly of weakly shaly sandstones, also occur. Intervals of soft, white, sometimes pinkish kaolinitic clay are also present; the latter usually occurs in relatively thin (20–30 cm thick) finely laminated layers that can be cross-cut by quartz veins (M65); these are considered to be weathered (and probably also partly reworked) pyroclastite intercalations representing Unit 1.2. (see below). Three of these intercalations, two of which occur very close to the basal contact – represented by an angular unconformity – of Unit 1.1 with the underlying marine turbidites, were sampled for zircon U–Pb geochronology investigations (i.e. samples LL16, LL17, LL18; see Supplementary information 1). Remarkably, despite their overall tuff-like appearance in the field, these sampled beds turned

Fig. 10. The relationships of the marine turbidite beds, the base conglomerate (Unit 1.1) and the pyroclastite layers (Unit 1.2). Base conglomerate with large rounded clasts (A), and in contact with the hardened pyroclastic bed (see text for details), the sandstone is dark grey (B).The contact of the marine turbidites and the base conglomerate is shown on (C) and (D). The weathered zone of the turbidites with still recognizable clasts (1 in C) is covered by a red contact zone and by the reworked pyroclastic intercalations of the overlying base conglomerate containing larger rounded clasts (2 in C). Rectangle in photo (D), showing a wider image of the contact zone, indicates the location of photo (C). In the well-cemented tuff layers, xenoliths (E) and planes indicating shear (F) are visible.

out to be mixed siliciclastic-volcaniclastic cinerites, as documented by the presence of important, albeit variable, amounts of significantly older, reworked (detrital) zircon grains in their composition (see Supplementary information 2). The mixed, siliciclastic-volcanoclastic nature of at least one of these intercalations is further supported by the presence of a notable amount of particulate organic matter (sample LL17-ST1). Although quasi-barren in identifiable palynomorphs, this sample and a closely spaced second one (LL17-ST3; see Supplementary information 1) were nevertheless rich in large-sized and well-preserved plant tissue fragments and stomata-bearing cuticles (Fig. 7.9); this palynofacies indicates a short-distance transport of the organic clasts, corresponding to a delta or proximal siliciclastic fan facies (Tyson, 1995).

This unit marks the onset of continental deposition in the study area, with coarse-grained deposits accumulated unconformably on top of the Răchitova Formation and dominated by locally sourced coarse clastic material. Based on the predominance of FA 1 deposits as well as its coarse material, depositional Unit 1.1 likely represents the proximal reaches of an alluvial fan, built up by mass-flow events. The fining upward nature of the deposits coupled with the presence of fluvial deposits point to a transition towards the medial zone of the alluvial fan, which could indicate that the main coarse sediment influx was shifted either towards the catchment area or else laterally. It is worth noting that while the presence of fluvial deposition was already suggested in previous descriptions of the lower subunit of the Densuş-Ciula Formation (Grigorescu, 1992), the coarse grained, poorly sorted nature of the deposits with a sandy-clay matrix, and the locally high proportion of volcanic debris suggest that Unit 1.1 is an alluvial-conglomerate, which might be a partially reworked lahar. Occurrence of lahar deposits was already mentioned south of the mapped area, at Densuş, within the Lower Member of the Densuş-Ciula Formation (Anastasiu and Csobuka, 1989).

As a transition to the overlying unit, a dark grey coarse-grained sandstone shows bedding-parallel flake-like features that are suspected to be post-sedimentary in origin. The clasts appear to be mainly of volcanic origin. The sandstone also contains large, rounded clasts (derived from the underlying conglomerate), and above it, a finer-grained pyroclastite layer appears as a hard, well-cemented pad (Fig. 10B).

The zircon U–Pb geochronology analyses (Supplementary informations 1 and 2) derived from samples LL16, LL17 and LL18 (for their geographic and sedimentary context, see Figs. 2 and 9) revealed a wide temporal spread of the identified zircon populations (Supplementary information 2) – in accordance with their suggested partly reworked nature (see above).Nonetheless, all samples include relatively young zircon grains that can be genetically linked to the latest Cretaceous (so-called 'banatitic') volcanism active in south-eastern Europe during this time period (e.g., Berza et al., 1998; Gallhofer et al., 2015). Although there were only two latest Cretaceous zircons out of 34 separated grains in sample LL16 (5.88 %), their proportion rises to about 38 % (19 out of 50) in sample LL17, and reaches almost half of the total (31 out of 63,

49.2 %) in sample LL18. The weighed mean ages of the banatitic zircon populations recovered from the latter two samples are clustered tightly around an early late Campanian maximum depositional age (MDA; 79.75 ± 0.69 Ma for LL17, and 79.10 ± 0.73 Ma for LL18; Fig. 11 A-C), in good accordance with the latest Cretaceous individual zircon U–Pb age values recorded in sample LL16. Furthermore, the relatively high percentage contribution of the banatitic zircon population in sample LL18 suggests that accumulation of this particular cinerite-bearing bed occurred quasi-synchronously with the volcanic activity that generated the banatitic population, i.e., that the calculated MDA is temporally close to its actual depositional age (see discussion for a similar case in Bălc et al., 2024).

4.2.3. *Unit 1.2 –pyroclastites*

Intercalated within the base conglomerate (Unit 1.1), at least three layers of volcanogenic deposits were mapped in the east-side gullies of Geat Valley. Two lithotypes could be noticed in the field: one that is unconsolidated, clayey, kaolinitic light grey or sometimes pinkish grey in colour (Fig. 10C) with a dominant clast size below 0.1 mm, and a second one which is consolidated, greyish brown, and granular in texture with a dominant clast size between 0.5 and 5 mm (Fig. 10E). Both lithotypes may contain larger rounded aggregates. The first variety is intercalated between coarse-grained layers of the base conglomerate, and appears lower in stratigraphic position, while the harder variety is exposed in two levels, a thinner (~1–2 m) lower layer and a thicker (~5–10 m) upper layer. As a continuous stratigraphic sequence could not be reconstructed in the field, their stratigraphic thickness can only be estimated from their dips.

As the softer, kaolinitic material is very weathered and mostly of small grain size, with only occasional larger rounded clasts, it may represent secondary volcanic ash accumulations probably interbedded into the conglomerate layers by reworking the original cinerites (Fig. 10C; and see above). Geochronological analyses of samples collected from this lithotype were discussed in the previous section.

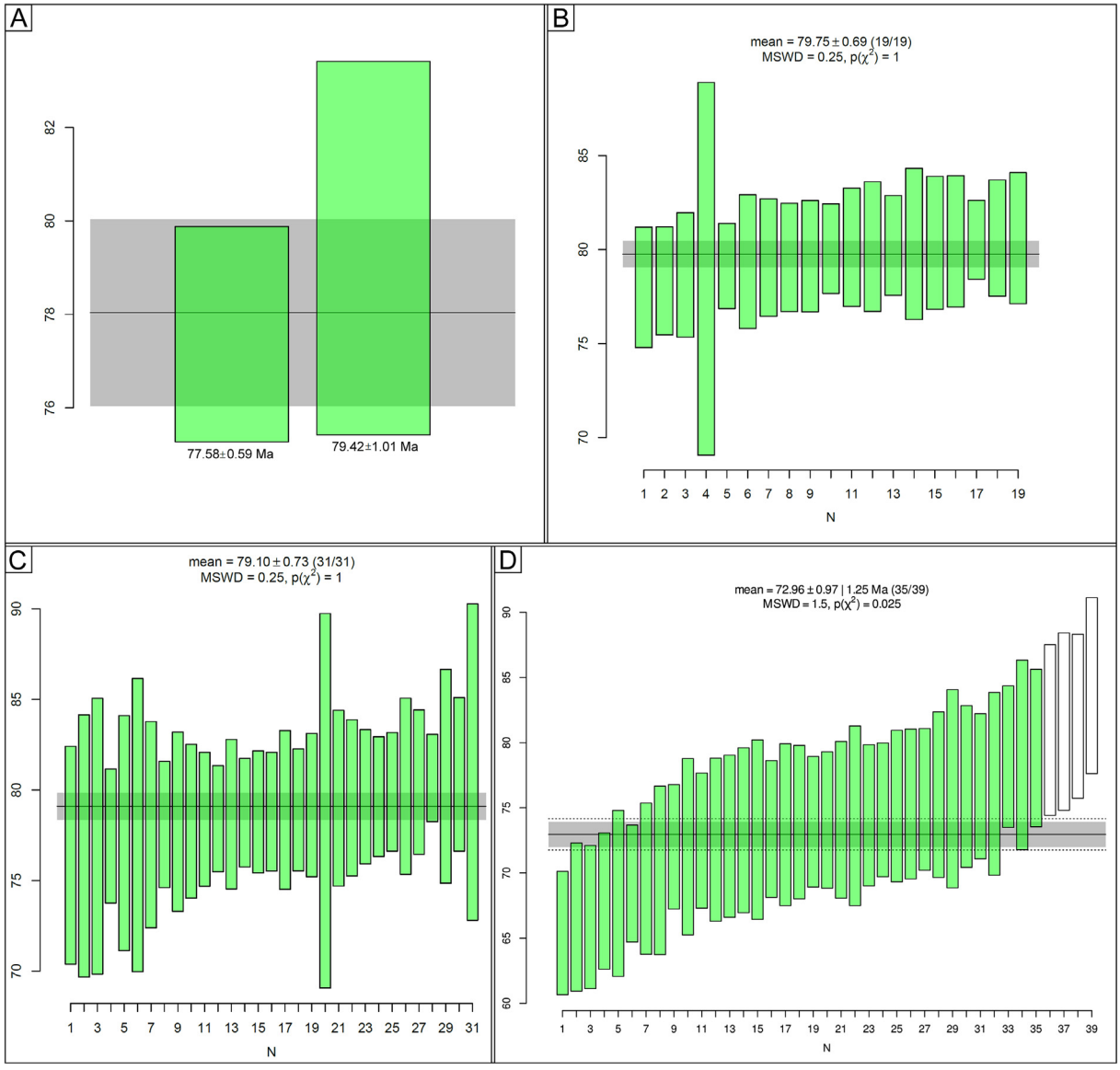

Fig. 11. Distribution of $^{206}Pb/^{238}U$ ages and individual errors of the Late Cretaceous (banatitic) zircons, with weighted mean Maximum Depositional Ages (shown only in B, C, and D), from the zircon U–Pb geochronology analyses for samples: (A) LL16; (B) LL17; (C) LL18; and (D) BUD (see more details in text and Supplementary information 1).

The harder pyroclastite first appears above a dark grey flaky-textured coarse-grained sandstone with a rough erosional contact (Fig. 10B). About 40 m further upward in the grey conglomeratic sandstone succession, the same lithotype crops out once more with a greater thickness, and below this second occurrence there is again a darker grey, about 50 cm thick layer composed mainly of clasts of volcanic origin within the sandstone. These darker layers beneath the pyroclastites may be due to the large amount of pyroclast fragments, which indicate reprocessing immediately prior to contact. As medium-grained dark to light grey grains are mixed with rounded xenolith grains (Fig. 10E) and a large number of intrinsic white plagioclase phenocrysts are clearly visible, this lithotype may represent either a lapilli-tuff or an ignimbrite of andesitic composition (Fisher and Schmincke, 1984). The entire succession is highly tectonised in this part, almost shale-like in character, and the original stratigraphy is completely overwritten by shear planes (Fig. 10F). Along the shear planes, displacement scars and scales are also common, and are more likely related to transpressional forces. The hardness of the rock is due to its high silica content, which can be the result of secondary alteration and is visible as microcrystalline quartz veins in thin sections (Fig. 12).

The hard pyroclastite is found in the middle section of the eastern side of Geat Valley, striking parallel to the axis of the valley for a length of about 400 m. It thins out towards the north, and is interrupted to the south by a fault. Above the upper pyroclastite layer, cyclic sandstones and conglomerates reappear.

The occurrence of yellowish-grey hard 'tuffites' with varying thicknesses between Ciula Mică and Densuș, roughly along the same strike, was already mentioned by Laufer (1925) who indicated these as 'porphyrites' on his map. In addition to Laufer's description, Grigorescu (1992) also notes briefly the occurrence of such intercalations, which he placed in the Lower Member of the Densuș-Ciula Formation.

In addition to the three samples originating from the softer, altered ash-bearing layers discussed above (LL16, LL17, LL18), a fourth sample for zircon U–Pb geochronology was also collected from this unit, from the hardened, darker pyroclastite layer (sample M73, see Supplementary information 1), in order to further constrain the chronostratigraphic position of Units 1.1–1.2. (i.e., basal part of the Densuș-Ciula Formation) in this area. Unfortunately, an extremely small number of zircon grains (4) could be extracted for analysis, of which only one yielded a Late Paleozoic age (middle Carboniferous, ~343 Ma). Given the nature of the host rock, it seems highly likely that it represents an inherited zircon crystal from within the original magmatic source, whereas the very low overall zircon yield of sample M73 is the result of the relatively more basic (i.e. andesitic) composition of the pyroclastite.

4.2.4. Unit 1.3 – proximal alluvial fan– "lower" Vălioara breccia

Breccia deposits (Fig. 13) outcropping in Neagului Valley, were previously thought to represent the oldest deposits in the uppermost Cretaceous continental succession (Botfalvai et al., 2021), deposited prior to the formation of the main bone-bearing layers (e.g., site K2). However, this coarse proximal lithofacies (Gms) also recur on top of the otherwise stratigraphically higher-lying fine-grained cyclic strata (interpreted here as Unit 1.6). This observation was further confirmed by subsequent mapping, and this second, recurring coarse-grained facies was re-interpreted as the "upper" Vălioara breccia (see below, Unit 2.1.), an isofacial unit different from (and younger than) the basal ("lower" Vălioara) breccia overlying the base conglomerate (Figs. 2 and 9).

This depositional unit conformably overlies the lower coarse-grained and tuffaceous-volcaniclastic part (Units 1.1. and 1.2) of the Densuș-Ciula Formation, as can be observed in Geat Valley; given the absence of associated volcanogenic material within it, it is considered to correspond to the basal part of the Middle Member of the Densuș-Ciula Formation, following the subdivision scheme introduced by Grigorescu (1992). Its cover units in the study area are either the Conglo-breccia (Unit 1.4) or the "upper" Vălioara breccia (Unit 2.1), from which it is separated by the shear zone of the Vălioara Valley. The unit is bounded to the north by the tectonic boundary ("main fault") of the metamorphic Mesteacăn Range, while towards the south, it merges with the finer-grained conglomerates and sandstones of depositional Unit 1.4 (Figs. 2 and 8).

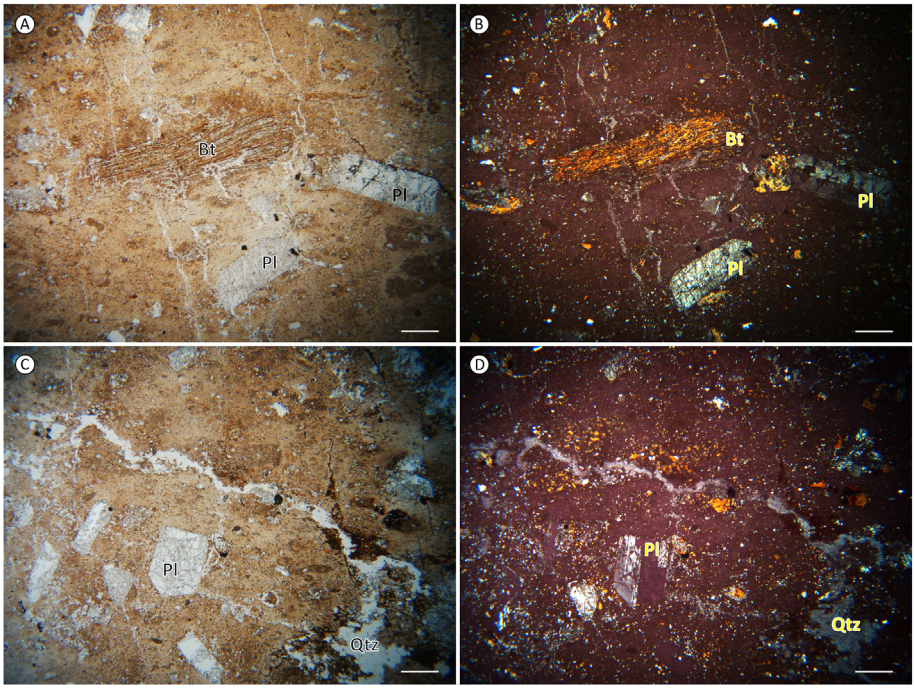

Fig. 12. Thin sections of the hard pyroclastite from Unit 1.2 in PPL (left) and XPL (right). Pl = plagioclase; Bt = biotite; Qtz = quartz. Scale bars = 1000 μm.

Fig. 13. Characteristic field appearance of the "lower" Vălioara breccia (Unit 1.3). Thick gravel bed (facies Gms) overlying floodplain mudstones (Fsg) (A); colour variation between floodplain (Fsg) and mass-flow deposits (Gms) (B); characteristic upward fining but without well-defined cycles of gravel (Gms) and mudstones (Fsg), a few metres in thickness (C); unsorted and weakly rounded clasts within coarse-grained conglomerate (D); steeply dipping beds of gravel (Gms and Gcs) and floodplain mudstone (Fsg) (E); rounded and weathered volcanic clast between angular sericite schist clasts (F).

The measured dip of the beds belonging to this unit decreases towards east while their azimuth changes as well: in the western part of the study area, recorded values are generally around ~60/60° (azimut/dip), whereas in its eastern parts, they change to ~120/30 (Fig. 2). The thickness of this unit, calculated from the dip data, is estimated to be 700–750 m in the study area. Although the overlying Unit 2.1 represents the same facies (proximal alluvial fan), the two units must be kept separated since they belong to different depositional sequences (see above).

Depositional Unit 1.3. is dominated by the coarse FA 1, and its Gms lithofacies (Fig. 13), especially in the vicinity of the basin bounding fault. Similarly to the entire studied continental succession, gravel clasts in Unit 1.3 are composed of a mixed angular metamorphic material, and the deposits are therefore considered breccias (Fig. 13D). Individual clasts can reach up to 50 cm in size, but sometimes even larger boulders may occur. The material of the matrix is represented by fine to medium-grained sand and clay, also composed mainly of metamorphic phyllite grains that are quite clayey due to weathering. The unit is mainly built up by cyclic alterations of coarser and finer beds of Gcs, Gms and Gx facies (Fig. 13C), while beds of muddy sand and cross-stratified gravelly sand (Sxg) also occur (Fig.13A, B, D, F). Based on the dominance of FA 1 within depositional Unit 1.3., it represents proximal alluvial fan deposition through mass-flow events, while the presence of Sxg and Gx facies shows that fluvial channels were also present (Fig. 13A), similarly to the case of Unit 1.1.; these fluvial deposits become more frequent towards the south.

As near the main fault the dominance of FA 1 deposits is more pronounced, the suggested depositional environment corresponds to a fragmented landscape of hillslopes, where subaerial erosion was active and generated alluvial fan systems characterised by gravitational debris flows on the northern, steeper parts of the landscape, and intermittent water flows on its lower-lying, southern parts.

4.2.5. Unit 1.4– medial and distal alluvial fan– conglo-breccias

This unit gradually overlies the base conglomerate (Unit 1.1.) and the "lower" Vălioara breccia (Unit 1.3.), while being also laterally interbedded with the latter (Fig. 9A). Its thickness varies between 20 and 300 m, increasing towards south, further downdip from the basin bounding fault, where it becomes dominant as it replaces the breccia completely. It is overlain by Unit 1.5 (grey Vălioara beds) (e.g. at site K2). The general dip of its deposits is to the east-northeast, at about 70° in the west and 60-50° in the east.

The alternation of Gms and Fsg lithofacies characterizes the entire unit; its colour, albeit dependent on the clastic material, is usually a reddish greenish-grey. Finer-grained deposits may record much higher thicknesses (0.8–1.5 m) and thus make up a larger portion of the unit than the coarse-grained ones. Its matrix-supported gravelly deposits are 30–40 cm thick and composed of a clastic material of varied origin and size, with the flattened clasts showing imbrication in places. The imbricated clasts – after rotating the beds to horizontal position – suggest an estimated SW flow direction according to current cardinal directions (Fig. 3B). The

clast-supported layers are more cemented (Gcs) in places. In these, the rounded clasts are mostly 10–20 cm in size, more flattened, and are composed of sericite schists and quartzite.

Based on the increased presence of floodplain fines and the reduced gravel bed thicknesses compared to the underlying units, this unit likely represents medial to distal alluvial fan environments. This interpretation is also supported by its interfingering with the coarser unit of the "lower" Vălioara breccia (Unit 1.3.), and by its increasing prominence with increasing distance from the basin bounding fault.

4.2.6. Unit 1.5 – fluvial deposition – grey (Vălioara) beds

This stratigraphic unit includes several lithologically distinct strata (Fig. 14), mostly assigned to FA 4 and FA 3, but also to FA 2 (see Table 2, Fig. 9B). Their occurrence is associated with a well-traceable stratigraphic level that extends throughout the study area with a NNW-SSE strike (Fig. 2). This unit includes previously described, palaeontologically significant outcrops from the area yielding abundant vertebrate remains, continental molluscs, and plant remains (Kadić, 1916; Botfalvai et al., 2021; Páll-Gergely et al., 2023; Magyar et al., 2024).

The lithology of the unit can vary both along strike and dip, but it is overall characterized, and distinguished from the under- and overlying units, by its greyish colour, as well as the cyclic alteration of fine-grained and sandy or sandy-gravelly deposits belonging to FA 2 and FA 3, respectively. It also uniquely hosts the lacustrine FA 4, which does not occur in any other unit recognized in this area.

In the studied outcrops, the sedimentary succession of the unit starts with a 1–1.5 m thick layer of sandy-claystones and sandy-siltstones with a slightly variegated greyish appearance, which is

Fig. 14. Characteristics of the grey (Vălioara) beds (Unit 1.5). Laminated grey mudstone layer (facies Fl), upper part of Ogradiilor Valley, sampled for palynology (A); fault lineations along the bedding plane and calcitic lithoclase in the bluish-grey clayey sands (Smg) (B); cemented cross-bedded gravelly sandstone layer (Sxg) (C); vertebrate remains in grey sandstone (Sm) (D); sheared and fractured beds: dark grey clayey sandstone (Fs) on the right, brownish grey sandstone (Sm) on the left, with dark grey sheared clay between the two, forming a fault zone (E); flattened wood remains in grey fine-grained, mica-rich, clayey sandstone (Smg) (F); grey sandstone (Sxg) overlying a red paleosol layer (Ptc) (G); pebbly greyish brown clay with charcoal plant remains, calcareous concretions and clay pebbles with limonitic crust (Ptc) (H).

also represented within the site K2 outcrop in Neagului Valley (Botfalvai et al., 2021) (Fig. 9C). Here, it hosts a rich vertebrate assemblage, together with gastropod shells and small flattened wood remains, as encountered at site K2 (Fig. 14D, F).

The most thoroughly examined outcrops of this unit occur along Neagului Valley. South of it, however, the same succession of strata was also found in ravines and tributaries of the Neagului, Ogradiilor and South Ogradiilor valleys (Fig. 2.).

In the uppermost section of the main branch of Ogradiilor Valley, dark grey-blueish claystones and mudstones crop out in 0.5–1.5 m thickness above cross-bedded sand beds (Fl); this homogeneous, 1.5m thick hard bluish grey mudstone layer was not observed elsewhere in the studied succession. It is criss-crossed by plate-like fractures that seem post-diagenetic, as the surface of these cracks are coated with a limonitic film. The cracks are furthermore calcitic in places, and there are also scratches along the planes indicating displacement. This bluish grey mudstone (Fig. 14A) from the middle-upper part of Ogradiilor Valley was preliminarily sampled for palynology during our first fieldwork in 2019 (sample P1; see Supplementary information 1), revealing poorly preserved palynomorphs and a particulate organic matter (POM) content dominated by small, rounded opaque phytoclasts (Botfalvai et al., 2021). This palynofacies was interpreted at that moment as indicating a distal basinal, possibly marine environment located farther away from a continental source area (see also below).

The blueish grey mudstone is conformably overlain by grey clayey sandstones and palaeosols. Up in the section, at site L15, a bone fragment was found broken during a sliding movement and fused along the lithoclase; some of the sandstone beds contain abundant white clay clasts suggestive of weathered pyroclastite grains or intraclastic kaolinitic clays. A well-developed shear zone was mapped in the grey beds at the head of the southern tributary of Ogradiilor Valley. The “fault gouge” is a dark grey clay wedged between a grey clayey sandstone with molluscs and a brownish grey sandstone (Fig. 14E). In this section, the succession of the unit continues with brownish grey, thinly bedded marly claystones, grey conglomerates, sandstones, and calcareous-clayey reddish palaeosol cycles (Fig. 14C, G). The same succession includes the fossil-rich site NVS of Botfalvai et al. (2021), the deposits at the fossiliferous bed belong to FA 2, on their turn being under- and overlain by FA 3 deposits.

The thickness of the bone-bearing sequence of Unit 1.5. changes spatially along-strike. To the north it is only 15 m thick in Neagului Valley, thickening to 60–80 m in Ogradiilor Valley, and can reach a thickness of over 100 m in the South Ogradiilor and Vârtopilor valleys. However, the recorded thicknesses do not necessarily equate with depositional thickness, as signs of tectonic displacement along the beds were noted in almost all observation points (Fig. 14B, E). The character of the displacement is generally oblique lateral, so both thinning and thickening of the successions, associated with duplex formation, are possible. The original stratigraphic thickness of the unit therefore must fit between the two end values (15 and ~100 m).

Field observations of the grey mudstone layers and their estimated general geometry yielded a dip direction of 63° and a dip angle of 61°, which is consistent with previous field measurements (Lupu et al., 1993; Botfalvai et al., 2021). In some places, the dip of cross-bedding was also measured. After adjusting the general dip to horizontal, the foresets show a dip direction to the present-day SE, indicating the probable original transport direction (Fig. 3C).

The facies and FA types recorded in this depositional unit, and the presence of fluvial, lacustrine and floodplain deposits indicate a predominantly wet, fluvial and marshy environment, as already suggested by previous studies (Kadić, 1916; Botfalvai et al., 2021). Compared to the underlying units that were dominated mainly by coarse-grained material in the vicinity of the basin bounding fault, this unit suggests a reduced coarse sediment flux into the depositional area. Such reduction in grain size can be due to a reduced activity along the fault (Steel, 1988); however, based on the thickness of the unit, the area clearly underwent subsidence during the deposition of the grey (Vălioara) beds. Alternatively, it is also conceivable that the coarse sediment input via alluvial fans was transferred to another location along the basin bounding fault, whereas a mainly fluvially dominated depositional environment became established in the study area.

This unit and its outcrops have been long been known for its well-preserved vertebrate remains (Kadić, 1916), hosting several fossiliferous sites where the bone-bearing strata are represented by bluish-grey mudstones and marls with plant remains (Botfalvai et al., 2021).

Due to its palaeontological significance (Kadić, 1916; Botfalvai et al., 2021; Magyar et al., 2024) and the possible marine influence within the grey beds based on palynological sample P1 reported by Botfalvai et al. (2021), Unit 1.5. was extensively sampled to estimate its origin and age. In addition to the two samples collected from beds of this unit and previously reported by Botfalvai et al. (2021), 18 more biostratigraphic samples were collected from this area subsequently, alongside one detrital zircon sample for U–Pb geochronology (M74) from a sandstone body in the immediate proximity of vertebrate site NVS (see Supplementary information 1).

Of these16 samples were analysed for their palynological content and palynofacies, whereas a smaller number were also investigated for their marine micropalaeontological content (12 for calcareous nannoplankton and 5 for foraminifera; Supplementary information 1). In the case of micropalaeontologically investigated samples, their selection was guided by the lithofacial characteristics of the sampled rocks, assessed to preliminarily suggest a potentially marine origin. The samples analysed from Unit 1.5 can be grouped into two clearly distinct clusters: a smaller number of samples (5 in total) show hints of at least some degree of marine influence, whereas for their largest part a definitive continental origin could be assessed.

The ‘marine-influenced’ samples are also rather tightly grouped spatially, being restricted to the upper reaches of the main course of Ogradiilor Valley, upstream of vertebrate locality Nvs (section L14, with samples 5B, 7B, P292 and P293; see Figs. 9 and 14A as well as Supplementary information 1); one exception to this general rule is sample 2B that shares some features with the former subset, but was collected from deposits cropping out in the uppermost end of the southern tributary to Ogradiilor Valley, also upstream of site Nvs (section L21). Although all these samples are rather poor in identifiable palynomorphs, their palynofacies is very characteristic, with a mixture of granular amorphous organic matter of marine origin (Fig. 7.10) and small-sized opaque phytoclasts of continental origin, suggesting a transitional or nearshore marine depositional environment. This assessment is also supported by their palynological content that includes mainly terrestrial taxa (e.g., common *Classopollis* div. sp. pollen, Fig. 7.12, and *Polypodiaceoisporites hojrupensis* spores), but associated with rare fragments of the marine dinocyst *Odontochitina* sp. Furthermore, some of these samples, collected from an extreme upstream location (5B, P293) – thus stratigraphically lower in position, taking into account the local dip of the beds – also yielded very poor nannoplankton assemblages (a few specimens each); meanwhile, other nannoplankton samples from this subset were barren, as were all the samples analysed for foraminifera (Supplementary information 1). The nannoplankton taxa identified in sample P293 (*Micula staurophora* and *Watznaueria barnesiae*) are often regarded as dissolution-resistant (e.g.,

Mahanipour et al., 2022), and their low-abundance occurrence may be the result of reworking from underlying marine beds. However, the species identified in sample 5B (*Tranolithus orionatus*) is reported to occur in relatively low numbers compared to other taxa in nannoplankton assemblages affected by dissolution (e.g., Linnert et al., 2010) and thus appears to be more susceptible to the effects of potential dissolution processes, making it less likely to be reworked from older beds.

Accordingly, our extended sampling does appear to support a marine (albeit transitional, near-shore) depositional setting for the hard bluish claystone beds from the stratigraphic section cropping out along the main Ogradiilor Valley as was tentatively hinted at previously by Botfalvai et al. (2021). It is worth noting here that sample P1, reported earlier by Botfalvai et al. (2021) as suggesting possible marine influences within the Densuș-Ciula Formation, also comes from the same L14 local section that yielded most of the samples from this subset. Given the shallow-marine, near-shore depositional setting identified for the hard, bluish grey claystones, the absence of ostracods and benthic foraminifera in the sample subset originating from them is puzzling; however, similar patterns of microfossil and palynofacies distribution had been reported previously from the transitional, brackish shallow-marine part of the Petrești succession near Sebeș in the southwestern Transylvanian Basin (e.g. Ţabără et al., 2022; Bălc et al., 2024), and these patterns may reflect the highly turbid nature of the palaeoenvironment.

The second subset of samples recovered from the grey Valioara beds shows a markedly different microfossil content. All samples from this subset analysed micropalaeontologically (i.e., samples 13B, P289, P290, LL5-15-1, LL5-15-2, LL5-15-3) turned out to be completely barren both for calcareous nannoplankton and for foraminifera (Supplementary information 1). On the other hand, all of them yielded at least some palynological content, either in the form of identifiable palynomorphs or as particulate organic matter. Samples P289 and P290 have an intermediate stratigraphic position along the southern tributary to Ogradiilor Valley, between the stratigraphically lower sample 2B from the first subset and the overlying fossiliferous locality Nvs. Their palynological content is rather poor, with only a few occurrences of *Classopollis* sp. gymnosperm pollen recorded; their palynofacies is reminiscent of that found in sample 2B, but with a progressively increasing proportion of translucent phytoclasts (woody tissues) that suggests a shift towards a deltaic/fluvial depositional environment (e.g., Aggarwal, 2022). Sample 13B, slightly even higher in this local section, but still below the Nvs level, yielded a small amount of continental organic matter, with a palynofacies composed of a mixture of opaque phytoclasts and large cuticle and woody tissue fragments that indicate a wholly continental sedimentary setting and a short-distance transport of these organic components.

All other samples collected from the outcropping area of the grey Vălioara beds (samples LL5-15-1, LL5-15-2, LL5-15-3, 8B, 9B, LL56, LL7, 6B) have revealed exclusively the presence of palynomorphs and palynofacies of continental affinities (Supplementary information 1). Of particular note is sample LL5-15-3 (Fig. 14E), in which the organic content is represented mainly by fossil resin (Fig. 7.14), amounting to about 50–60 % of the total organic matter extracted. According to Tyson (1995), most fossil resin-enriched accumulations are associated with deltaic deposits. The palynological assemblages are well preserved, with terrestrial palynomorphs such as *Polypodiaceoisporites hojrupensis* (Fig. 7.15), *Suemegipollis triangularis* (Fig. 7.16) and *Trudopollis capsula* (Fig. 7.17). In Vârtopilor Valley, the samples yielded poor and low-diversity assemblages, in which most remarkable are the occurrence of freshwater algae (i.e. *Chomotriletes fragilis*) in sample LL56, supporting the presence of standing water bodies (small lakes or marshes), and an assemblage in sample 8B consisting almost exclusively of ferns spores (i.e. *Deltoidospora* div. sp.) related to a Cretaceous–Paleocene fern taxon that is usually regarded as very early colonizer of disturbed habitats, e.g., after volcanic eruptions (Vajda and Bercovici, 2014; Thomas and Cleal, 2022).

Although the microfossil assemblages recovered from Unit 1.5. are not very rich or diverse, they nevertheless offer relatively useful biostratigraphic information concerning these vertebrate fossil-rich grey Vălioara beds. The co-occurrence of *Polypodiaceoisporites hojrupensis* with *Odontochitina* sp. in sample P292 suggests a latest Campanian age (Siegl-Farkas, 2001; Williams et al., 2004); meanwhile, assemblages reported from samples LL5-15-3 support a probably slightly younger, terminal Campanian to earliest Maastrichtian age, in good accordance with the higher relative stratigraphic position of these samples.

On the other hand, the detrital zircon sample M74 (collected from a sandstone bed lying stratigraphically slightly below the fossiliferous NVS level, in the southern tributary of Ogradiilor Valley) has yielded a population dominated by Mesoproterozoic to Cambrian grains, and with only one (out of 40 analysed) latest Cretaceous-aged (probably banatitic) grain (see Supplementary information 2) that, nevertheless, showed an older age (83.6 ± 5.3 Ma) than those recorded in the samples analysed from the underlying beds of Unit 1.1 (samples LL16, LL17 and LL18; ~78–79 Ma). The differences in banatitic zircon abundance and age patterns between this sample and those from the basal part of Unit 1.1. may indicate that by the time the lower grey Vălioara beds were formed (around the Campanian/Maastrichtian boundary), the magmatic sources that were active and fed the depositional basin of the Lower Member of Densuș-Ciula Formation became dormant and/or were largely removed by erosion, ceasing to supply cineritic or volcanoclastic material into the northwestern Hațeg Basin, concomitantly with the activation of a somewhat older, but also quantitatively less important volcanogenic source area.

4.2.7. Unit 1.6 – distal alluvial fan with palaeosols –red cyclic beds with palaeosols

This unit outcrops mostly in Neagului Valley, in the upper part of South Ogradiilor Valley, and in the upper part of East Vârtopilor Valley, and has a thickness of about 20–40 m (Fig. 2). It has a gradual contact both with the dominantly grey beds of the underlying Unit 1.5 as well as towards the overlying deposits, from which it differs mainly in its more pronounced stratification, generally finer grain size, and the presence of palaeosol layers, all of which imply different, more distal sedimentary environment for this unit (Figs. 9A and 15). Rare vertebrate remains were also found in this unit (e.g., at LL9; Magyar et al., 2024). In Ogradiilor Valley, this unit is thinner, represented only by a ca. 2 m thick red palaeosol above the grey, fluvial beds of Unit 1.5, and is followed by massive conglobreccias of Unit 2.1.

The bulk of the unit is built up by FA 2 and FA 3 deposits, its main distinctive features being the absence of FA 4 deposits compared to the underlying grey unit, and the presence and dominance of FA 3 deposits compared to the overlaying conglo-breccias (Fig. 9A). It is dominated by red-coloured sandy-gravelly and clayey deposits (Fig. 15B-C), but in places, near its contact with the underlying unit, grey, bluish-grey sandstone and conglomerate layers may also occur (Fig. 15A, D). In this interval (Sx), the gravels are more rounded, and the deposit is better sorted, compared to the underlying unit. In the reddish clayey beds (Fsg), the gravel clasts are more angular, and sand of varying grain size classes is present. In both cases, some of the beds show normal grading and are characterized by an erosional lower contact. The material of the clasts is dominated by metamorphic rocks, although the more rounded clasts are usually of igneous origin.

Fig. 15. Features of the red cyclic beds with palaeosols (Unit 1.6). Distinctive bluish-grey to greenish-grey coarser-grained sandy-gravel layer (Gms) overlying red palaeosol (Ptc) (A); characteristic rhythmic alternations of palaeosol (Pct) and more cemented gravelly-sandy layers (Gms) rare bone fragments occur in the palaeosol layers (B); lamination observed in thin, cemented sandstone beds (Sl) (C); Cross lamination in coarse-grained beds (Sxg) (D).

The average dip direction is NE (68°) and the dip is around 64°, similarly to the underlying unit. The imbrication of the gravels suggests an easterly transport direction (Fig. 3C). Deposits of the unit showed slips along the bedding planes due to subsequent tectonic movements. The finer-grained clayey layers are best suited to accommodate such slips, and their presence is indeed observed regularly in the red palaeosol layers (e.g. L3).

The presence of palaeosols and the characteristic red colour of the unit document an environmental shift in the depositional zone compared to the underlying grey, fluvial-lacustrine unit. Its characteristics indicate that the main fluvial axes were located farther away from the present outcropping areas, which resulted in more oxidative conditions, due to lower water table levels, and in the formation of moderately to well developed red-coloured palaeosol sequences.

4.2.7.1. Depositional sequence 2. Above the intervening finer-grained grey Vălioara beds (Unit 1.5) and red cyclic beds (Unit 1.6), coarse-grained deposits showing sedimentological characteristics similar to the stratigraphically lower-lying deposits of Unit 1.3 were mapped. These deposits that, nonetheless, occurr above Unit 1.6 indicate a renewed intensity in sediment supply and thus were classified into a new, younger depositional sequence composed of 3 distinct units (Fig. 9A).

4.2.8. Unit 2.1— proximal alluvial fan — "upper" Vălioara breccia

The unit was encountered in the lower section of Neagului Valley and the lower-middle section of Ogradiilor Valley; furthermore, the hill range stretching in the northern part of the study area between the upper part of Vălioara Valley and Fântânele Valley is also built up mostly of these strata (Fig. 2). They are dominated by matrix-supported, poorly sorted and poorly rounded gravel with the addition of coarse clayey sand layers of considerable thickness (Gms, Gx, Smg), while palaeosol levels are missing (Fig. 9). In its field appearance and sedimentary architecture, the unit is very similar to the succession described previously as the "lower" Vălioara breccia (Unit 1.3), but shows a higher proportion of finer-grained sands and rounded gravel, and is also interpreted as proximal alluvial fan deposition through mass flow events. Consistent with this overall similarity, deposits of this unit belong predominantly to FA 1, although those of FA 2 are also present.

Similarly to Unit 1.3, this unit includes deposits that were accumulated in the proximal zone of an alluvial fan located in the proximity of the basin bounding fault. The presence of the unit indicates that after an episode of relatively slow rate of sedimentation represented by Units 1.5 and 1.6, coarse-grained influx has restarted to the northwestern part of the basin, either due to renewed activity of the basin bounding fault or to lateral shift in the sediment influx (e.g., Steel, 1988).

West of Vălioara Valley, the "upper" Vălioara breccia dips typically to ENE with 60°, as are deposits in the underlying unit. Moving up-sequence towards east, the dip direction becomes easterly, and the dip decreases to 30°. Near the main fault, the rotation is even greater and a SE azimuth was measured, while the dip of the strata remains around 60°. In the immediate vicinity of the main fault, shear phenomena (deformation bands) and drag folds are present in the beds.

4.2.9. Unit 2.2— medial distal alluvial fan— greenish red conglo-breccias

This unit crops out in the lower sections of Ogradiilor and South Ogradiilor valleys, and on the southern tip of the hilly range north of Vălioara, between Fântânele and Vălioara valleys (Fig. 2). It is almost identical to previously described Unit 1.4 (Conglo-breccia), is typically reddish in colour, but the conglomerate layers are mostly greenish grey (Fig. 16). The unit is built up by deposits of FA 1, FA 2 and FA 3, and is characterized by a succession of coarse-grained (Gcs, Gms) and fine-grained (Smg, Sxg) beds (Fig. 9). In some places, the fine-grained beds may also show soil features (Fsg), but these do not usually reach a high degree of maturity (such as Ptc). The succession of beds, as well as the start and end of cycles are difficult to determine due to the massive, lenticular character of the deposits, but an upward change from coarser to finer grain size is evident within each cycle of about 3–5 m thickness (Fig. 16D). Calcareous layers (Ptc) appear only in very few places in the upper cycles of the unit (e.g., AG29), documenting soil formation (Fig. 16C).

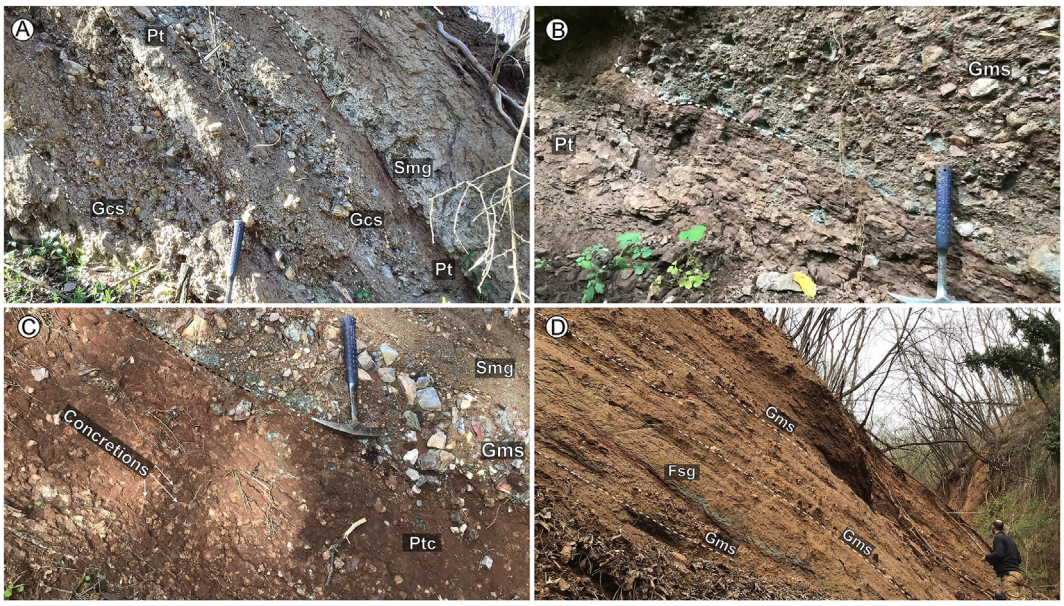

Fig. 16. Characteristics of the conglo-breccia beds (Unit 2.2). Small cycles of upwardly fining beds (alternating beds of facies (Gcs, Smg and Pt) in Ogradiilor Valley (A); reddish greenish-grey matrix-supported conglomerate (Gms) deposited on fine-grained floodplain deposits (Pt) (B); floodplain deposits containing calcrete nodules (Ptc) overlain by gravel (Gms) and sandstone deposits (Smg) (C); alteration of thin fine (Fsg) and coarser-grained (Gms) beds (D).

This unit interfingers laterally with Unit 2.1, replacing it completely in the southern areas. It has an east-northeast dip of 50° and a thickness of about 300–400 m; the general eastward dipping was estimated based on measurements made in several places on the conglomerates. Further eastwards in the lower part of Ogradiilor Valley, the thickness of the cycles decreases, and the grain size becomes finer (L38). Here, reddish variegated medium-grained sand followed by clay forms the finer interval (Fsg) of the cycles, and fine-grained, unsorted, subangular pebbles form their ~40 cm thick coarser-grained part (Smg, Sm) (Fig. 16A), marking a transition to more "distal" fluvial deposits. In the NE part of the study area, in the eastern side of Fântânale Valley, the beds are tilted at 35° to the east here, a succession of dominantly fluvial facies (FA 2) beds was observed marking the transition to the overlying Unit 2.3.

Similarly to the previously described relationship between Units 1.3 and 1.4, this unit marks the medial and distal portions of an alluvial fan body while the previous unit (2.1) represents its proximal area. The unit is deposited, through a continuous transition, on top of the red cyclic beds containing palaeosols from the previous depositional sequence (Unit 1.6.); in its upper part, it supports the overlying unit (2.3 – Fântânele and Budurone beds), although their direct contact is not recorded.

4.2.10. Unit 2.3 – distal alluvial fan –Fântânele and Budurone beds

Two, sedimentologically and palaeontologically slightly different successions make up this unit; nevertheless, these are similar to each other in their general depositional setting assessment, and are thus included together in Unit 2.3. The Fântânele beds are reduced in areal extent (Fig. 2), and their distinction within this depositional unit is due to the fact that no other deposits that would be similar in overall appearance and richness in fossils were found in the eastern-northeastern side of Vălioara Valley (Fig. 17A-B). The strata exposed in the lower part of Fântânele Valley, at the northern end of Vălioara settlement, in the fork of the branching gully at the village boundary, and in the area around the Fântânele excavation area (Grigorescu et al., 1999; Vasile and Csiki, 2010; Csiki-Sava et al., 2023) belong to this local division of Unit 2.3 (Fig. 9D).

The Budurone beds (Fig 17C-D) outcrop on the eastern side of the lower and middle sections of Vălioara Valley, to the east and southeast of the village (Fig. 2). The cyclical fluvial-floodplain sequence described by Botfalvai et al. (2021) from the Budurone ravine containing site K6 that yielded some vertebrate remains is representative for this unit. Previous studies have also revealed the presence of a rich assemblage of microvertebrates and other associated fossil remains in other gullies running parallel to the valley containing site K6 (Grigorescu et al., 1999; Csiki et al., 2008).

Two facies associations can be distinguished within this unit: fluvial channel (FA 2), and floodplain (FA 3). The beds of FA 3 are built up by cycles of gravelly sandstone beds (Smg) and yellowish red mudstone deposits containing calcrete horizons and nodules (Fig. 17A-B). The fine-grained layers are also characterized by laminated fine-sand (Sl), and reddish variegated clay and paleosols (Pt, Ptc). The abundance of muscovite mica in all layers is indicative of disintegrated metamorphic debris. The cycles are normal-graded, with a thickness of around 1–2.5 m (Fig. 17B-D), although they can reach as much as 2.5–4 m. Within the beds of FA 3, fluvial beds of FA 2 occur with thicknesses varying between 10 cm and 1.5 m. The individual fluvial channels can be either deposited on top of each other, forming thick amalgamated bodies or else are isolated within floodplain fines. Channel fills usually show fining upward sequences, and are occasionally capped by fine sandy siltstones; these are the ones that host vertebrate remains in the Fântânele section.

Based on the FA proportions found in Unit 2.3, it likely represents distal alluvial fan environments (Table 2), where thick debris flow beds are less frequent and floodplain to fluvial sedimentation occur. The layers are tilted at 37° to the southeast in Fântânele Valley, and at 32° to the east in Budurone ravine. The basal contact of the unit with the underlying ones is largely unexposed. The scarce available data suggest a continuous transition from the underlying conglo-breccia (Unit 2.2), but the presence of lateral faults and

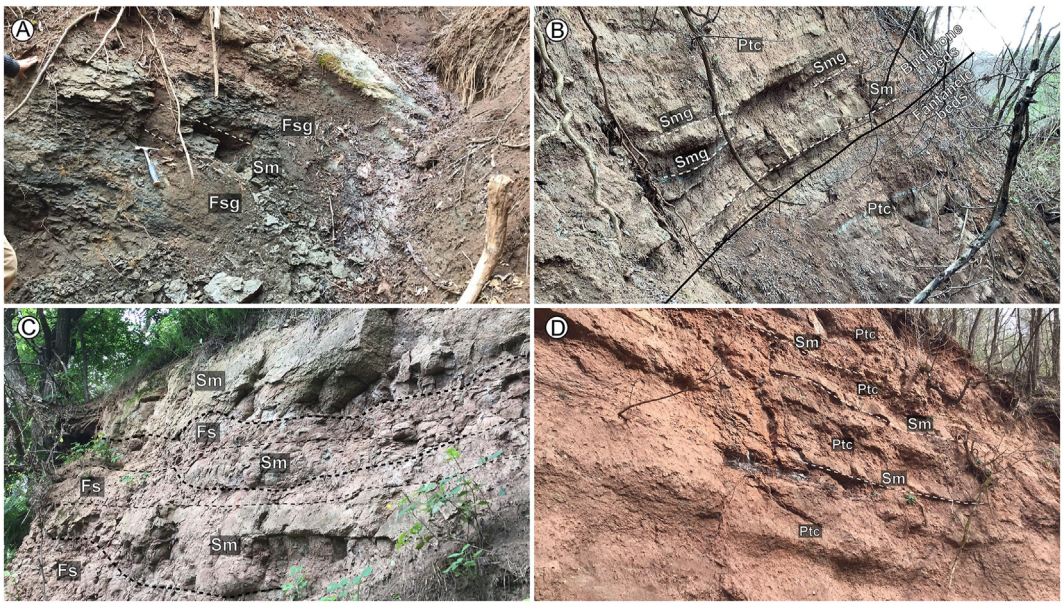

Fig. 17. Characteristics of the Fântânele and Budurone beds (Unit 2.3). Fânânele beds-type locality: greyish red, clayey-sandy (facies Sm), bone-bearing strata, (location LL73) (A); Fântânele beds-1, and overlying Budurone beds-2 (B); typical facies organization of the Budurone beds, with alternating Sm and Fs facies seposits (C); finer-grained sandstone (Sm), and sandy mudstones (Ptc) forming 1-1. 5 m thick cycles in the Budurone beds (D).

deformation bands parallel to Fântânele Valley probably means that this continuous transition is partly tectonically disturbed. In many of the outcrops, deformation bands and lateral fault scarps divide the sedimentary strata. The structural planes strike parallel to Vălioara Valley, and have steep dips in the vicinity of Budurone ravine.

Several sediment samples were collected from Unit 2.3 (see Supplementary information 1), focusing mainly on the close proximity of important vertebrate occurences from this unit such as Fântânele 1 microvertebrate site (e.g., Grigorescu et al., 1999; Csiki and Grigorescu, 2000; Vasile and Csiki, 2010 – sample P294), Budurone microvertebrate site (Grigorescu et al., 1999; Csiki et al., 2008 – sample BUD), K6 site (Botfalvai et al., 2021) and closely spaced/identical site VI of Kadić (1916 – sample P295), as well as the newly discovered site Fântânele-3 (Csiki-Sava et al., 2023 – samples P424 to P428). Most of these were collected from grey or greenish gray fine-grained beds for palynological analyses (given the purely continental nature of these deposits, no attempt was made to check for calcareous nannoplankton or foraminifera in Unit 2.3), except for sample BUD that was retrieved for detrital zircon U–Pb geochronometry from a grey sandstone bed directly overlying the bed that hosts the Budurone microvertebrate bonebed.

Of the palynological samples analysed from this unit, sample P294 proved to be quasi-barren, whereas sample P295 yielded only a few poorly preserved specimens, suggesting oxidizing conditions during and immediately after the deposition of the sampled beds. Nevertheless, the palynofacies identified in sample P295, composed mainly of gelified amorphous organic matter of entirely continental origin, independently supports the sedimentological interpretation of these deposits. Meanwhile, sample P425 (collected near site Fântânele-3) has proven remarkably rich, yielding a diversified and well-preserved terrestrial palynomorph assemblage dominated by angiosperm pollen referred to *Proteacidites* div. sp. (Fig. 7.19-20), a taxon also encountered in sample 6B (Neagului Valley, Unit 1.5). The assemblage also includes fern spores such as *Polypodiaceoisporites hojrupensis* and primitive angiosperm pollen with *Pseudopapillopollis praesubhercynicus* (Fig. 7.23), *Krutzschipollis crassis* (Fig. 7.22), *Trudopollis conrector* (Fig. 7.21) and *Subtriporopollenites constans* (Fig. 7.24). The corresponding palynofacies is represented by a mixed assemblage of translucent and opaque continental phytoclasts, including frequent large-sized cuticle fragments (Fig. 7.13); overall, the palynofacies suggests short-distance transport of the vegetal debris within a wider fluvial/deltaic setting. Meanwhile, the Proteaceae pollen frequently occurring in sample P425 is considered to be derived from a vegetation commonly associated with lignitic coaly deposits (Milne, 1998), and thus indicates a swampy/lacustrine sedimentary setting. This assessment is independently confirmed by the presence of the freshwater algae spore *Schizosporis* sp., also identified, albeit with a low relative frequency, in the same sample.

The taxon *Polypodiaceoisporites hojrupensis* (also reported from sample LL5-15-3 from South Ogradiilor Valley; see above) has its first occurrence around the Campanian/Maastrichtian boundary in the Tercis les Bains section from France (Siegl-Farkas, 2001), whereas *Pseudopapillopollis praesubhercynicus* and *Krutzschipollis crassis* have their currently accepted last occurrence in the basal Maastrichtian (Góczán and Siegl-Farkas, 1990; Ion et al., 1998; Bălc et al., 2024).

Overall, these biostratigraphic constraints suggest a probably earliest Maastrichtian age for this sample and thus for the Fântânele-3 site, as well. Interestingly, the palynological assemblage reported by Csiki et al. (2008) from the Budurone microvertebrate site, situated within the same unit but in a somewhat higher stratigraphic position, lacks the important marker taxon *Pseudopapillopollis praesubhercynicus*, suggesting that the age of this assemblage (and site) may be younger than earliest Maastrichtian, and (based on the estimated thickness of the unit) is thus probably an early (but not earliest) Maastrichtian.

Such an age assessment at Budurone is broadly supported by the detrital zircon U–Pb data derived from the BUD sample (Supplementary information 1 and 2). Unlike the other geochronology samples from the study area reported previously, the rich zircon grain population recovered from this sample is remarkable

in that it contains a large number of latest Cretaceous ('banatitic') zircons (51 out of 100), including many with relatively young crystallization ages (see Supplimentary information 2) unlike any other U–Pb age data previously reported from Haţeg Basin area and nearby regions (e.g., Gallhofer et al., 2015; Vornicu et al., 2023; this paper). Indeed, the calculated maximum depositional age (MDA) for this sample is 72.96 ± 0.97 Ma (Fig. 11D), and may be even somewhat younger, as it is definitively biased towards an older age value by part of the banatitic zircon sample that appears to originate from a more 'classical', ~79 Ma age magmatic source, already identified in other, stratigraphically lower geochronology samples (e.g. LL18). Such a young MDA and the high frequency of banatitic grains (51 %) within the BUD zircon population indicate the activation of a relatively young volcanic source around the Campanian/Maastrichtian boundary in the neighbourhood of Haţeg Basin. Furthermore, the abundance of banatitic zircons within this sample suggests that accumulation of the sampled bed was probably only slightly delayed relative to its calculated mean MDA, as stratovolcanic bodies (the potential source for these zircons, based on the nature of their parent magmatism; e.g., Gallhoferet al., 2015) are transient features swiftly dismantled by subsequent erosion (Ducea et al., 2015; see also similar discussion in Bălc et al., 2024: p. 17). Accordingly, we posit that deposition of the Budurone beds in this area took place sometimes during the later part of the early Maastrichtian, in good accordance with the available palynostratigraphy data (see above).

4.3. Structural settings

The structural setting of the mapped area was reconstructed using measurements as well as stratigraphic and morphotectonic features. During the measurements, the directions of faults, lateral displacements, thrusts, lithoclases, deformation bands and folds were recorded. The occurrence of strata tilting and indirect features, such as abrupt changes in lateral distribution of sedimentary units, the occurrence of fault breccias and fault clay, or the relationship between morphological features (valleys, ridges) and nearby measured directions also helped to interpret the observed phenomena. Based on these observations, several groups of structural features (S1-4) and deformation phases (D1-3) were distinguished, the former partially mentioned earlier but summarized here.

4.3.1. Description of structural features

The structural features observed in the outcrops are generally small in scale, with only a few centimeters of displacement in the case of faults, but they are typically found as dense, parallel planar layers, often nearly parallel to the stratification. The mapped area is overall characterised by a significant degree of shear deformation, already mentioned by Laufer (1925) as a phenomenon affecting both marine and continental strata. In clayey layers, shear planes are marked by slickenside lineations and, in places, by broken larger grains (even bone fragments). Due to the loose, fractured nature of the medium to coarse-grained depositss, fault zones can be recognised by the different colouration of the rock, their clayey nature, the roundness of the grains, and the occasional calcitic, limonitic fissure fills. The character of the displacements is given by the fibrous mineral steps and slickensides visible in the calcitic fissure fills.

The most prominent structural feature is the West-East striking fault line (S1) in the northern part of the study area, which also represents the boundary between the Upper Cretaceous deposits of Haţeg Basin and the crystalline basement rocks (Fig. 18). This major fault has been interpreted previously both as a normal fault (Lupu et al., 1993; Iancu et al., 2005) and a right-lateral strike-slip fault (Bărzoi and Şeclăman, 2010). The latter interpretation is also consistent with our observations and suggests either a NW-SE transpression or a SW-NE transtension. Although the fault surface is generally not exposed, the damage zone with associated fault-breccia, red-clayed cataclastite zone, and drag folds are dominant features in the mapped area (Fig. 18A, C, D respectively).

The planes showing smaller-scale displacement are arranged in two dominant structural directions, with strike directions NE-SW (S2) and NW-SE (S3), respectively. Both are mostly associated with oblique faults, whose kinematics can be both right and left (Fig. 19). The mapped structures suggest that the S3 displacements are younger than the S2 ones, as can be observed, for example, in the main branch of Ogradiilor Valley, where the former displaces the latter.

Three more subordinate structural directions were also observed, which also take the form of shear planes and appear as a few

Fig. 18. Appearance of the main boundary fault and the associated damage zone in the field: calcareous cemented fault breccia – L55 (A); fault scarp with 180/82 azimut and dip (B); cataclasic red clayey zones formed in the proximal alluvial fan deposits (C); shear zones (red) and drag fold in the proximal alluvial fan deposits – L66 (D).

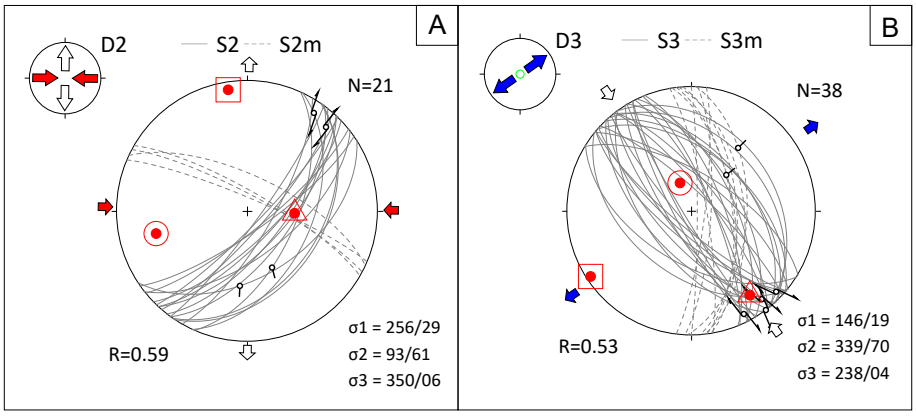

Fig. 19. Stereonet diagrams of structural elements and deformation phases. The Equal area stereograms (southern hemisphere projection) show the faults and the slickensides: structural elements S2 and S2m show a W-E compression, corresponding to deformation phase D2 (A); structural elements S3 and S3m show a SW-NE extension, corresponding to deformation phase D3 (B). Stereograms computed using the Win-tensor program (Delvaux and Sperner, 2003).

measurements only at a site. S2m is a group of generally right-lateral oblique faults with ~290-110 (WNW-ESE) strike, measured almost exclusively in the grey clayey beds. S3m is a structural direction with a ~0–180 (N–S) strike, a ~90° azimut and 60–70° dip. It can be associated with normal fault scarps, suggesting a W-E extension. These faults were observed in the upper Geat Valley and in Fântânele Valley close to the major (S1) fault. S4 contains near-vertical planes with a ~270–90 (W-E) strike, but no displacement direction was measured; they were more numerous on the hillside above Ciula Mică.

Fault-shear deformation affects both the marine deposits and the overlying continental strata. As the dip of the two formations is nearly similar, the displacements along the bedding planes are dominant in both. The measured directions cannot be distinguished by the separated units, although S3 is relatively more pronounced in the "grey Vălioara beds", which can be explained by the rheology of the rocks and the near parallel dip of the bedding planes to S3.

The dip of the marine turbidite deposits is generally steep (~67° on average), sometimes nearly vertical, and the sedimentary structures (e.g. solemarks, see Fig. 4B) show either an easterly or westerly dip, suggesting intense folding due to W-E compression. This trend in the marine turbidites is also confirmed by previous studies (Grigorescu and Melinte, 2001). The presence of boudin-structures in the sandstone layers (Fig. 4C) further indicates that this unit was exposed to shearing, parallel to the bedding plane.

The base conglomerate (Unit 1.1), the lower conglo-breccia (Unit 1.4) and the grey Vălioara beds (Unit 1.5) are tilted approximately NE, with a dip of 60° over most of the area but can reach 70–80° in the west. Towards east, the upper conglo-breccia (Unit 2.2) as well as the Fântânele and Budurone beds (Unit 2.3) become gradually less steeper (~30°) and switch to east-dipping (Fig. 8).

The bedding planes of the "lower" Vălioara breccia (Unit 1.3) show greater variability. Near the northern main fault the strike of the strata turns to ~290–110 (WNW-ESE) nearly parallel to the main fault, while at locations away from the main fault, similarly to the lower conglo-breccia and the grey beds, the dip direction is typically NE. At sites close to the main fault, a cataclastic breccia with a very similar appearance to the breccia can be found, which marks the damage zone along the fault and is difficult to be distinguished from the original sedimentary breccia (Fig. 18C).

In the immediate vicinity of the main fault, folded zones of clastic deposits were detected (Fig. 18D). The zones may have been former sedimentary strata associated with the proximal alluvial fan (Unit 1.3), whose structure was rearranged by the shear stress of the main fault, and the larger flat clasts became more oriented. The folding is indicative of a ~NW-SE compression.

4.3.2. Deformation phases

The northern main fault, interpreted as a strike-slip fault elongated in the present-day W-E direction, can be related to a present-day NW-SE transpression and perpendicular transtension tectonics (hereafter referred to as D1). Based on the size of the structural element (= main fault − S1), it was active for a long time and may have favoured the creation of an elongated pull-apart basin through its activity. This phase may also have been associated with the exhumation of crystalline schists in the vicinity of the study area (on the basin margins), which provided the debris material for the breccias (and subsequent deposits). Due to the transtension, the basin filling sequence was tilted in the direction of the basin depocenter.

The formation of S2 structures occurred after the deposition of thick clastic deposits filling the pull-apart basin and is associated with a W-E compression environment (hereafter referred to as D2). During this process, the more ductile deposits (such as the marine turbidites) were folded, and the SW-NE striking right lateral faults observed in the area may have formed.

The S3 structural elements displace the faults and the folded beds resulting from the previous structural phase, and are therefore younger than those. They are characterised by NW-SE oblique faults, which are generally normal component right lateral displacements and dip to the NE. This direction is associated with a SSW-NNE transtensional stress field (hereafter referred to as D3) in which the synthetic Riedel shears (e.g. Naylor et al., 1986) correspond to the observed structures. The displacement surfaces are mostly shear faults along the bedding planes and mainly occur in the grey Vălioara beds, but can also be found in all other units. In the plastic turbidite layers, which were already steeply inclined to the NE due to D1 tilting, such a stress field could have produced small-scale drag folds and boudin structures. The direction of the S3m structures also coincides with the direction of the antithetic Riedel shears of this stress field. Both the S3 and S3m structural directions had an impact on the formation of the present day geomorphology, as the main valley directions in the area are parallel to them. D3 also includes the folds with a SW-NE striking axial plane observed near the main fault, which deformed the layers of the neighboring coarse-grained unit ("lower" Vălioara breccia; Unit 1.3) indicating that the main fault was also active during this phase.

Structures associated with S4 are not distinguished here as the result of a separate deformation event, as few measurements are included. Based on the orientation (~W-E steep faults), this deformation could also be a lateral displacement associated with D3. Although they are parallel to the main fault, they are certainly not

related to it because they displace the uppermost Cretaceous clastic sedimentary sequence.

5. Discussion

The detailed geological mapping was carried out primarily to obtain a detailed lithostratigraphic framework for the Geat Valley – Vălioara area and to place the known vertebrate sites in the reconstructed sedimentary sequences (Figs. 2, 8, 9, 20). To that end, the geological make-up of the mapped area had to be established both spatially and temporally, considering all the newly assembled and previously published data. These effort resulted in an integrated geological dataset serving as a model for the stratigraphic and structural evolution of the area, discussed below.

5.1. Sedimentary-stratigraphic evolution of the uppermost Cretaceous in the northwestern Haţeg Basin, and implication for its vertebrate fossil record

The Densuș-Ciula Formation around Vălioara was interpreted so far as being deposited by braided rivers, in which deposits generally suffered short transportation and were rapidly accumulated (Grigorescu, 1983, 1992, 2005). Our recent data, however, allow a more accurate reconstruction of the temporal and spatial evolution of the northwestern Haţeg Basin area near the end of the Cretaceous (see Fig. 20).

The direct, albeit erosional, contact between the marine turbidites of the Răchitova Formation representing the lower Campanian to lower part of upper Campanian and the overlying fossiliferous Densuș-Ciula Formation was observed in Geat Valley, represented by a slight angular unconformity. Deposition of the first continental units overlying the turbidite sequence (the base conglomerates – Unit 1.1 – and interbedded pyroclastic and volcanoclastic bodies – Unit 1.2), corresponding to the Lower Member of the Densuș-Ciula Formation (Grigorescu, 1992), was dated using detrital zircon U–Pb geochronology. This was carried out on altered and partly reworked tuffitic intercalations deposited on top of the turbidites (Fig. 10C-D), most probably in the latest early to earliest middle part of the late Campanian (Fig. 20). Together these age constraints leave a short temporal window around the boundary between the informal early and middle parts of the late Campanian (see Methods chapter) during which marine deposition ceased and continental conditions were installed, more or less concomitanly with a flare-up in banatitic magmatic activity in nearby areas. During this time interval, the tilting and emergence of the marine beds before their erosion was initiated. Since it was noted that the extent of erosion increases in S and SW direction in present-day azimuth (Grigorescu and Melinte, 2001), the former subaerially exposed areas may had been in this direction at the start of continental sedimentation. In the study area, transport direction data confirm this assessment, with the imbrications measured in the base conglomerate (Unit 1.1) showing a present-day NE-oriented flow direction (Fig. 3A). Furthermore, the presence of igneous clasts and possible volcano-sedimentary deposits within the base conglomerates attests to contemporaneous volcanic activity taking place in the catchment area, to the west of Vălioara.

Our new age constraints have important implications for the stratigraphic framework of the Upper Cretaceous deposits from northwestern Haţeg Basin. Sofar, it was assumed that deposition of the continental beds (grouped in the Densuș-Ciula Formation) started sometime during the early Maastrichtian (Grigorescu, 1992; Csiki-Sava et al., 2016), although a somewhat earlier date for this event (at the Campanian/Maastrichtian boundary) had been suggested tentatively by Melinte-Dobrinescu (2010) mainly based on the assessed age of the underlying turbidites of the Răchitova Formation. New biostratigraphic/geochronologic constraints from around the unconformable Răchitova/Densuș-Ciula formational contact indicate that this lithostratigraphic boundary, marking an important environmental shift as well as contemporary tectonic and magmatic activity, should be placed significantly earlier, in the early part of the late Campanian, and that sedimentation of the volcano-siliciclastic Lower Member of the Densuș-Ciula Formation (represented in the study area by Units 1.1 and 1.2) actually covers a large portion of the middle and later parts of the late Campanian (Fig. 20). Remarkably, this reinterpretation is in line with recently published igneous zircon U–Pb geochronology results from Densuș Valley (Vornicu et al., 2023). There, the Lower Member is significantly better developed, and usually coarser-grained volcanoclastic beds represent a large proportion of the outcropping succession; dating of andesitic and dacitic volcanoclasts from these beds have yielded late early Campanian to earliest late Campanian (81.88 ± 0.17 Ma to 80.22 ± 0.25 Ma) crystallization ages, indicating subaerial magmatic activity by this time already, quasi-contemporaneously with the cessation of marine deposition and initiation of continental sedimentation. Accordingly, we propose that the base of the continental Densuș-Ciula Formation should be placed in the middle part of the upper Campanian (Fig. 20).

In the study area, the mixed siliciclastic-volcanoclastic deposition corresponding to the Lower Member of the Densuș-Ciula Formation is less well developed than in the Răchitova-Densuș sector (western part of Haţeg Basin), and is covered by the coarse-grained, laterally interfingering deposits of Units 1.3 and 1.4. These deposits mark the next stage in the evolution of the basin, interpreted as a longitudinal, rapidly subsiding pull-apart basin, in which alluvial fans developed and were fed by source areas that became more and more elevated (Fig. 21A). One of the basin's marginal faults is the main boundary fault (S1) identified during the fieldwork. The “lower” Vălioara breccia (Unit 1.3) formed continuously during this stage along the main fault while this was active, and was interfingered with more distal, alluvial deposits at several stratigraphic levels (Fig. 21B). As is typical of terrestrial pull-apart basins in general (Noda, 2013), fluvial and floodplain facies have developed towards the interior of the basin, away from the bounding marginal faults, and alluvial fans formed at the basin margins due to the greater relief existing there. The sediments of the basin margin alluvial fans were derived mainly from the footwall of the fault. The main fault of the study area was located on the present-day northern side of the basin, so that sediment transport direction was from present-day north towards the south, which identifies the metamorphic formations of the Poiana-Ruscă Mountains as the source of the clastic material (Fig. 21B). At the same time, another fault was active along the southern margin of the basin which potentially also had alluvial fans attached to it, but these preferentially accumulated metamorphic material from the Retezat Mountains and transported it from south northwards, as confirmed by previous sedimentological and petrological studies of uppermost Cretaceous alluvial deposits of the Sînpetru Formation and potentially correlative units (Van Itterbeeck et al., 2004; Bojar et al., 2010). Away from the basin margins, however, axial transport parallel to the basin elongation was typical, corresponding to today's west-east direction, a transport direction that was indeed documented by us in the grey Vălioara beds (Unit 1.5) and the red cyclic deposits (Unit 1.6) (Fig. 21C).

The coarsening and reddening of the debris towards the basin rim have both been noted previously (Grigorescu, 1992), but the basin was then considered to be post-tectonic in nature. Given the largely alluvial nature of the deposits representing this stage, without any significant contribution from magmatic input, Units 1.3 and 1.4 should be regarded as the basal units of the Middle Member of the Densuș-Ciula Formation as defined by Grigorescu (1992).

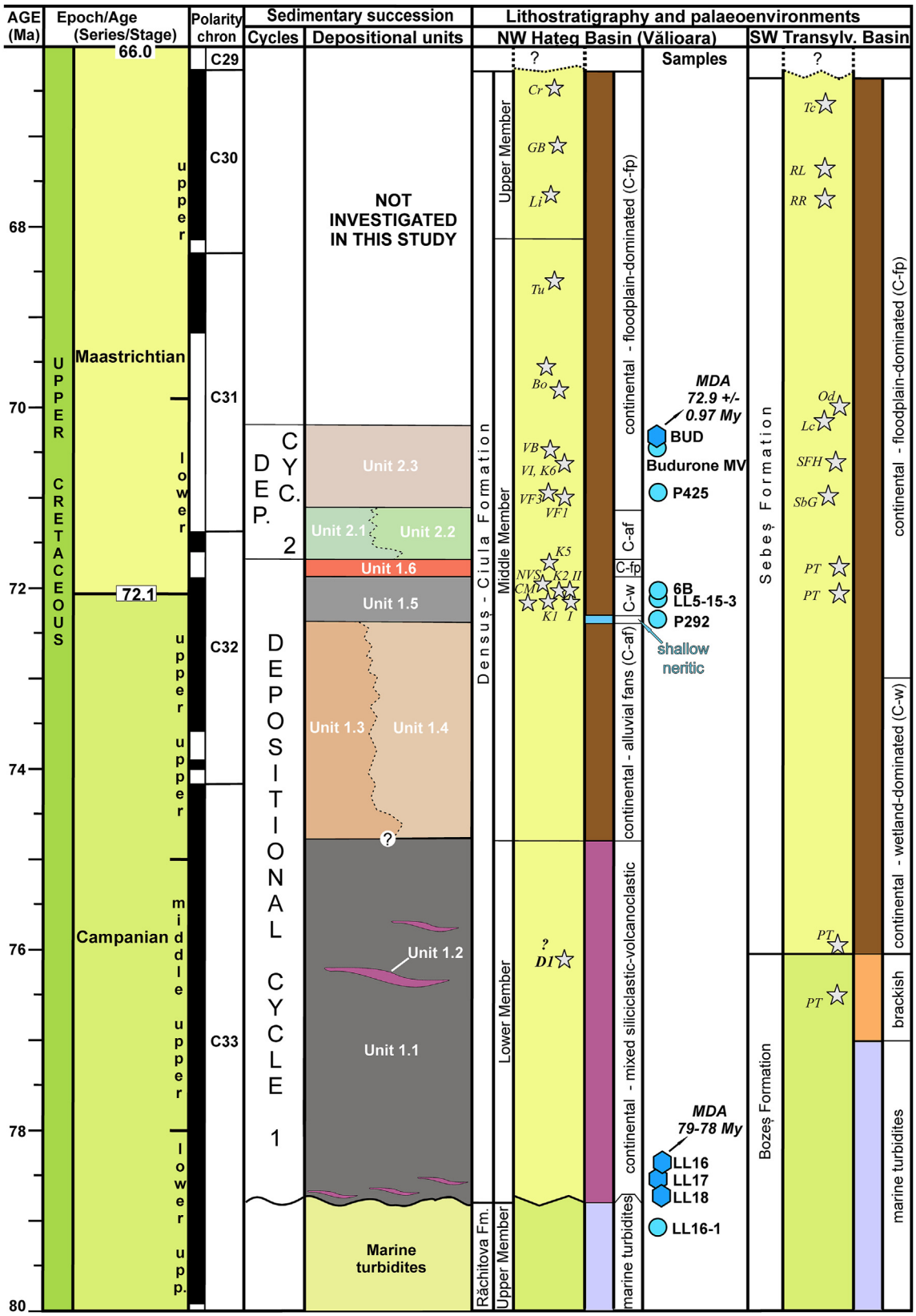

Fig. 20. Synthetic overview of the sedimentological and stratigraphical results, Vălioara study area, with reinterpretation of the chronostratigraphy and sedimentological make-up of the lower part of the continental Densuș-Ciula Formation (Lower Member and lower part of Middle Member), Hațeg Basin, with main depositional cycles and units (color coding according to Fig. 2), interpreted palaeoenvironments, approximate position of important vertebrate occurrences (grey stars), and most significant samples reported (light blue circles – biostratigraphy, dark blue hexagons – geochronology; see details in text; Budurone MV - palynological sample reported by Csiki et al. (2008) from the Budurone microvertebrate bonebed), in comparison with the Sebeș Formation, southwestern Transylvanian Basin; updated and completed from Csiki-Sava et al. (2016) based on Bălc et al. (2024), Țabără and Csiki-Sava (2024), and present study. Abbreviations of localities and sites (see also Csiki-Sava et al., 2016; Botfalvai et al., 2021): I, II, VI – Kadić's sites I, II and VI,

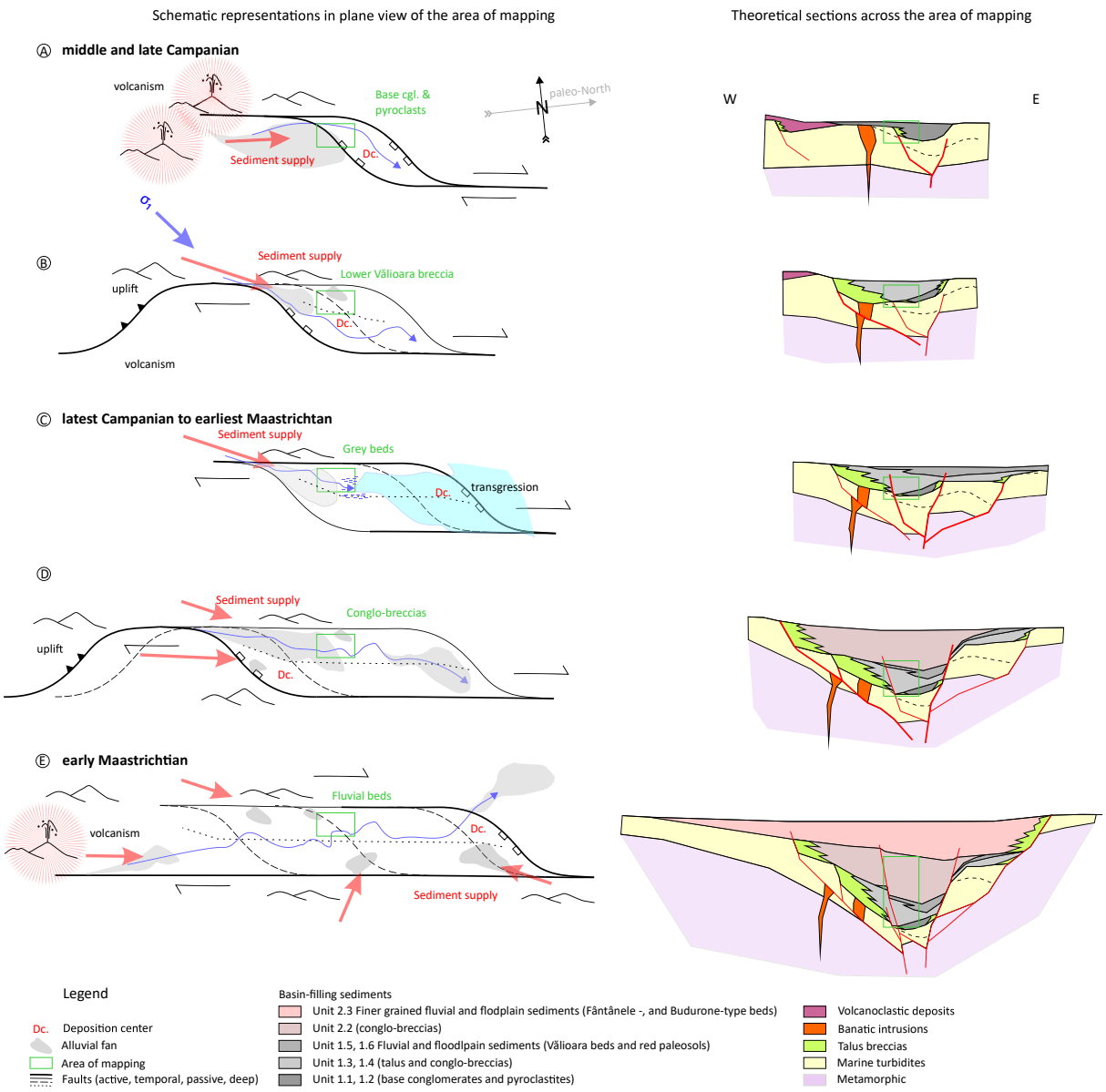

Fig. 21. Reconstruction of the main stages of the latest Cretaceous basin evolution in the northwestern Hațeg Basin.

Unfortunately, no direct chronostratigraphic constraints are currently available for these units, except their intermediate geometric position between the geochronologically constrained Lower Member and the overlying finer-grained alluvial units that end the first sedimentary cycle (see below). The grey Vălioara beds (Unit 1.5) include organic matter-rich deposits of floodplain lakes connected to the river systems, besides the wetland-type environments suggested previously by Botfalvai et al. (2021). Lithologically, they would indicate a more distal (i.e., away from the basin margin) depositional setting within the pull-apart basin, but as these beds can be traced laterally almost to the main fault, they are here interpreted instead to represent a subsequent evolutionary stage characterized by expansion of more quiet, lower-relief energy environments, at a time of important decrease in relief difference between the erosion base and the northern source area (Fig. 21C).

This study showed that, marine intercalations were indicated locally in the basal part of Unit 1.5 by the occurrence of rare individuals of dinocysts and calcareous nannoplankton, as well as by a marine palynofacies suggesting relatively shallow, nearshore environments (see also Botfalvai et al., 2021). Their presence suggests a transient transgression event that may have also temporarily raised the erosion base in the area (Fig. 21C). Available biostratigraphic data place this event in the latest Campanian, close to the Campanian/Maastrichtian boundary. Two major sequence boundaries roughly corresponding to this time interval had been identified by Haq (2014), with short-term (third-order) sea-level highstands occurring at aprox. 74 Ma and 72.4 Ma, respectively, and any of these could potentially account for this short-lived marine ingression. However, it is far more likely that – given the tectonically active intermontane setting of the study area – this

Bo – Boița, CM – Ciula Mică, Cr – Crăguiș, D1 – Densuș, GB – General Berthelot, K1, K2, K6 – sites K1, K2 and K6 of Botfalvai et al. (2021), Vălioara, Lc – Lancrăm, Li – Livezi, Nvs – New Vertebrate Site, Vălioara, Od – Oarda de Jos, PT – Petrești (different sites), RL – Râpa Lancrămului, RR – Râpa Roșie, SbG – Sebeș-Glod, SFH – Secaș Fetii Hill, Tc – Teleac, Tu – Tuștea, VB – Vălioara Budurone, VF1 – Vălioara Fântânele 1, VF3 – Vălioara Fântânele 3; '?' marks tentative (i.e., not well constrained) position of sites/boundaries.

event is a reflection of locally acting dynamic topographic (i.e., eurybatic) effects instead of being purely eustasy-driven (see Haq, 2014 for comments on these terms). The brevity of this ingression event is emphasized both by the limited areal presence of the corresponding deposits (identified only in the upper reaches of Ogradiilor Valley) and by the fact that biostratigraphic constraints from slightly higher-lying deposits of Unit 1.5 (e.g., samples 6B, LL5-15-3) indicate the re-establishment of purely continental settings by the earliest Maastrichtian (Fig. 20).

The well-developed red palaeosols (Unit 1.6) covering the grey, bone-rich Vălioara beds (Unit 1.5) also represent a quieter accumulation period when aggradation nearly ceased or largely shifted to other areas. However, unlike the underlying unit, they document a relative expansion of better-drained floodplain environments and more widespread pedogenesis. Macroscopic, outcrop-level examination of these brick-red calcareous palaeosols pointed out high levels of similarity to well-developed pedogenic successions described previously from the middle part of the Densuș-Ciula Formation at Tuștea, as well as from roughly correlative continental beds cropping out either along the Bărbat River south of Pui in Hațeg Basin, or else in the southwestern Transylvanian Basin (e.g. Therrien, 2005; Botfalvai et al., 2017), and that were interpreted as indicative of relatively dry, well-drained and higher-lying distal floodplain environments. Meanwhile, they are clearly different from the palaeosol-bearing successions reported from the uppermost Cretaceous Sînpetru Formation or the coeval 'Râul Mare beds' cropping in the central part of Hațeg Basin, that are quantitatively dominated by grey-green hydromorphic palaeosols, with subordinate brown-red calcareous ones, indicating a dynamic palaeoenvironmental mosaic of poorly to at most moderately drained floodplain settings (Van Itterbeeck et al., 2004; Therrien, 2006).

Moving up-sequence, an episode of renewed erosion and increased sediment influx is indicated by the re-appearance of coarser-grained sedimentary successions (Units 2.1 and 2.2). These units largely replicate the lithofacies and patterns of lateral interfingering described previously in the case of Units 1.3 and 1.4, with coarser proximal alluvial facies found near the main boundary fault (Unit 2.1), replaced farther away from the basin margin by generally finer-grained floodplain and fluvial deposits (Unit 2.2; Fig. 21D). Accordingly, these units are interpreted to mark the basal part of a second, distinct depositional sequence, most probably due to a second episode of tectonic activation along the northern main fault and source area and/or to a lateral shift of the axes of major sediment transport back into the study area. As a further similarity with depositional sequence 1, these coarse, conglomerate- and breccia-dominated units are replaced up-section by dominantly finer-grained deposits of Unit 2.3 (Fântânele and Budurone beds; Fig. 21E) hosting again several important vertebrate fossil accumulations (e.g., sites Fântânele-1,2,3 and the Budurone microvertebrate site). Available biostratigraphic and geochronologic constraints from Unit 2.3 place its basal part (Fântânele beds) into the lower part of the lower Maastrichtian, but also indicate that it extends into the upper part of the lower Maastrichtian within the Budurone beds (Fig. 20). Incidentally, these constraints further underline the magnitude of tectonic reactivation at this stage of basin evolution, with a large amount of coarse detritic material being brought into the basin during a relatively brief amount of time during the early part of early Maastrichtian, a time interval bracketed by the largely isofacial grey beds of Units 1.5 and 2.3, respectively. We finally emphasize that despite the rather important sedimentological and palaeoenvironmental changes tracked by us across the largest part of depositional sequence 1 and within depositional sequence 2, all these deposits belong to the lower part of the Middle Member of the Densuș-Ciula Formation, as still younger deposits of this subunit are known to extend farther to the east, beyond the borders of our study area (see Grigorescu and Csiki, 2008; Vasile et al., 2011).

There are several implications of these lithostratigraphic/chronostratigraphic, sedimentary evolution, and palaeoenvironmental reassessments resulting from the newly acquired data from the Vălioara area. The first of these concerns currently existing scenarios about the overall evolution of the latest Cretaceous Hațeg Island. Until recently, the main emergence phase of this landmass was placed in the second part of the late Campanian, based on the biostratigraphically well constrained marine-to-continental transitional succession from Petrești, in the southwestern Transylvanian Basin (e.g., Vremir et al., 2014; Ţabără et al., 2022; Bălc et al., 2024). There, a gradual base level fall first led to establishment of brackish-water environments up until the second half of the middle part of late Campanian, with the first moments of fluvial deposition within an estuarine-coastal lowland setting placed at around 75–76 Ma, roughly coeval with a moment of important magmatic (banatitic) activity (Bălc et al., 2024), but otherwise lacking episodes of coarse-grained sedimentation almost completely. By contrast, our Geat Valley data documents a somewhat earlier emergence in the western Hațeg Basin areaat the beginning of the middle part of the late Campanian, and with clearly distinct sedimentary and magmatic signatures of this event, as marked by the accumulation of the mixed volcanoclastic-siliciclastic succession of the base conglomerate (Units 1.1 and 1.2). Together, these indicate a tectonically and magmatically more active setting and even a brief period of unconformity-producing tectonic activity that ended abruptly the preceding marine deposition. These differences emphasize the presence of high levels of spatial and temporal heterogeneity among the geological evolution pathways that characterized different parts of Hațeg Island, underscoring its very dynamic history at the end of the Cretaceous.

Besides these sedimentological differences, there are also important distinctions between the early fossil records of the uppermost Cretaceous of Hațeg Basin, respectively that of the southwestern Transylvanian Basin (Csiki-Sava et al., 2016). In the southwestern Transylvanian Basin the first, albeit isolated, remains of continental vertebrates are recorded in the still brackish segment of the succession corresponding to the middle part of the upper Campanian, and the first indications of a diversified continental vertebrate fauna derive from the uppermost Campanian (Vremir et al., 2014, 2015; Bălc et al., 2024). Meanwhile, the first known vertebrate fossil occurrences in our study area are located most probably in the lowermost Maastricthtian near to the Campanian-Maastrichtian boundary, postdating those from the Transylvanian Basin by about 3–4 Ma. Admittedly, however, the generally coarse nature of the older continental sedimentary record from the Vălioara area is not favourable to fossil preservation, thus the differences we note may be partly biased by environment-driven preferential preservation of fossils.

On the other hand, the oldest known important fossil accumulations from the Vălioara area (K1, but especially K2 and Nvs; see also Botfalvai et al., 2021) reveal a more diversified faunal assemblage compared to that from Petrești, with significant presences of taxa otherwise common on the former Hațeg Island like the basal testudine *Kallokibotion*, the hadrosauroids and (in particular) the titanosaurs, all of which are currently unreported from the Petrești succession (Vremir et al., 2014). Furthermore, our new age constraints provide further support for the assessment of Botfalvai et al. (2021) according to which the local continental vertebrate assemblages are probably the oldest ones documented in Hațeg Basin. Nonetheless, in order to more properly understand the place and importance of these local assemblages in the evolutionary history of the Hațeg Island palaeofaunas, a detailed investigation of

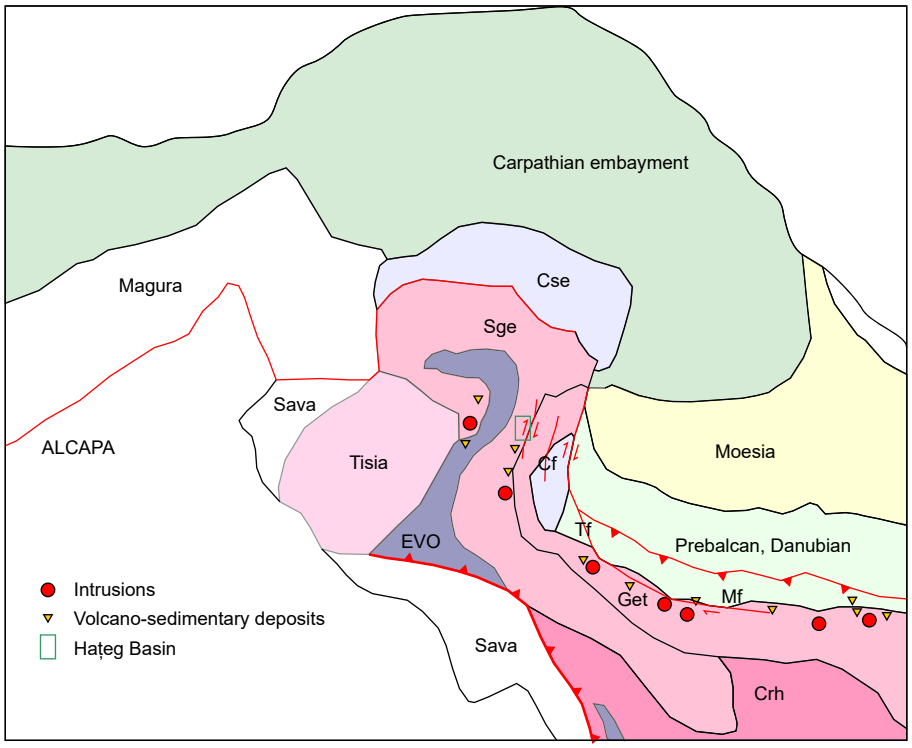

Fig. 22. Palinspastically reconstructed position of Hațeg Basin (boxed area) and the right-lateral strike-slip fault that generated the latest Cretaceous pull-apart basin, in relation with the regional plate-tectonic setting. The latest Cretaceous (Maastrichtian) palaeogeography is based on palaeomagnetic data (Pătrașcu et al., 1993; Gallhofer et al., 2015; van Hinsbergen et al., 2020). Sge: Supragetic Unit, Get: Getic Unit, Cse: Ceahlău-Severin Unit, EVO: East Vardar Ophiolites, Crh: Circum-Rhodope, Mf: Maritsa Fault, Tf: Timok Fault, Cf: Cerna Fault.

the newly discovered rich fossil material is required – an effort that is currently underway (e.g., Magyar et al., 2024).

5.2. Reconstruction of Late Cretaceous basin development

Arguments for the activity of the main fault and for the syn- instead of post-tectonic nature of the continental lower Densuș-Ciula Formation are presented here through a reconstruction of the Late Cretaceous tectono-structural evolution of the Hațeg Basin area (Fig. 22). The location of Hațeg Basin within a regional plate tectonic setting is a key factor in determining the possible model that synthesizes convincingly the explanatory interpretations derived from our observations. Therefore, although our specific study area is more spatially restricted, our results are discussed starting from regional-scale context and phenomena.

The Densuș-Ciula Formation is one of the cover units of the major Getic Nappe tectonic unit. Due to late Campanian to early Maastrichtian southwest-to-northeast plate motions, the contemporaneous stress field was characterized by a W-E compression, which, considering a post-Cretaceous clockwise rotation of nearly 90°, corresponds to the present-day NNW-SSE orientation in this area of the Getic unit (Pătrașcu et al., 1993; Mațenco and Schmid, 1999; van Hinsbergen et al., 2020). The Getic unit moved towards and overthrusted the Severin and Danubian units during the latest Early to Late Cretaceous; during the same time period, a piggy-back basin was formed behind the arc of the main thrust front, in which marine sediments, mainly turbidites were deposited over a large area during the Cenomanian to early late Campanian, including within Hațeg Basin (Grigorescu and Melinte, 2001; Willingshofer et al., 2001; Iancu et al., 2005; Melinte-Dobrinescu, 2010; Țabără and Slimani, 2019). The final, latest Cretaceous accretion of the Getic units (corresponding to the second Getic/Laramian tectonic phase) was roughly NE-vergent, corresponding to today's SE, ESE direction, and caused a displacement of more than 100 km (Iancu et al., 2005; Golonka et al., 2006). Magmatic activity developed along the entire subduction line, forming volcanic arcs along faults south of the piggy-back basin, partly due to transtensional movements, and in some places volcanic-volcaniclastic sediments deposited simultaneously with the deepening of dextral pull-apart basins (Gallhofer et al., 2015). Dextral shear propagated westward between the colliding plates as the Apulian plate moved NE-ward along the rigid Moesian Platform.

The next tectonic phase was mainly characterised by right lateral displacements between two crustal segments: the superposed Danubian-Severin-Getic units with a greatly thickened crust through nappe stacking, and the remainder of the Getic-Supra-Getic units; it coincided with the beginning of the "Danubian unroofing" event, i.e. the start of the erosion of the nappe cover stacked on top of the lowermost, Danubian unit in the South Carpathians (Willingshofer et al., 2001). The uplift has caused erosion over most of the area of the western Southern Carpathians, but simultaneously a rapidly deepening pull-apart basin has formed roughly along the line of the former piggy-back basin, the basal sedimentary succession of which is documented in the study area by the present research.

Previous studies generally emphasized the post-orogenic character of Hațeg Basin, which led to the deposition of talus-breccia, then alluvial debris cones, and finally fluvial and occasional lacustrine deposits within the Densuș-Ciula Formation (e.g., Grigorescu, 1983, 1992). Although we consider this reconstruction of local tectono-sedimentary evolution as largely correct, there are nevertheless several indications that sedimentation was syn-tectonic rather than purely post-tectonic, and that the formerly active Danubian-Getic continent-continent collision zone

(including the Haţeg Basin area) was already shifted into the peri-orogenic zone, where orogenesis in the Wilsonian sense (Wilson et al., 2019), as a phase of the Wilson cycle, had indeed already been completed. These peri-orogenic zones are characterised by thick sedimentary successions, including turbidites and volcano-sedimentary deposits as pre- and synorogenic sediments, and also by thick molasse-type deposits in the late and post-orogenic phases (François et al., 2022). In the study area, we encounter both of these types of successions intertwined, since the Densuş-Ciula Formation itself is an intramontane molasse, but the volcanoclastic deposits and reworked igneous clasts in the lower part of the formation, overlying marine turbidites, are related to synorogenic magmatic activity (i.e. banatites) found to the west (Bojar et al., 2005; Iancu et al., 2005). The banatites are associated with the Laramide phase of the Alpine orogeny (Berza et al., 1998; Iancu et al., 2005), and currently available dating suggests that this magmatism began in the late Turonian (89.48 ± 0.35 Ma) and continued into the Campanian-earliest Maastrichtian (74-71 Ma; Strutinski, 1986; Gallhofer et al., 2015). The well-developed volcano-sedimentary sequences of the Rusca Montană Basin, in the immediate western vicinity of our study area, also date from this period (Strutinski, 1986; Pătraşcu et al., 1993). During the Late Cretaceous these basins were located along a several hundred km-long line including other dextral pull-apart basins (in Timok and Srednogorje) that also host similar uppermost Cretaceous (Campanian-Maastrichtian) stratigraphic sequences (Banjesevic, 2010; Gallhofer et al., 2015).

The peri-orogenic basin formation and right lateral strike-slip displacement documented by our data for the northwestern Haţeg Basin is therefore not a local but a regional phenomenon, one that was active for an extended time period due to its size, and the easternmost member of this displacement front, the Maritsa Fault, was demonstrably operational in the early Late Cretaceous (Gallhofer et al., 2015). The Haţeg Basin, formed as a dextral pull-apart basin, may have been part of the horsetail structure at the continuation of the Cerna-Timok Fault System, at the then end of the displacement zone (Fig. 22), and based on palaeomagnetic measurements (Pătraşcu et al., 1993) its contemporary orientation was indeed parallel to it. The rapid deepening of the Haţeg molasse basin is indicated by the thick (approximately 2500−4000 m) uppermost Cretaceous continental sequence deposited. In the mapped area, the association of the breccia layers with the main fault further supports the syntectonic nature of the basin-filling sequence.

5.3. Post-Cretaceous basin development

In the mapped area, no post-Cretaceous deposits predating the Quaternary are currently present, so the post-Cretaceous evolution of the basin can only be inferred from the mapped structural elements and the data available in literature. The interpretation of the observed structures is thus here related to the known wider-scale episodes of regional geological history, referred to in the following text, and is discussed accordingly.

Among the structural elements, the formation of the folded and sheared structures (D2) can be explained by regional structural motions that caused orogenic-parallel extension and then clockwise rotation of about 50° in the Southern Carpathians during the Paleogene (Maţenco and Schmid, 1999; Fügenschuh and Schmid, 2005; Iancu et al., 2005). The main activity of the Cerna-Timok Fault System south of the study area can also be dated to this period (Linzer et al., 1998; Krézsek et al., 2013; Krstekanić et al., 2021). The rotation can be traced well by the track of these faults and took place in a W-E compressional force field (Maţenco and Schmid, 1999), during which the previously NNE-SSW positioned (Pătraşcu et al., 1993) Haţeg Basin and its surroundings became WSW-ENE striking. The study area itself was therefore still in a dextral shear force field, but whereas the Late Cretaceous to middle Paleogene was dominated by transtension, at the end of the Paleogene this was replaced by transpression that could conceivably also produce the larger, basin-scale deformations (e.g. folds) associated with D2. The main fault of the mapped area may also have been reactivated in this stress field, but the main movements were probably along SW-NE striking lateral displacements and oblique thrusts, which are typical of the restraining bend of a transpressional strike-slip fault system (Mann, 2007).

The youngest identified deformation event (D3) had a major impact on morphotectonics, producing NW-SE strike-slip fault-shear structures that deformed the mapped units, and especially those that are softer, such as the grey bone-bearing Vălioara beds (Unit 1.5) and sometimes even the fossils themselves. Fractures of this orientation may have been generated by the Middle and Late Miocene structural phases identified by Maţenco and Schmid (1999). The former was characterised by a SSW-NNE transtension, the latter by a NW-SE transpression stress field. Since by this time, the wider study area was already close to its present-day position (Linzer et al., 1998), and we mainly observed normal component oblique displacements on the fractures, we propose that the transtensional stress field could be the main cause of the deformation. Due to the previous deformations, the Upper Cretaceous strata were parallel to the faults by this time, so shear deformations along the bedding planes could easily occur. Nevertheless, as Middle Miocene (Badenian - lower Sarmatian) shallow marine formations found in Haţeg Basin and deposited on top of Paleogene erosion surface are affected by the NW-SE strike-slip fault system (Lupu et al., 1993), we hypothesize that both Miocene structural phases left their mark on these deposits; however, deciphering the post-Cretaceous basin development more accurately is beyond the scope of the present work.

6. Conclusions

The geological mapping realized recently in the Geat Valley - Vălioara area (northwestern Haţeg Basin), involving GIS recording, as well as sedimentological, structural geological and petrological studies, covered an area of about 10 km^2 that hosts some of the palaeontologically most important vertebrate sites known from the Haţeg Basin area. These geological investigations were complemented by intense exploration for, and excavation of, vertebrate fossil sites, together with a broad coverage of palynological and marine micropalaeontological (calcareous nannofossil and foraminifera) investigations as well as zircon U−Pb geochronology, in order to better constrain the ages of the different sedimentary successions cropping out in the study area and to refine their palaeoenvironmental interpretation. The synthesis of the newly amassed data from this complex multiproxy research contributed to a more detailed understanding of the tectonic and palaeoenvironmental evolution of this area during the latest Cretaceous, with the following main results:

1. The new field data and observations demonstrate that the major environmental shift from marine to continental deposition in Haţeg Basin, accompanied by important contemporary tectonic

and magmatic activity, occurred significantly earlier than previously considered, in the early part of the late Campanian, and that the lowermost part of the Densuș-Ciula Formation – once thought to belong to the Maastrichtian – covers a good part of the middle and late Campanian as well.
2. Two vertically superimposed fining upward depositional cycles could be separated within the uppermost Cretaceous continental basin fill succession from this area, both characterized by an upward increase in the proportion of fluvial and floodplain deposits in tandem with a decrease in the prevalence of proximal alluvial fan deposits. Significant fossil vertebrate assemblages discovered in both the lower (K2, Nvs sites) and the upper (Fântânele and Budurone sites) depositional sequences accumulated in largely similar palaeoenvironments (e.g. fluvial deposits formed during periods of lowered sedimentation rates) but represent different deposition times.
3. We identified minor marine intercalations locally in the basal part of the fossil vertebrate-bearing grey Vălioara beds (Unit 1.5), indicated by the occurrence of rare individuals of dinocysts and calcareous nannoplankton, as well as of a marine palynofacies that suggest relatively shallow, nearshore environments. The presence of these intercalations documents a transient transgression event that may have also temporarily raised the erosion base in the area; available biostratigraphic data place this event in the latest Campanian, close to the Campanian/Maastrichtian boundary.
4. Deposition of the lower part of the continental Densuș-Ciula Formation (investigated in the study area) took place associated with intermittent subsidence of a syntectonic dextral pull-apart basin. This rapidly subsiding basin was formed during the late Campanian in a peri-orogenic zone, coeval with the banatitic magmatic activity, and within a trans-tensional stress field along a N–S (E-W, in present-day coordinates) striking tectonic line.
5. The highly diverse vertebrate sites excavated in the study area represent the oldest currently known and temporally well-constrained bone-bearing horizons in the entire Hațeg Basin, and also rank among the oldest ones from the entire latest Cretaceous Hațeg Island, formed during a time interval ranging from near the Campanian/Maastrichtian boundary to the late early Maastrichtian. Accordingly, the currently ongoing study of these sites and their fossil content will contribute greatly to our knowledge concerning the composition of the earliest faunal assemblages of Hațeg Island, and the spatial patterning of the local palaeogeographical-palaeoenvironmental conditions within which these early faunas evolved. Furthermore as well as will shed new light onto the timing of evolution and diversification of these peculiar latest Cretaceous Eastern European island faunas.

CRediT authorship contribution statement

Gáspár Albert: Writing – review & editing, Writing – original draft, Software, Methodology, Investigation, Formal analysis, Data curation, Conceptualization. **Soma Budai:** Writing – review & editing, Writing – original draft, Methodology, Investigation, Data curation. **Zoltán Csiki-Sava:** Writing – review & editing, Writing – original draft, Resources, Methodology, Investigation, Data curation, Conceptualization. **László Makádi:** Writing – review & editing, Investigation, Data curation. **Daniel Ţabără:** Writing – review & editing, Writing – original draft, Methodology, Investigation, Data curation. **Valentin Árvai:** Software, Data curation. **Ramona Bălc:** Writing – review & editing, Writing – original draft, Methodology, Investigation. **Raluca Bindiu-Haitonic:** Writing – review & editing, Writing – original draft, Methodology, Investigation, Data curation. **Mihai N. Ducea:** Writing – review & editing, Writing – original draft, Methodology, Investigation, Data curation. **Gábor Botfalvai:** Writing – review & editing, Writing – original draft, Supervision, Resources, Project administration, Methodology, Investigation, Data curation, Conceptualization.

Declaration of competing interest

The authors declare that they have no known competing financial interests or personal relationships that could have appeared to influence the work reported in this paper.

Acknowledgements

The authors would like to thank Eduardo Koutsoukos and an anonymous reviewer, as well as the Editor (Maria Rose Petrizzo), for their insightful and constructive comments and observation on a previous version of this manuscript, and which contributed to a great extent to its improvment. We are grateful to the 2019–2024 field crews for their assistance in the Vălioara fieldwork. Field and laboratory investigations were supported by Hungarian Scientific Research Fund and National Research, Development and Innovation Office (Grant no. NKFIH OTKA PD 131557 and FK146097 to GB), Supervisory Authority for Regulatory Affairs, Hungarian Natural History Museum, Eötvös Loránd University, HUN-REN Hungarian Research Network, Valiora Dinosaur Research Group and János Bolyai Research Scholarship of the Hungarian Academy of Sciences. This is HUN-REN-MTM-ELTE Paleo contribution No. 415. The research was further supported by grants of the Romanian Ministry of Research, Innovation and Digitization, CNCS/CCCDI -UEFISCDI through projects PN-III-P4-ID-PCE-2020-2570, within PNCDI III (to ZCs-S) and PNRR–III–C9-2023–I8 (64/30.07.2023) (to MND); RBH acknowledges financial support from the Babeș-Bolyai University through project SRG-UBB 32938/22.06.2023. We are grateful to the following colleagues for their help: János Magyar (ELTE), Pál Pelikán† (MÁFI), Cristian Ciobanu (Hațeg Country UNESCO Global Geopark), Ștefan Vasile, Maria-Raluca Văcărescu (University of Bucharest), Ádám Csicsek, Réka Lukács, Zsófia Farkas (ELTE). Fieldwork in the Vălioara area had been conducted under permits issued by the Hațeg Country UNESCO Global Geopark and by the National Agency for Natural Protected Areas (437/STDH/08.04.2022 and 468/STDH/09.04.2024).

Data availability

Data will be made available on request.

References

Abramovich, S., Keller, G., Stüben, D., Berner, Z., 2003. Characterization of late Campanian and Maastrichtian planktonic foraminiferal depth habitats and vital activities based on stable isotopes. Palaeogeography, Palaeoclimatology, Palaeoecology 202, 1–29. https://doi.org/10.1016/S0031-0182(03)00572-8.

Abramovich, S., Yovel-Corem, S., Almogi-Labin, A., Benjamini, C., 2010. Global climate change and planktic foraminiferal response in the Maastrichtian: Maastrichtian climate and foraminifera. Paleoceanography 25, 1–15. https://doi.org/10.1029/2009PA001843.

Aggarwal, N., 2022. Sedimentary organic matter as a proficient tool for the palaeoenvironmental and palaeodepositional settings on Gondwana coal deposits. Journal of Petroleum Exploration and Production Technology 12, 257–278. https://doi.org/10.1007/s13202-021-01331-x.

Albert, G., Csiki-Sava, Z., Botfalvai, G., 2024. Public database of geological-paleontological mapping in the surroundings of Vălioara. https://doi.org/10.5281/ZENODO.13286551.

Alberti, G., 1961. Zur Kenntnis mesozoischer und alttertiärer Dinoflagellaten und Hystrichosphaerideen von Nord- und Mitteldeutschland sowie einigen anderen europäischen Gebieten. Palaeontographica Abteilung A 116, 1–58.

Amaglio, G., Petrizzo, M.R., Holbourn, A., Kuhnt, W., Wolfgring, E., 2023. Benthic foraminiferal response to the Oceanic Anoxic Event 2 (Late Cretaceous) and evidence of bottom water re-oxygenation during the Plenus Cold Event at Clot Chevalier (Vocontian Basin, SE France). Palaeogeography, Palaeoclimatology, Palaeoecology 623, 111598. https://doi.org/10.1016/j.palaeo.2023.111598.

Anastasiu, N., Csobuka, D., 1989. Non-marine uppermost Cretaceous deposits in the Stei-Densuş region (Haţeg Basin): sketch for a facial model. Revue Roumaine de Géologie, Géophysique et Géographie. Geologie 33, 43–53.

Antonescu, E., Lupu, D., Lupu, M., 1983. Correlation palinologique du Crétacé terminal du sud-est des Monts Metaliferi et des Depressions de Haţeg et de Rusca Montană. Anuarul Institutului de Geologie şi Geofizică 59, 71–77.

Archangelsky, S., 1977. *Balmeiopsis*, a new generic name for the palynomorph *Inaperturopollenites limbatus*, Balme,1957. Ameghiniana 14 (1), 122–126.

Arkhangelsky, A.D., 1912. Upper Cretaceous deposits of east European Russia. Materialien zur Geologie Russlands 25, 1–631.

Bălc, R., Bindiu-Haitonic, R., Kövecsi, S.-A., Vremir, M., Ducea, M., Csiki-Sava, Z., Ţabără, D., Vasile, Ş., 2024. Integrated biostratigraphy of Upper Cretaceous deposits from an exceptional continental vertebrate-bearing marine section (Transylvanian Basin, Romania) provides new constraints on the advent of 'dwarf dinosaur' faunas in Eastern Europe. Marine Micropaleontology 187, 102328. https://doi.org/10.1016/j.marmicro.2023.102328.

Banjesevic, M., 2010. Upper cretaceous magmatic suites of the Timok magmatic complex. Geološki Anali Balkanskog Poluostrva 71, 13–22. https://doi.org/10.2298/GABP1071013B.

Bărzoi, S.C., Şecläman, M., 2010. Petrographic and geochemical interpretation of the Late Cretaceous volcaniclastic deposits from the Hateg Basin. Palaeogeography, Palaeoclimatology, Palaeoecology 293, 306–318. https://doi.org/10.1016/j.palaeo.2009.08.028.

Berza, T., Constantinescu, E., Vlad, S.-N., 1998. Upper Cretaceous Magmatic Series and Associated Mineralisation in the Carpathian – Balkan Orogen. Resource Geology 48, 291–306. https://doi.org/10.1111/j.1751-3928.1998.tb00026.

Black, M., Barnes, B., 1959. The structure of Coccoliths from the English Chalk. Geological Magazine 96 (5), 321–328.

Blair, T.C., 1999. Sedimentology of the debris-flow-dominated Warm Spring Canyon alluvial fan, Death Valley, California. Sedimentology 46, 941–965. https://doi.org/10.1046/j.1365-3091.1999.00260.x.

Blair, T.C., McPherson, J.G., 1994. Alluvial Fans and their Natural Distinction from Rivers Based on Morphology, Hydraulic Processes, Sedimentary Processes, and Facies Assemblages. Journal of Sedimentary Research 64A, 450–489. https://doi.org/10.1306/D4267DDE-2B26-11D7-8648000102C1865D.

Bojar, A.-V., Bojar, H.-P., Ottner, F., Grigorescu, D., 2010. Heavy mineral distributions of Maastrichtian deposits from the Haţeg Basin, South Carpathians: Tectonic and palaeogeographic implications. Palaeogeography, Palaeoclimatology, Palaeoecology 293, 319–328. https://doi.org/10.1016/j.palaeo.2009.10.002.

Bojar, A.-V., Grigorescu, D., Ottner, F., Csiki, Z., 2005. Palaeoenvironmental interpretation of dinosaur-and mammal-bearing continental Maastrichtian deposits, Haţeg Basin, Romania. Geological Quarterly 49, 205–222.

Botfalvai, G., Csiki-Sava, Z., Grigorescu, D., Vasile, Ş., 2017. Taphonomical and palaeoecological investigation of the Late Cretaceous (Maastrichtian) Tuştea vertebrate assemblage (Romania; Haţeg Basin) - insights into a unique dinosaur nesting locality. Palaeogeography, Palaeoclimatology, Palaeoecology 468, 228–262. https://doi.org/10.1016/j.palaeo.2016.12.003.

Botfalvai, G., Csiki-Sava, Z., Kocsis, L., Albert, G., Magyar, J., Bodor, E.R., Ţabără, D., Ulyanov, A., Makádi, L., 2021. 'X' marks the spot! Sedimentological, geochemical and palaeontological investigations of Upper Cretaceous (Maastrichtian) vertebrate fossil localities from the Vălioara valley (Densuş-Ciula Formation, Haţeg Basin, Romania). Cretaceous Research 123, 104781. https://doi.org/10.1016/j.cretres.2021.104781.

Bramlette, M.N., Martini, E., 1964. The great change in calcareous nannoplankton fossils between the Maestrichtian and Danian. Micropaleontology 10 (2), 291–322.

Breiman, L., 2001. Random forests. Machine Learning 45, 5–32. https://doi.org/10.1023/A:1010933404324.

Brotzen, F., 1942. Die Foraminiferengattung *Gavelinella* nov. gen. und die Systematik der Rotaliiformes. Sveriges Geologiska Undersökning 36 (8), 1–60.

Buffetaut, E., Grigorescu, D., Csiki, Z., 2002. A new giant pterosaur with a robust skull from the latest Cretaceous of Romania. Naturwissenschaften 89, 180–184. https://doi.org/10.1007/s00114-002-0307-1.

Bukry, D., 1969. Upper Cretaceous coccoliths from Texas and Europe. University of Kansas Paleontological Contributions 51 (Protista 2), 1–79.

Bull, W.B., 1997. Discontinuous ephemeral streams. Geomorphology 19, 227–276. https://doi.org/10.1016/S0169-555X(97)00016-0.

Burnett, J., 1998. Upper Cretaceous. In: Bown, P.R. (Ed.), Calcareous Nannofossil Biostratigraphy. British Micropalaeontological Society Publication Series. Chapman & Hall, London, pp. 132–199.

Bykova, N.K., Balakhmatova, V.T., Vasilenko, V.P., Voloshinova, N.A., Grigelis, A., Dain, l.G., Ivanova, L.V., Kuzina, V.I., Kuznetsova, Z.V., Kozyreva, V.F., Morozova, V.G., Myatlyuk, E.V., Subbotina, N.N., 1958. New genera and species of foraminifera. Microfauna of the USSR. Proceedings of the Oil Research Geological Institute 9 (115), 5–106.

Cant, D.J., Walker, R.G., 1978. Fluvial processes and facies sequences in the sandy braided South Saskatchewan River, Canada. Sedimentology 25, 625–648. https://doi.org/10.1111/j.1365-3091.1978.tb00323.x.

Carpenter, W.B., 1869. On the Rhizopodal Fauna of the Deep Sea. Proceedings of the Royal Society of London 18 (114–122), 59–62.

Carvalho, M.D.A., Ramos, R.R.C., Crud, M.B., Witovisk, L., Kellner, A.W.A., Silva, H.D.P., Grillo, O.N., Riff, D., Romano, P.S.R., 2013. Palynofacies as indicators of paleoenvironmental changes in a Cretaceous succession from the Larsen Basin, James Ross Island, Antarctica. Sedimentary Geology 295, 53–66. https://doi.org/10.1016/j.sedgeo.2013.08.002.

Chan, S.A., Bălc, R., Humphrey, J.D., Amao, A.O., Kaminski, M.A., Alzayer, Y., Duque, F., 2022. Changes in paleoenvironmental conditions during the Late Jurassic of the western Neo-Tethys: Calcareous nannofossils and geochemistry. Marine Micropaleontology 173, 102116. https://doi.org/10.1016/j.marmicro.2022.102116.

Clarke, R.F.A., Verdier, J.P., 1967. An investigation of microplankton assemblages from the Chalk of the Isle of Wight, England. Verhandelingender Koninklijke Nederlandse Akademie van Wetenschappen, Afdeeling Natuurkunde, Eerste Reeks 24 (3), 1–96.

Codarcea, A., 1940. Vues nouvelles sur la tectonique du Banat meridional et du Plateau de Mehedinţi. Dări de Seamă ale Institutului Geologic al Romăniei 20, 1–74.

Cookson, I.C., Dettmann, M.E., 1959. On Schizosporis, a new form genus from Australian Cretaceous deposits. Micropaleontology 5 (2), 213–216.

Couper, R.A., 1953. Upper Mesozoic and Cainozoic spores and pollen grains from New Zealand. N.Z. Geological Survey Paleontological Bulletin 22, 77.

Couper, R.A., 1960. New Zealand Mesozoic and Cainozoic plant microfossils. New Zealand Geological Survey Paleontological Bulletin 32, 1–88.

Cracknell, M.J., Reading, A.M., 2014. Geological mapping using remote sensing data: A comparison of five machine learning algorithms, their response to variations in the spatial distribution of training data and the use of explicit spatial information. Computers & Geosciences 63, 22–33. https://doi.org/10.1016/j.cageo.2013.10.008.

Cushman, J.A., 1926. The foraminifera of the Velasco Shale of the Tampico Embayment. Bulletin of the American Association of Petroleum Geologists 10, 581–612.

Csiki, Z., Grigorescu, D., 2000. Teeth of multituberculate mammals from the Late Cretaceous of Romania. Acta Palaeontologica Polonica 45 (1), 85–90.

Csiki, Z., Grigorescu, D., Codrea, V., Therrien, F., 2010. Taphonomic modes in the Maastrichtian continental deposits of the Haţeg Basin, Romania—Palaeoecological and palaeobiological inferences. Palaeogeography, Palaeoclimatology, Palaeoecology 293, 375–390. https://doi.org/10.1016/j.palaeo.2009.10.013.

Csiki, Z., Ionescu, A., Grigorescu, D., 2008. The Budurone microvertebrate site from the Maastrichtian of the Haţeg Basin-flora, fauna, taphonomy and paleoenvironment. Acta Palaeontologica Romaniae 6, 49–66.

Csiki-Sava, Z., Ţabără, D., Bălc, R., Bindiu-Haitonic, R., Botfalvai, G., Albert, G., Vasile, Ş., 2023. New biostratigraphic and palaeoenvironmental constraints in the uppermost Cretaceous deposits from the Ciula Mică (Geat Valley) - west Vălioara area, northwestern Haţeg Basin (Romania). In: Csiki-Sava, Z., Floroiu, A., Văcărescu, R.-M., Lazăr, I. (Eds.), Abstract Book, 14th Romanian Symposium on Palaeontology Bucharest. University Press, Bucharest, pp. 43–44.

Csiki-Sava, Z., Vremir, M., Vasile, Ş., Brusatte, S.L., Dyke, G., Naish, D., Norell, M.A., Totoianu, R., 2016. The East Side Story – The Transylvanian latest Cretaceous continental vertebrate record and its implications for understanding Cretaceous–Paleogene boundary events. Cretaceous Research 57, 662–698. https://doi.org/10.1016/j.cretres.2015.09.003.

Cushman, J.A., 1927. An outline of a re-classification of the Foraminifera. Contributions from the Cushman Laboratory for Foraminiferal Research 3 (1), 1–105.

Deák, M.H., Combaz, A., 1967. "Microfossiles organiques" du Wealdien et du Cénomanien dans un sondage de Charente-Maritime. Revue de Micropaleontologie 10, 69–96.

Deflandre, G., 1937. Microfossiles des silex crétacés, Deuxième partie, Flagellés incertae sedis, Hystrichosphaeridés, Sarcodinés, Organismes divers. Annales de paléontologie 26, 51–103.

Deflandre, G., 1959. Sur les nannofossiles calcaires et leur systématique. Revue de Micropaleontologie 2, 127–152.

Delvaux, D., Sperner, B., 2003. New aspects of tectonic stress inversion with reference to the TENSOR program. SP, pp. 75–100. https://doi.org/10.1144/GSL.SP.2003.212.01.06, 212.

Doeven, P., 1983. Cretaceous nannofossil stratigraphy and paleoecology of the Canadian Atlantic Margin. Geological Survey of Canada. Bulletin. Geological Survey of Canada 356, 1–70.

Drusch, M., Del Bello, U., Carlier, S., Colin, O., Fernandez, V., Gascon, F., Hoersch, B., Isola, C., Laberinti, P., Martimort, P., Meygret, A., Spoto, F., Sy, O., Marchese, F., Bargellini, P., 2012. Sentinel-2: ESA's Optical High-Resolution Mission for GMES Operational Services. Remote Sensing of Environment 120, 25–36. https://doi.org/10.1016/j.rse.2011.11.026.

Ducea, M.N., Saleeby, J.B., Bergantz, G., 2015. The Architecture, Chemistry, and Evolution of Continental Magmatic Arcs. Annual Review of Earth and Planetary Sciences 43, 299–331. https://doi.org/10.1146/annurev-earth-060614-105049.

Erba, E., 1992. Middle Cretaceous calcareous nannofossils from the western Pacific (Leg 129): evidence for paleoequatorial crossings. In: Proceedings of the Ocean Drilling Program, Scientific Results. Ocean Drilling Program College Station, TX, pp. 189–201.

Erba, E., Castradori, D., Guasti, G., Ripepe, M., 1992. Calcareous nannofossils and Milankovitch cycles: the example of the Albian Gault Clay Formation (southern England). Palaeogeography, Palaeoclimatology, Palaeoecology 93, 47–69. https://doi.org/10.1016/0031-0182(92)90183-6.

Ezquerro, L., Luzón, A., Simón, J.L., Liesa, C.L., 2019. Alluvial sedimentation and tectono-stratigraphic evolution in a narrow extensional zigzag basin margin

(northern Teruel Basin, Spain). Journal of Palaeogeography 8, 2–25. https://doi.org/10.1186/s42501-019-0044-4.
Forchheimer, S., 1972. Scanning electron microscope studies of Cretaceous coccoliths from the Köpingsberg Borehole No. 1, SE Sweden. Sveriges Geologiska Undersökning. Series C 668 (65), 1–141.
Fidolini, F., Ghinassi, M., Aldinucci, M., Billi, P., Boaga, J., Deiana, R., Brivio, L., 2013. Fault-sourced alluvial fans and their interaction with axial fluvial drainage: An example from the Plio-Pleistocene Upper Valdarno Basin (Tuscany, Italy). Sedimentary Geology 289, 19–39. https://doi.org/10.1016/j.sedgeo.2013.02.004.
Fielding, C.R., 1984. Upper delta plain lacustrine and fluviolacustrine facies from the Westphalian of the Durham coalfield, NE England. Sedimentology 31, 547–567. https://doi.org/10.1111/j.1365-3091.1984.tb01819.x.
Fisher, N.I., Lewis, T., Embleton, B.J.J., 1987. Statistical analysis of spherical data. Cambridge University Press, Cambridge [Cambridgeshire] ; New York.
Fisher, R.V., Schmincke, H.-U., 1984. Pyroclastic Fragments and Deposits. In: Pyroclastic Rocks. Springer Berlin Heidelberg, Berlin, Heidelberg, pp. 89–124. https://doi.org/10.1007/978-3-642-74864-6_5.
Flaig, P.P., Fiorillo, A.R., McCarthy, P.J., 2014. Dinosaur-bearing hyperconcentrated flows of Cretaceous arctic Alaska: Recurring catastrophic event beds on a distal paleopolar coastal plain. PALAIOS 29, 594–611. https://doi.org/10.2110/palo.2013.133.
François, C., Pubellier, M., Robert, C., Bulois, C., Jamaludin, S.N.F., Oberhänsli, R., Faure, M., St-Onge, M.R., the IGCP 667 Team, 2022. Temporal and spatial evolution of orogens: a guide for geological mapping. Episodes 45, 265–283. https://doi.org/10.18814/epiiugs/2021/021025.
Fügenschuh, B., Schmid, S.M., 2005. Age and significance of core complex formation in a very curved orogen: Evidence from fission track studies in the South Carpathians (Romania). Tectonophysics 404, 33–53. https://doi.org/10.1016/j.tecto.2005.03.019.
Gallhofer, D., Quadt, A.V., Peytcheva, I., Schmid, S.M., Heinrich, C.A., 2015. Tectonic, magmatic, and metallogenic evolution of the Late Cretaceous arc in the Carpathian-Balkan orogen. Tectonics 34, 1813–1836. https://doi.org/10.1002/2015TC003834.
Gao, C., Ji, Y., Wu, C., Jin, J., Ren, Y., Yang, Z., Liu, D., Huan, Z., Duan, X., Zhou, Y., 2020. Facies and depositional model of alluvial fan dominated by episodic flood events in arid conditions: An example from the Quaternary Poplar Fan, northwestern China. Sedimentology 67, 1750–1796. https://doi.org/10.1111/sed.12684.
Gardet, M., 1955. Contribution à l'étude des coccolithes des terrains néogènes de l'Algérie, vol. 5. Publications du Service de la Carte Géologique de l'Algérie, pp. 477–550.
Gardin, S., 2002. Late Maastrichtian to early Danian calcareous nannofossils at Elles (Northwest Tunisia). A tale of one million years across the K–T boundary. Palaeogeography, Palaeoclimatology, Palaeoecology 178, 211–231. https://doi.org/10.1016/S0031-0182(01)00397-2.
Gartner, S., 1968. Coccoliths and related calcareous nannofossils from Upper Cretaceous deposits of Texas and Arkansas. University of Kansas Paleontological Contributions 48, 1–56. Protista 1.
Georgescu, M.D., Huber, B.T., 2009. Early evolution of the cretaceous serial planktic foraminifera (late Albian-Cenomanian). Journal of Foraminiferal Research 39 (4), 335–360.
Góczán, F., 1964. Stratigraphic palynology of the Hungarian Upper Cretaceous. Acta Geologica Academiae Scientiarum Hungaricae 8, 229–264.
Góczán, F., Siegl-Farkas, Á., 1990. Palynostratigraphical zonation of Senonian sediments in Hungary. Review of Palaeobotany and Palynology 66, 361–377. https://doi.org/10.1016/0034-6667(90)90047-M.
Góczán, F., Groot, J.J., Krutzsch, W., Pacltová, B., 1967. Die Gattungen des "Stemma Normapolles Pflug 1953b" (Angiospermae) – Neubeschreibungen und Revision europäischer Formen (Oberkreide bis Eozän). Paläontologische Abhandlungen, Abteilung B 2, 429–540.
Golonka, J., Gahagan, L., Krobicki, M., Marko, F., Oszczypko, N., Ślączka, 2006. Plate-tectonic evolution and paleogeography of the circum-Carpathian region. In: Golonka, J., Picha, F.J. (Eds.), The Carpathians and their foreland: Geology and hydrocarbon resources, vol. 84. AAPG Memoir, pp. 11–46.
Grigorescu, D., 1992. Nonmarine Cretaceous formations of Romania. In: Matter, N.J., Chen, P.-J. (Eds.), Aspects of Nonmarine Cretaceous Geology. China Ocean Press, Beijing, pp. 142–164.
Gradstein, F.M., Ogg, J.G., Schmitz, M.D., Ogg, G.M., 2020. Geologic Time Scale 2020. In: Elsevier. https://doi.org/10.1016/C2020-1-02369-3.
Grigorescu, D., 1983. A stratigraphic, taphonomic and paleoecologic approach to a" forgotten land": the dinosaur-bearing deposits from the Haţeg Basin (Transylvania-Romania). Acta Palaeontologica Polonica 28 (1–2), 103–121.
Grigorescu, D., 2005. Rediscovery of a "forgotten land". The last three decades of research on the dinosaur-bearing deposits from the Haţeg Basin. Acta Palaeontologica Romaniae 5, 191–204.
Grigorescu, D., Csiki, Z., 2008. A new site with megaloolithid egg remains in the Maastrichtian of the Haţeg Basin. Acta Palaeontologica Romaniae 6, 115–121.
Grigorescu, D., Melinte, M., 2001. The stratigraphy of the Upper Cretaceous marine sediments from the NW Haţeg area (South Carpathians, Romania). Acta Palaeontologica Romaniae 3, 153–160.
Grigorescu, D., Venczel, M., Csiki, Z., Limberea, R., 1999. New latest Cretaceous microvertebrate fossil assemblages from the Haţeg Basin (Romania). Geologie en Mijnbouw 78, 301–314. https://doi.org/10.1023/A:1003890913328.
Grün, W., Allemann, F., 1975. The Lower Cretaceous of Caravaca (Spain): Berriasian Calcareous Nannoplankton of the Miravetes Section (Subbetic Zone, Prov. of Murcia). Eclogae Geologicae Helvetiae 68, 147–211.
Grzybowski, J., 1898. Foraminifera of oil-bearing strata in the neighbourhood of Krosno. Rozprawy Wydziału Matematyczno-Przyrodniczego Akademii Umiejętności 33, 257–305.
Haq, B.U., 2014. Cretaceous eustasy revisited. Global and Planetary Change 113, 44–58. https://doi.org/10.1016/j.gloplacha.2013.12.007.
Herrle, J.O., Pross, J., Friedrich, O., Hemleben, Ch, 2003. Short-term environmental changes in the Cretaceous Tethyan Ocean: micropalaeontological evidence from the Early Albian Oceanic Anoxic Event 1b. Terra Nova 15, 14–19. https://doi.org/10.1046/j.1365-3121.2003.00448.x.
Iancu, V., Berza, T., Seghedi, A., Gheuca, I., Hann, H.-P., 2005. Alpine polyphase tectono-metamorphic evolution of the South Carpathians: A new overview. Tectonophysics 410, 337–365. https://doi.org/10.1016/j.tecto.2004.12.038.
Ion, J., Antonescu, E., Melinte, M.C., Szasz, L., 1998. Tentative for an integrated standard biostratigraphy-on the basis of Macrofauna, planktonic foraminifera, calcareous nannoplankton, dinoflagellates, pollen-for the Upper Cretaceous deposits from Romania. Romanian Journal of Stratigraphy 77, 65–83.
Jeffery, D.L., Bertog, J.L., Bishop, J.R., 2011. Sequence stratigraphy of dinosaur lake: small scale fluvio-deltaic stratal relationship of a dinosaur accumulation as the Aaron Scott quarry, Morrison Formation, San Rafael Swell, Utah. PALAIOS 26, 275–283. https://doi.org/10.2110/palo.2010.p10-104r.
Kadić, O., 1916. Report on my excavations in 1915, vol. 40. Annual reports of the Royal Geological Institute of Hungary, pp. 568–576.
Kaiho, K., 1994. Benthic foraminiferal dissolved-oxygen index and dissolved-oxygen levels in the modern ocean. Geology 22, 719–722. https://doi.org/10.1130/0091-7613(1994)022<0719:BFDOIA>2.3.CO;2.
Kaiho, K., Hasegawa, T., 1994. End-Cenomanian benthic foraminiferal extinctions and oceanic dysoxic events in the northwestern Pacific Ocean. Palaeogeography, Palaeoclimatology, Palaeoecology 111, 29–43. https://doi.org/10.1016/0031-0182(94)90346-8.
Kedves, M., 1980. Palynological investigations on sediments of the lower Danian (Fish Clay, Denmark). Acta Mineralogica-Petrographica 24 (2), 355–376.
Kranner, M., Harzhauser, M., Beer, C., Auer, G., Piller, W.E., 2022. Calculating dissolved marine oxygen values based on an enhanced Benthic Foraminifera Oxygen Index. Scientific Reports 12, 1376. https://doi.org/10.1038/s41598-022-05295-8.
Krézsek, C., Lăpădat, A., Maţenco, L., Arnberger, K., Barbu, V., Olaru, R., 2013. Strain partitioning at orogenic contacts during rotation, strike–slip and oblique convergence: Paleogene–Early Miocene evolution of the contact between the South Carpathians and Moesia. Global and Planetary Change 103, 63–81. https://doi.org/10.1016/j.gloplacha.2012.11.009.
Krstekanić, N., Willingshofer, E., Broerse, T., Maţenco, L., Toljić, M., Stojadinovic, U., 2021. Analogue modelling of strain partitioning along a curved strike-slip fault system during backarc-convex orocline formation: Implications for the Cerna-Timok fault system of the Carpatho-Balkanides. Journal of Structural Geology 149, 104386. https://doi.org/10.1016/j.jsg.2021.104386.
Krutzsch, W., 1962. Stratigraphic or botanic importance of new spore and pollen forms from the German Tertiary. Geologie 11 (3), 265–287.
Laufer, F., 1925. Contribuţiuni la studiul geologic al împrejurimilor oraşului Haţeg. Anuarul Institutului Geologic al Romaniei 10, 301–333.
Leeder, M.R., 1999. Sedimentology and sedimentary basins: from turbulence to tectonics. Blackwell Science, Oxford.
Lentin, J.K., Williams, G.L., 1981. Fossil dinoflagellates: index to genera and species, 1981 edition. Bedford Institute of Oceanography, Report Series, no.BI-R-81-12, p. 345.
Leschik, G., 1955. Die Keuperflora von Neuewelt bei Basel. II. Die Iso-und Mikrosporen. Schweizerische Paläontologische Abhandlungen 72 (1), 5–70.
Linnert, C., Mutterlose, J., Erbacher, J., 2010. Calcareous nannofossils of the Cenomanian/Turonian boundary interval from the Boreal Realm (Wunstorf, northwest Germany). Marine Micropaleontology 74, 38–58. https://doi.org/10.1016/j.marmicro.2009.12.002.
Linzer, H.-G., Frisch, W., Zweigel, P., Girbacea, R., Hann, H.-P., Moser, F., 1998. Kinematic evolution of the Romanian Carpathians. Tectonophysics 297, 133–156. https://doi.org/10.1016/S0040-1951(98, 00166-8Loeblich, A. R., 1946. Foraminifera from the Type Pepper Shale of Texas. Journal of Paleontology 20(2), 130–139.
Loeblich, A.R., 1946. Foraminifera from the type Pepper shale of Texas. Journal of Paleontology 20 (2), 130–139.
Loeblich, A.R., Tappan, H., 1986. Some New and Revised Genera and Families of Hyaline Calcareous Foraminiferida (Protozoa). Transactions of the American Microscopical Society 105 (3), 239–265.
Long, D.G.F., 2006. Architecture of pre-vegetation sandy-braided perennial and ephemeral river deposits in the Paleoproterozoic Athabasca Group, northern Saskatchewan, Canada as indicators of Precambrian fluvial style. Sedimentary Geology 190, 71–95. https://doi.org/10.1016/j.sedgeo.2006.05.006.
Long, D.G.F., 2011. Architecture and Depositional Style of Fluvial Systems Before Land PlantsA Comparison of Precambrian, Early Paleozoic, and Modern River Deposits. In: From River to Rock Record: The Preservation of Fluvial Sediments and Their Subsequent Interpretation. SEPM Society for Sedimentary Geology. https://doi.org/10.2110/sepmsp.097.037.
Lund, J.J., 1977. Rhaetic to Lower Liassic palynology of the onshore south-eastern North Sea Basin. Danmarks Geologiske Undersøgelse 109, 6–128.

Lunt, I.A., Bridge, J.S., Tye, R.S., 2004. A quantitative, three-dimensional depositional model of gravelly braided rivers. Sedimentology 51, 377–414. https://doi.org/10.1111/j.1365-3091.2004.00627.x.
Lupu, M., Popescu, G., Munteanu, T., Pop, G., Bindea, G., Stelea, I., Munteanu, E., 1993. Harta geologică a României 1:50000 105/b Hațeg L-34-94-B.
Magyar, J., Csiki-Sava, Z., Ősi, A., Augustin, F.J., Botfalvai, G., 2024. Rhabdodontid (Dinosauria, Ornithopoda) diversity suggested by the first documented occurrence of associated cranial and postcranial material at Vălioara (uppermost Cretaceous Densuș-Ciula Formation, Hațeg Basin, Romania). Cretaceous Research 156, 105810. https://doi.org/10.1016/j.cretres.2023.105810.
Mahanipour, A., Mutterlose, J., Parandavar, M., 2022. Integrated bio- and chemostratigraphy of the Cretaceous – Paleogene boundary interval in the Zagros Basin (Iran, central Tethys). Palaeogeography, Palaeoclimatology, Palaeoecology 587, 110785. https://doi.org/10.1016/j.palaeo.2021.110785.
Maier, O., Lupu, M., 1979. Harta Geologică a României 1:50000, 105/a Băuțar L-34-94-A.
Mann, P., 2007. Global catalogue, classification and tectonic origins of restraining- and releasing bends on active and ancient strike-slip fault systems, vol. 290. Geological Society, London, Special Publications, pp. 13–142. https://doi.org/10.1144/SP290.2.
Marie, P., 1941. Les Foraminifères de la craie à *Belemnitella mucronata* du Bassin de Paris. Mémoires du Muséum National d'Histoire Naturelle de Paris. Nouvelle Série 12, 1–296.
Mațenco, L., Schmid, S., 1999. Exhumation of the Danubian nappes system (South Carpathians) during the Early Tertiary: inferences from kinematic and paleostress analysis at the Getic/Danubian nappes contact. Tectonophysics 314, 401–422. https://doi.org/10.1016/S0040-1951(99)00221-8.
Melinte-Dobrinescu, M.C., 2010. Lithology and biostratigraphy of Upper Cretaceous marine deposits from the Hațeg region (Romania): Palaeoenvironmental implications. Palaeogeography, Palaeoclimatology, Palaeoecology 293, 283–294. https://doi.org/10.1016/j.palaeo.2009.04.001.
Melinte-Dobrinescu, M.C., Grigorescu, D., 2014. Marine deposits (Urgonian and Gosau Facies) and continental Upper Cretaceous deposits with dinosaur remains of the Hațeg Basin (Southern Carpathians, Romania). Field trip guide. Universitatea Din Bucuresti.
Miall, A.D., 2006. The Geology of Fluvial Deposits: Sedimentary Facies, Basin Analysis, and Petroleum Geology. Springer, Berlin/Heidelberg, Berlin, Heidelberg.
Milne, L.A., 1998. Tertiary palynology: Beaupreaidites and new Conospermeae (Proteoideae) affiliates. Australian Systematic Botany 11, 553–603. https://doi.org/10.1071/SB97013.
Miner, E.L., 1935. Paleobotanical examinations of Cretaceous and Tertiary Coals. 1. Cretaceous Coals from Greenland. 2. Cretaceous and Tertiary Coals from Montana. The American Midland Naturalist 16 (4), 585–625.
Miniati, F., Petrizzo, M.R., Falzoni, F., Erba, E., 2020. Calcareous plankton biostratigraphy of the Santonian-Campanian boundary interval in the Bottaccione Section (Umbria-Marche Basin, Central Italy). Rivista Italiana di Paleontologia e Stratigrafia 126, 771–789. https://doi.org/10.13130/2039-4942/14399.
Montgomery, H., Barnes, K., 2012. Paleolimnology of Uppermost Cretaceous lacustrine deposits in western Texas. PALAIOS 27, 386–394. https://doi.org/10.2110/palo.2011.p11-020r.
Murgoci, G., 1912. The geological synthesis of the South Carpathians. C.R. du XI Congres. Géol. International. Stockholm 871–881.
Murray, J.W., 2006. Ecology and applications of benthic foraminifera. Cambridge University Press, Cambridge ; New York.
Murray, J.W., 1991. Ecology and Palaeoecology of Benthic Foraminifera, first ed. Routledge. https://doi.org/10.4324/9781315846101.
Naylor, M.A., Mandl, G., Supesteijn, C.H.K., 1986. Fault geometries in basement-induced wrench faulting under different initial stress states. Journal of Structural Geology 8, 737–752. https://doi.org/10.1016/0191-8141(86)90022-2.
Nemec, W., Steel, R.J., 1984. Alluvial and coastal conglomerates: their significant features and some comments on gravelly mass-flow deposits. In: Koster, E.H., Steel, R.J. (Eds.), Sedimentology of Gravels and Conglomerate. Canadian Society of Petroleum Geologists, Memoir, pp. 1–31.
Noda, A., 2013. Strike-Slip Basin – Its Configuration and Sedimentary Facies. In: Itoh, Y. (Ed.), Mechanism of Sedimentary Basin Formation - Multidisciplinary Approach on Active Plate Margins. InTech. https://doi.org/10.5772/56593.
Nopcsa, F., 1915. Erdély dinosaurusai. Magyar Állami Földtani Intézet Évkönyve 23, 1–24.
Orbigny, A.D. d', 1840. Mémoire sur les foraminifères de la craie blanche du bassin de Paris. Mémoires de la Société géologique de France 4 (1), 1–51.
Páll-Gergely, B., Magyar, J., Csiki-Sava, Z., Botfalvai, G., 2023. *Ferussina petofiana* sp. n. (Gastropoda, Caenogastropoda, Cyclophoridae), the oldest representative of its subfamily from the Late Cretaceous of Romania. Acta Zoologica Academiae Scientiarum Hungaricae 69, 337–352. https://doi.org/10.17109/AZH.69.4.337.2023.
Parker, W.K., Jones, T.R., 1859. On the nomenclature of the Foraminifera. II. On the species enumerated by Walker and Montagu. Annals and Magazine of Natural History 4 (23), 333–351.
Pătrașcu, Șt, Șeclăman, M., Panaiotu, C., 1993. Tectonic implications of paleomagnetism in Upper Cretaceous deposits in the Hațeg and Rusca Montană basins (South Carpathians, Romania). Cretaceous Research 14, 255–264. https://doi.org/10.1006/cres.1993.1021.
Perch-Nielsen, K., 1968. Der Feinbau und die Klassifikation der Coccolithen aus dem Maastrichtien von Danemark. Biologiske Skrifter. Kongelige Danske Videnskabernes Selskab 16, 1–96.
Perch-Nielsen, K., 1985. Mesozoic calacareous nannofossils. In: Bolli, H.M., Saunders, J.B., Perch-Nielsen, K. (Eds.), Plankton Stratigraphy. Cambridge University Press, Cambridge, pp. 329–426.
Peryt, D., Dubicka, Z., Wierny, W., 2022. Planktonic Foraminiferal Biostratigraphy of the Upper Cretaceous of the Central European Basin. Geosciences 12, 22. https://doi.org/10.3390/geosciences12010022.
Petrizzo, M.R., 2002. Palaeoceanographic and palaeoclimatic inferences from Late Cretaceous planktonic foraminiferal assemblages from the Exmouth Plateau (ODP Sites 762 and 763, eastern Indian Ocean). Marine Micropaleontology 45, 117–150. https://doi.org/10.1016/S0377-8398(02)00020-8.
Petrizzo, M.R., Falzoni, F., Silva, I.P., 2011. Identification of the base of the lower-to-middle Campanian Globotruncana ventricosa Zone: Comments on reliability and global correlations. Cretaceous Research 32, 387–405. https://doi.org/10.1016/j.cretres.2011.01.010.
Pflug, H.D., 1953. Zur Entstehung und Entwicklung des angiospermiden Pollens in der Erdgeschichte. Palaeontographica Abteilung B 95, 60–171.
Plint, A.G., Helm, C.W., Lockley, M.G., 2023. Crocodylian and dinosaur trace fossil assemblages from crevasse splay/levee and floodplain lake environments: middle Cenomanian Dunvegan Formation, northeast British Columbia, Canada. Historical Biology 35, 403–429. https://doi.org/10.1080/08912963.2022.2043294.
Pocock, S.A.J., 1962. Microfloral analysis and age determination of strata at the Jurassic-Cretaceous boundary in the Western Canada Plains. Palaeontographica Abteilung B 111, 1–95.
Pocock, S.A.J., 1970. Palynology of the Jurassic sediments of Western Canada. Part 1. Terrestrial species. Palaeontographica Abteilung B 130 (1–2), 12–72. Pop, G., Neagu, T., Szász, L., 1972. Senonianul din regiunea Hațegului (Carpatii Meridionali). Dări de Seamă, Institutul de Geologie și Geofizică 58(4), 95–118.
Potonié, R., 1956. Synopsis of the genera of the sporae dispersae. Part 1. Beihefte zum Geologischen Jahrbuch 23, 1–103.
Premoli Silvá, I., Erba, E., Emilia Tornaghi, M., 1989. Paleoenvironmental signals and changes in surface fertilityin Mid Cretaceous Corg-Rich pelagic facies of the Fucoid Marls (Central Italy). Geobios 22, 225–236. https://doi.org/10.1016/S0016-6995(89)80059-2.
Potonié, R., 1934. Zur Mikrobotanik des eozänen Humodils des Geiseltals. Arbeiten aus dem Institut für Paläobotanik und Petrographie der Brennstein 4, 25–125.
Reinhardt, P., 1966a. Fossile Vertreter coronoider und styloider Coccolithen (Family Coccolithaceae Poche 1913). Monatsberichte der Deutschen Akademie der Wissenschaften zu Berlin 8, 513–524.
Reinhardt, P., 1966b. Zur Taxonomie und Biostratigraphie des fossilen Nannoplanktons aus dem Malm, der Kreide und dem Alttertiär Mitteleuropas. Freiberger Forschungshefte - A C196, 5–109.
Ridgway, K.D., Decelles, P.G., 1993. Stream-dominated alluvial fan and lacustrine depositional systems in Cenozoic strike-slip basins, Denali fault system, Yukon Territory, Canada. Sedimentology 40, 645–666. https://doi.org/10.1111/j.1365-3091.1993.tb01354.x.
Roth, P.H., 1989. Ocean circulation and calcareous nannoplankton evolution during the Jurassic and Cretaceous. Palaeogeography, Palaeoclimatology, Palaeoecology 74, 111–126. https://doi.org/10.1016/0031-0182(89)90022-9.
Roth, P.H., Krumbach, K.R., 1986. Middle Cretaceous calcareous nannofossil biogeography and preservation in the Atlantic and Indian oceans: Implications for paleoceanography. Marine Micropaleontology 10, 235–266. https://doi.org/10.1016/0377-8398(86)90031-9.
Săndulescu, M., 1994. Overview on Romanian geology. Romanian Journal of Tectonics and Regional Geology 75, 3–15.
Schafarzik, F., 1910. Geological conditions around Gyalár [in Hungarian: Gyalár környékének földtani viszonyai], vol. 35. Annual reports of the Royal Geological Institute of Hungary, pp. 58–66.
Schwager, C., 1866. Fossile Foraminiferen von Kar Nikobar. Reise der Österreichischen Fregatte Novara um die Erde in den Jahren 1857, 1858, 1859 unter den Befehlen des Commodore B. von Wüllerstorf-Urbair. Geologischer Theil (Zweite Abtheilung, Paläontologische Mittheilungen) 2(2), 187–268.
Sheldon, E., Ineson, J., Bown, P., 2010. Late Maastrichtian warming in the Boreal Realm: Calcareous nannofossil evidence from Denmark. Palaeogeography, Palaeoclimatology, Palaeoecology 295, 55–75. https://doi.org/10.1016/j.palaeo.2010.05.016.
Siegl-Farkas, A., 2001. Palynological examination of samples from the Campanian-Maastrichtian succession at Tercis les Bains: A preliminary view on spores and pollen. In: Odin, G.S. (Ed.), Developments in Palaeontology and Stratigraphy, IUGS Special Publication (Monograph) Series. Elsevier, pp. 184–191.
Silvestri, A., 1924. Fauna Paleogenica di Vasciano presso Todi. Bollettino della Societa Geologica Italiana 42, 7–29.
Sissingh, W., 1977. Biostratigraphy of Cretaceous calcareous nannoplankton. Geologie en Mijnbouw 65 (1), 37–65.
Slimani, H., Benam, V.M., Țabără, D., Aassoumi, H., Jbari, H., Chekar, M., Mahboub, I., M'Hamdi, A., 2021. Distribution of Dinoflagellate cyst assemblages and palynofacies in the Upper Cretaceous deposits from the neritic Bou Lila section, External Rif (northwestern Morocco): Implications for the age, biostratigraphic correlations and paleoenviromental reconstructions. Marine Micropaleontology 162, 101951. https://doi.org/10.1016/j.marmicro.2020.101951.
Soliman, H.A., 1972. New Upper Cretaceous foraminifera from Soviet Carpathian (USSR). Revue de Micropaleontologie 15, 35–44.
Soltan, R., Mountney, N.P., 2016. Interpreting complex fluvial channel and barform architecture: Carboniferous Central Pennine Province, northern England. Sedimentology 63, 207–252. https://doi.org/10.1111/sed.12224.

Steel, R.J., 1988. Coarsening-upward and skewed fan bodies: symptoms of strike-slip and transfer fault movement in sedimentary basins. In: Nemec, W., Steel, R.J. (Eds.), Fan Deltas: Sedimentology and Tectonic Settings. Blackie & Son, Glasgow, pp. 75–83.
Stelea, I., Ghenciu, M., 2020. The evolution of structural knowledge of the South Carpathians reflected by old geological maps (1890-1940). Oltenia Journal for Studies in Natural Sciences 36, 7–14.
Stover, L.E., 1966. Cretaceous coccoliths and associated nannofossils from France and the Netherlands. Micropaleontology 12 (2), 133–167.
Stover, L.E., Evitt, W.R., 1978. Analyses of pre-Pleistocene organic-walled dinoflagellates, vol. 15. Stanford University Publications, Geological Sciences, p. 300.
Stradner, H., 1962. Über neue und wenig bekannte Nannofossilien aus Kreide und Alttertiär. Verhandlungen der Geologischen Bundesanstalt 2, 363–377.
Stradner, H., 1963. New contributions to Mesozoic stratigraphy by means of nannofossils. In: Proceedings of the Sixth World Petroleum Congress. Section 1 Paper 4, pp. 167–183.
Strutinski, C., 1986. Upper Cretaceous formations south of Ruschița. Paleotectonic significance. Dări de Seamă. Institutul de Geologie și Geofizică 70–71 (5), 247–254.
Țabără, D., Csiki-Sava, Z., 2024. Palynostratigraphic and palaeoenvironmental investigations of the Maastrichtian from Oarda de Jos (southwestern Transylvanian basin). Acta Palaeontologica Romaniae 20, 87–107. https://doi.org/10.35463/j.apr.2024.01.07.
Țabără, D., Slimani, H., 2019. Palynological and palynofacies analyses of Upper Cretaceous deposits in the Hațeg Basin, southern Carpathians, Romania. Cretaceous Research 104, 104185. https://doi.org/10.1016/j.cretres.2019.07.015.
Țabără, D., Vasile, Ș., Csiki-Sava, Z., Bălc, R., Vremir, M., Chelariu, M., 2022. Palynological and organic geochemical analyses of the Upper Cretaceous Bozeș Formation at Petrești (southwestern Transylvanian Basin) – biostratigraphic and palaeoenvironmental implications. Cretaceous Research 134, 105148. https://doi.org/10.1016/j.cretres.2022.105148.
Tantawy, A.A.A.M., 2003. Calcareous nannofossil biostratigraphy and paleoecology of the Cretaceous–Tertiary transition in the central eastern desert of Egypt. Marine Micropaleontology 47, 323–356. https://doi.org/10.1016/S0377-8398(02)00135-4.
Thalmann, H.E., 1939. Bibliography and index to new genera, species and varieties of foraminifera for the year 1936. Journal of Paleontology 13, 425–465.
Therrien, F., 2005. Palaeoenvironments of the latest Cretaceous (Maastrichtian) dinosaurs of Romania: insights from fluvial deposits and paleosols of the Transylvanian and Hațeg basins. Palaeogeography, Palaeoclimatology, Palaeoecology 218, 15–56. https://doi.org/10.1016/j.palaeo.2004.12.005.
Therrien, F., 2006. Depositional environments and fluvial system changes in the dinosaur-bearing Sânpetru Formation (Late Cretaceous, Romania): post-orogenic sedimentation in an active extensional basin. Sedimentary Geology 192, 183–205.
Thibault, N., Gardin, S., 2007. The late Maastrichtian nannofossil record of climate change in the South Atlantic DSDP Hole 525A. Marine Micropaleontology 65, 163–184. https://doi.org/10.1016/j.marmicro.2007.07.004.
Thomas, B.A., Cleal, C.J., 2022. Pteridophytes as primary colonisers after catastrophic events through geological time and in recent history. Palaeobiodiversity and Palaeoenvironments 102, 59–71. https://doi.org/10.1007/s12549-021-00492-1.
Thomson, P.W., Pflug, H.D., 1953. Pollen und Sporen des Mitteleuropäischen Tertiärs. Palaeontographica Abteilung B Band 94, 1–138. Lieferung 1-4.
Tyson, R.V., 1995. Sedimentary Organic Matter: Organic facies and palynofacies. Springer, Netherlands, Dordrecht.
Vajda, V., Bercovici, A., 2014. The global vegetation pattern across the Cretaceous–Paleogene mass extinction interval: A template for other extinction events. Global and Planetary Change 122, 29–49. https://doi.org/10.1016/j.gloplacha.2014.07.014.
van der Meer, F., van der Werff, H., Van Ruitenbeek, F.J.A., 2014. Potential of ESA's Sentinel-2 for geological applications. Remote Sensing of Environment 148, 124–133. https://doi.org/10.1016/j.rse.2014.03.022.
van Hinsbergen, D.J.J., Torsvik, T.H., Schmid, S.M., Maţenco, L.C., Maffione, M., Vissers, R.L.M., Gürer, D., Spakman, W., 2020. Orogenic architecture of the Mediterranean region and kinematic reconstruction of its tectonic evolution since the Triassic. Gondwana Research 81, 79–229. https://doi.org/10.1016/j.gr.2019.07.009.
Van Itterbeeck, J., Săsăran, E., Codrea, V., Săsăran, L., Bultynck, P., 2004. Sedimentology of the Upper Cretaceous mammal- and dinosaur-bearing sites along the Râul Mare and Barbat rivers, Hațeg Basin, Romania. Cretaceous Research 25, 517–530. https://doi.org/10.1016/j.cretres.2004.04.004.
Varol, O., Girgis, M., 1994. New taxa and taxonomy of some Jurassic to Cretaceous calcareous nannofossils. Neues Jahrbuch für Geologie und Paläontologie - Abhandlungen 192, 221–253.
Vasile, Ș., 2010. Noi situri cu microvertebrate din Maastrichtianul Formațiunii de Densuș-Ciula, Bazinul Hațeg. In: Al X-lea Simpozion Național Studențesc "Geoecologia", Petroșani, pp. 90–93.
Vasile, Ș., Csiki, Z., 2010. Comparative paleoecological analysis of some microvertebrate fossil assemblages from the Hațeg Basin, Romania. Oltenia. Oltenia. Studii și comunicări. Științele Naturii 26, 315–322.
Vasile, Ș., Csiki, Z., Grigorescu, D., 2011. Reassessment of the spatial extent of the middle member, Densuș-Ciula Formation (Maastrichtian), Hațeg Basin, Romania. Acta Palaeontologica Romaniae 7, 335–342.
Vasilenko, V.P., 1961. Upper Cretaceous foraminifera of the Mangyshlak Peninsula. Proceedings of the Oil Research Geological Institute 171, 1–487.
Vekshina, V.N., 1959. Coccolithophoridae of the Maastrichtian deposits of the West Siberian lowlands. Trudyi Instituta Geologii i Geogiziki, Sibiriskoe Otlodelenie. Akademiya Nauk SSSR (Nauka) Moscow 2, 56–81.
Venczel, M., Gardner, J.D., Codrea, V.A., Csiki-Sava, Z., Vasile, Ș., Solomon, A.A., 2016. New insights into Europe's most diverse Late Cretaceous anuran assemblage from the Maastrichtian of western Romania. Palaeobiodiversity and Palaeoenvironments 96, 61–95. https://doi.org/10.1007/s12549-015-0228-6.
Vornicu, V.M., Seghedi, I., Csiki-Sava, Z., Ducea, M.N., 2023. Campanian U–Pb ages of volcaniclastic deposits of the Hațeg Basin (Southern Carpathians): Implications for future intrabasinal lithostratigraphic correlations. Geologica Carpathica 74, 407–422. https://doi.org/10.31577/GeolCarp.2023.21.
Vozzhennikova, T.F., 1967. *Iskopayemyye peridinei yurskikh, melovykh i paleogenovykh otlozheniy* SSSR. Izdatelstvo Nauka, Moscow, U.S.S.R., p. 347, 121 pl.
Vremir, M., Bălc, R., Csiki-Sava, Z., Brusatte, S.L., Dyke, G., Naish, D., Norell, M.A., 2014. Petrești-Arini – An important but ephemeral Upper Cretaceous continental vertebrate site in the southwestern Transylvanian Basin, Romania. Cretaceous Research 49, 13–38. https://doi.org/10.1016/j.cretres.2014.02.002.
Vremir, M., Dyke, G., Totoianu, R., 2015. Repertoire of the Late Cretaceous vertebrate localities from Sebeș area, Alba County (Romania). Terra Sebus. Acta Musei Sabesiensis 7, 695–724.
Watkins, D.K., 1989. Nannoplankton productivity fluctuations and rhythmically-bedded pelagic carbonates of the greenhorn limestone (upper cretaceous). Palaeogeography, Palaeoclimatology, Palaeoecology 74, 75–86. https://doi.org/10.1016/0031-0182(89)90020-5.
Weishampel, D.B., Jianu, C., Csiki, Z., Norman, D.B., 2003. Osteology and phylogeny of *Zalmoxes* (n. g.), an unusual Euornithopod dinosaur from the latest Cretaceous of Romania. Journal of Systematic Palaeontology 1, 65–123. https://doi.org/10.1017/S1477201903001032.
Williams, G., Brinkhuis, H., Pearce, M., Fensome, R., Weegink, J., 2004. Southern Ocean and global dinoflagellate cyst events compared: index events for the Late Cretaceous–Neogene. In: Exon, N.F., Kennett, J.P., Malone, M.J. (Eds.), Proceedings of the Ocean Drilling Program, Scientific Results 189, 1–98. College Station, Texas, USA.
Willingshofer, E., Andriessen, P., Cloetingh, S., Neubauer, F., 2001. Detrital fission track thermochronology of Upper Cretaceous syn-orogenic sediments in the South Carpathians (Romania): inferences on the tectonic evolution of a collisional hinterland: Detrital fission track data from the South Carpathians. Basin Research 13, 379–395. https://doi.org/10.1046/j.0950-091x.2001.00156.x.
Wilson, R.W., Houseman, G.A., Buiter, S.J.H., McCaffrey, K.J.W., Doré, A.G., 2019. Fifty years of the Wilson Cycle concept in plate tectonics: an overview. Geological Society, London, Special Publications 470, 1–17. https://doi.org/10.1144/SP470-2019-58.
Wright, V.P., Marriott, S.B., 1996. A quantitative approach to soil occurrence in alluvial deposits and its application to the Old Red Sandstone of Britain. Journal of the Geological Society 153, 907–913. https://doi.org/10.1144/gsjgs.153.6.0907.
Wright, V.P., Tucker, M.E., 1991. Calcretes. The international association of Sedimentologists, vol. 2. Blackwell Scientific Publications, Oxford, Reprint Series, p. 380.

Appendix A. Supplementary data

Supplementary data to this article can be found online at https://doi.org/10.1016/j.cretres.2025.106095.

Appendix 1. List of taxa mentioned in the text.

Foraminifera:

Brotzenella Vasilenko in Bykova et al. (1958)
Brotzenella monterelensis (Marie, 1941)
Chrysalogonium polystomum (Schwager, 1866)
Cibicidoides Thalmann, 1939
Cibicidoides voltzianus (d'Orbigny, 1840)
Contusotruncana morozovae (Vasilenko, 1961)
Ellipsoglandulina velascoensis Cushman (1926)
Globorotalites Brotzen, 1942
Globotruncana Cushman, 1927
Laevidentalina Loeblich and Tappan, 1986
Laevidentalina gracilis (d'Orbigny, 1840)
Paratrochamminoides Soliman, 1972
Paratrochamminoides deformis (Grzybowski, 1898)
Planoheterohelix Georgescu and Huber, 2009
Rhabdammina Sars in Carpenter (1869)
Saccammina Sars in Carpenter, 1869
Siphonodosaria Silvestri, 1924
Trochammina Parker and Jones, 1859
Trochammina wickendeni Loeblich, 1946

Calcareous nannoplankton

Arkhangelskiella cymbiformis Vekshina, 1959
Broinsonia parca subsp. *parca* Stradner (1963); Bukry (1969)
Calculites obscurus (Deflandre, 1959) Prins and Sissingh in Sissingh (1977)
Cylindralithus sculptus Bukry, 1969
Eiffellithus eximius Stover (1966); Perch-Nielsen (1968)
Eprolithus floralis (Stradner, 1962) Stover, 1966
Gorkaea pseudanthophorus Bramlette and Martini (1964); Varol and Girgis (1994)

Lucianorhabdus arcuatus Forchheimer (1972)
Lucianorhabdus maleformis Reinhardt (1966b)
Micula staurophora Gardet (1955); Stradner (1963)
Prediscosphaera cretacea Arkhangelsky (1912); Gartner (1968)
Reinhardtites anthophorus Deflandre (1959); Perch-Nielsen (1968)
Retecapsa crenulata (Bramlette and Martini, 1964); Grün in Grün and Allemann (1975)
Tranolithus orionatus Reinhardt (1966a); Reinhardt (1966b)
Watznaueria barnesiae (Black *in* Black and Barnes, 1959); Perch-Nielsen (1968)

Dinoflagellate cysts
Dinogymnium longicorne Vozzhennikova (1967)
Impagidinium Stover and Evitt, 1978
Isabelidinium microarmum bicavatum Slimani and Ţabără, 2019 in Ţabără and Slimani (2019)
Odontochitina Deflandre, 1937
Odontochitina costata Alberti (1961)
Pterodinium cingulatum subsp. *granulatum* Clarke and Verdier (1967); Lentin and Williams (1981)

Freshwater algae
Chomotriletes fragilis Pocock, 1962
Schizosporis Cookson and Dettmann, 1959

Pteridophyta
Deltoidospora Miner, 1935
Deltoidospora australis Pocock et al., 1970
Deltoidospora toralis (Leschik, 1955); Lund, 1977
Polypodiaceoisporites Potonié, 1956
Polypodiaceoisporites hojrupensis Kedves, 1980
Vadaszisporites sacali Deák and Combaz, 1967

Gymnospermatophyta
Balmeiopsis limbatus (Balme); Archangelsky, 1977
Classopollis Pflug, 1953

Angiospermatophyta
Hungaropollis Góczán, 1964
Krutzschipollis crassis (Góczán, 1964); Góczán in Góczán et al., 1967
Plicatopollis plicatus (Potonié, 1934); Krutzsch, 1962
Proteacidites Cookson ex Couper, 1953
Proteacidites scaboratus Couper, 1960
Pseudopapillopollis praesubhercynicus (Góczán, 1964); Góczán et al., 1967
Subtriporopollenites constans Pflug, 1953
Suemegipollis triangularis Góczán, 1964
Tricolporopollenites Pflug and Thomson, 1953 in Thomson and Pflug, 1953
Trudopollis capsula Pflug, 1953
Trudopollis conrector Pflug, 1953